DEVELOPMENT OF OXIDASE ENZYME AND NON-ENZYME BASED BIOSENSORS FOR
LACTATE AND CREATININE DETECTION

Miss Siraprapa Boobphahom

จุฬาลงกรณ์มหาวิทยาลัย
CHULALONGKORN UNIVERSITY

A Dissertation Submitted in Partial Fulfillment of the Requirements

for the Degree of Doctor of Philosophy in Biotechnology

Common Course

Faculty of Science

Chulalongkorn University

Academic Year 2019

การพัฒนาตัวรับรู้ชีวภาพแบบใช้เอนไซม์ออกซิเดสและแบบไม่ใช้เอนไซม์สำหรับการตรวจวัดแลคเตท
และครีแอทินิน

น.ส.สิรประภา บุบผาหอม

Thesis Title	DEVELOPMENT OF OXIDASE ENZYME AND NON-ENZYME BASED BIOSENSORS FOR LACTATE AND CREATININE DETECTION
By	Miss Siraprapa Boobphahom
Field of Study	Biotechnology
Thesis Advisor	Professor ORAWON CHAILAPAKUL, Ph.D.
Thesis Co Advisor	Professor SIRIRAT RENGPIPAT, Ph.D.
	NADNUDDA RODTHONGKUM, Ph.D.

Accepted by the Faculty of Science, Chulalongkorn University in Partial Fulfillment of the Requirement for the Doctor of Philosophy

.... Dean of the Faculty of Science

(Professor POLKIT SANGVANICH, Ph.D.)

DISSERTATION COMMITTEE

.... Chairman

(Associate Professor VUDHICHAI PARASUK, Ph.D.)

.... Thesis Advisor

(Professor ORAWON CHAILAPAKUL, Ph.D.)

.... Thesis Co-Advisor

(Professor SIRIRAT RENGPIPAT, Ph.D.)

.... Thesis Co-Advisor

(NADNUDDA RODTHONGKUM, Ph.D.)

.... Examiner

(Associate Professor NATTAYA NGAMROJANAVANICH, Ph.D.)

.... Examiner

(Associate Professor CHALEEDA BOROMPICHAICHARTKUL, Ph.D.)

.... External Examiner

(Assistant Professor Sarute Ummartyotin, Ph.D.)

สิรประภา บุบผาหอม : การพัฒนาตัวรับรู้ชีวภาพแบบใช้เอนไซม์ออกซิเดสและแบบไม่ใช้
เอนไซม์สำหรับการตรวจวัดแลคเตทและครีแอทินิน. (DEVELOPMENT OF OXIDASE
ENZYME AND NON-ENZYME BASED BIOSENSORS FOR LACTATE AND CREATININE
DETECTION) อ.ที่ปรึกษาหลัก : ศ. ดร.อรวรรณ ชัยลภากุล, อ.ที่ปรึกษาร่วม : ศ. ดร.ศิริรัตน์
เร่งพิพัฒน์,ดร.นาฏนัดดา รอดทองคำ

ในปัจจุบันการตรวจวิเคราะห์สารชีวโมเลกุลบ่งชี้โรค มีความสำคัญอย่างมากสำหรับการวินิจฉัยโรคเบื้องต้น
ทางการแพทย์และประเมินสถานะความรุนแรงโรคในผู้ป่วย สำหรับเทคนิคแบบดั้งเดิมที่ใช้วิเคราะห์สารบ่งชี้ทางชีวภาพที่
ผ่านมา มีขั้นตอนการดำเนินการที่ซับซ้อน ใช้เวลาในการวิเคราะห์นาน มีค่าใช้จ่ายสูง และต้องอาศัยผู้เชี่ยวชาญเฉพาะทาง
ดังนั้นตัวรับรู้ทางเคมีไฟฟ้า จึงเป็นอีกทางเลือกหนึ่งที่ได้รับความนิยมในการนำมาประยุกต์ใช้สำหรับวินิจฉัยโรคเบื้องต้น
ในทางการแพทย์ เนื่องจากการวิเคราะห์ด้วยวิธีนี้มีความไว แม่นยำ และราคาถูก ดังนั้นวิทยานิพนธ์นี้มุ่งเน้นการพัฒนาตัว
รับรู้ทางเคมีไฟฟ้าโดยใช้โลหะออกไซด์และแกรฟีนเพื่อการประยุกต์ใช้สำหรับตรวจวัดทางการแพทย์ โดยแบ่งออกเป็น 2
ส่วนหลัก ในส่วนแรกเป็นการพัฒนาตัวรับรู้โฟมนิกเกิลโดยการใช้โฟมนิกเกิลเป็นวัสดุรองรับชนิดใหม่และทำการดัดแปร
โฟมนิกเกิลด้วยแกรฟีน ไทเทเนียมไดออกไซด์โซล และเอนไซม์แลคเตทออกซิเดสเพื่อนำไปประยุกต์ใช้เป็นขั้วไฟฟ้า
สำหรับตรวจวัดแลคเตทแบบใช้เอนไซม์โดยการติดตามปริมาณไฮโดรเจนเปอร์ออกไซด์ที่เกิดขึ้นจากปฏิกิริยา การ
สังเคราะห์ไทเทเนียมไดออกไซด์โซลแกรฟีนนาโนคอมพอสิตสามารถเตรียมทำได้ง่ายโดยใช้วิธีไฮโดรไลซิส จากผล
การศึกษาพบว่าไทเทเนียมไดออกไซด์โซลสามารถกระจายตัวได้ดีบนแผ่นแกรฟีนซึ่งเคลือบอยู่บนแผ่นโฟมนิกเกิล ส่งผลให้
ตัวรับรู้มีความว่องไวในการตรวจวัดสูงขึ้นและมีความคงตัวที่ดียิ่งขึ้น ตัวรับรู้โฟมนิกเกิลสามารถนำไปประยุกต์สำหรับการ
ตรวจวัดปริมาณแลคเตทในตัวอย่างเซรัมได้ในช่วงกว้าง 0.05 ถึง 10.00 มิลลิโมลาร์ โดยมีค่าขีดจำกัดการวิเคราะห์ 0.019
ไมโครโมลาร์ ตัวรับรู้โฟมนิกเกิลนี้มีความว่องไวสูงพอสำหรับการตรวจวิเคราะห์แลคเตทเพื่อการวินิจฉัยสภาวะติดเชื้อใน
กระแสเลือด ในส่วนที่สองเป็นการพัฒนาตัวรับรู้กระดาษร่วมกับการใช้เทคนิคแบบพ่น (Dispensing technique) เพื่อ
การตรวจวัดครีอะทินินแบบไม่ใช้เอนไซม์ โดยตัวรับชนิดนี้สามารถเตรียมได้ง่ายด้วยการใช้เครื่อง HP D300 สำหรับพ่น
คอปเปอร์ออกไซด์คอมพอสิตลงบนรีดิวซ์แกรฟีนออกไซด์ที่ดัดแปรบนขั้วไฟฟ้าพิมพ์สกรีนคาร์บอนบนกระดาษ จากผล
การทดลองพบว่าการใช้เทคนิคแบบพ่นส่งผลต่อการเพิ่มประสิทธิภาพความว่องไวและความสามารถในการวัดซ้ำของตัว
รับรู้ อุปกรณ์ชนิดนี้สามารถนำไปประยุกต์ใช้ในการตรวจวิเคราะห์ครีอะทินินในตัวอย่างเซรัมของผู้ป่วยได้ในช่วง 0.01 ถึง
2.00 มิลลิโมลาร์ โดยมีค่าขีดจำกัดการวิเคราะห์ 0.22 ไมโครโมลาร์ ซึ่งทำให้ตัวรับรู้ชนิดนี้มีความสามารถในการตรวจ
วิเคราะห์ครีอะทินินสำหรับการวินิจฉัยโรคไตได้ในอนาคต

สาขาวิชา	เทคโนโลยีชีวภาพ	ลายมือชื่อนิสิต ....
ปีการศึกษา	2562	ลายมือชื่อ อ.ที่ปรึกษาหลัก ....
		ลายมือชื่อ อ.ที่ปรึกษาร่วม ....
		ลายมือชื่อ อ.ที่ปรึกษาร่วม ....

5872829023 : MAJOR BIOTECHNOLOGY

KEYWORD: Lactate, Creatinine, Titanium dioxide sol, Electrochemical sensor, Copper oxide, Graphene, Nickle form, Reduced graphene oxide

Siraprapa Boobphahom : DEVELOPMENT OF OXIDASE ENZYME AND NON-ENZYME BASED BIOSENSORS FOR LACTATE AND CREATININE DETECTION. Advisor: Prof. ORAWON CHAILAPAKUL, Ph.D. Co-advisor: Prof. SIRIRAT RENGPIPAT, Ph.D., NADNUDDA RODTHONGKUM, Ph.D.

This dissertation focused on the development of electrochemical sensors based on metal oxides and graphene modified electrodes for clinical applications, which is divided into two parts. The first part is development of a biosensor based on lactate oxidase (LOx) immobilized on titanium dioxide sol (TiO$_2$ sol)/graphene nanocomposite modified nickel (Ni) foam electrode for enzymatic electrochemical detection of lactate via hydrogen peroxide (H$_2$O$_2$) detection. A TiO$_2$/graphene nanocomposite was simply synthesized by hydrolysis and coated on Ni foam electrode to develop a novel electrode in biosensor. The results showed that the well intercalation of TiO$_2$ sol within graphene film covered on the Ni foam surface, leading to enhanced sensitivity and improved stability of the sensor. This electrode was successfully applied to detect lactate in a complex biological fluid. It exhibited a linear range from 0.05 to 10 mM with a detection limit of 19 µM. This platform was sensitive enough for early diagnosis of severe sepsis and septic shock via the detection of concerned lactate level. The second part is development of a paper-based analytical device (PAD) coupled with a dispensing technique for a non-enzymatic sensor of creatinine. The device was fabricated using a HP D300 dispenser for depositing a copper oxide and ionic liquid composite onto an electrochemically reduced graphene modified screen-printed carbon electrode (CuO/IL/ERGO/SPCE) on a PAD. The results revealed that the use of HP D300 dispenser in a novel approach for electrode modification, allowing for enhanced sensitivity and reproducibility. The CuO/IL/ERGO/SPCE was constructed and applied as a non-enzymatic sensor of creatinine in human serum samples. It exhibited a linear range from 0.01 to 2 mM with a detection limit of 0.22 µM, which make this device is applicable for detecting clinically relevant creatinine level in acute kidney injury diagnosis.

Field of Study:	Biotechnology	Student's Signature ....
Academic Year:	2019	Advisor's Signature ....
		Co-advisor's Signature ....
		Co-advisor's Signature ....

ACKNOWLEDGEMENTS

TABLE OF CONTENTS

LIST OF TABLES

LIST OF FIGURES

Page

No table of figures entries found.

LIST OF FIGURES

LIST OF TABLES

จุฬาลงกรณ์มหาวิทยาลัย

CHULALONGKORN UNIVERSITY

CHAPTER I

INTRODUCTION

1.1   Introduction

Nowadays, the determination of biomolecules is a prevalent importance for medical application. However, the conventional detecting techniques such as high performance liquid chromatography (HPLC), fluorescence spectroscopy, and chemiluminescence spectroscopy used for biological substances still have some limitations. These techniques are expensive, time-consuming, and complicated, also there is increasing a number of measurements of analytes performed in many locations, including hospital point-of-care testing, non-hospital and home healthcare settings. Among these techniques, an electrochemical technique has attracted a great interest for employing of the modified electrodes in recent years because of its simple measurements, qualitative and quantitative analysis, and low operating cost. Moreover, this technique can be used to develop an electrochemical sensor in a portable field-based size with fast response time, which is a promising device to analyze the amount of a biological sample providing precisely analytical information and rapidly obtained data about the health status of patients in clinical testing and point-of-care uses.

However, one of the main challenges in the development of electrochemical sensor is to make it sensitive and accurate, and able to determine various targeted analytes with different properties in real samples. Thus, the modification of working electrode is highly required, allowing for improved specific surface area, electrochemical performance and enhanced sensor sensitivity as well as analytical performances of sensors. The nanomaterials, including metal oxide and graphene have been gained more attention for electrode modification of electrochemical sensors in clinical fields because of theirs physical, chemical and electronic properties. Metal oxide sol-gels, such as titanium oxide (TiO_2) sol provide biocompatible property in which they have been frequently proposed as prospective for immobilization of enzymes. Besides, the metal oxides nanoparticles (*e.g.* copper oxide (CuO)) have a catalytic ability towards non-enzymatic electro-oxidation of

analytes, which is one of the attractive properties for the fabrication of enzyme-fee systems. In addition, graphene is one of the favorable materials used to modify the working electrode surface due to its excellent electrical conductivity and high surface area which can increase the electronic signal of analyte detection and improve electrochemical performance of the sensor.

In general, the electrochemical sensor can be categorized in various different ways, for instant, according to the sort of analytes or the sort of uses. Herein, we will focus on the development of electrochemical sensors both enzymatic and non-enzymatic systems for clinical diagnosis applications.

1.1.1   Enzymatic-based electrochemical sensors

To date, the electrochemical sensors have been increasingly developed for enzymatic detection of lactate level in patient's blood to diagnose some pathological conditions or sepsis shock status [1, 2]. Lactate is a key metabolite of anaerobic metabolic pathway and it significantly increases in the human body when the energy demand or liver and kidney functional failure. When these conditions are combined with the vital organ dysfunctions, the patient will develop severe sepsis [3, 4]. Thus, lactate level in patient's blood can act as an alarm signal for severity of illness and may also be used to develop the diagnosis and treatment for various diseases. Lactate can be interacted with lactate oxidase (LOx) and generate to H_2O_2 for monitoring of electrochemical signal. Hence, the development of lactate sensor by using an electrochemical technique has received more interest owing to its high sensitivity and more cost effective than the conventional techniques.

The fabrication of enzymatic based electrochemical biosensor is very challenge to make the immobilized enzymes remain functional over time since the enzyme structure is readily denatured and the life time of biosensors is limited by the loss of enzymatic activity. For biosensor design, the enlarge electrode surface area is capable to enhance interaction between bioreceptors and target analytes for sensor sensitivity improvement. The metallic foams, including nickel foam (Ni foam) has a porous structure, which can provide a high specific surface area, high porosity and a greater amount of enzyme entrapment. Thus, it could be an ideal electrode

platform material for the enzyme immobilization using as an electrochemical biosensor. To improve stability of the enzymatic biosensor, metal oxide sol-gel (*e.g.* titanium oxide sol: TiO_2-sol) is one of the interesting materials, which has been used to immobilize various enzymes and retain enzymatic activity on the modified electrode surface in electrochemical sensor. Although TiO_2-sol assistances to increase the stability of biosensor, the surface modification is still highly required to enhance the electrochemical sensitivity as well as analytical performance of the sensor. Graphene has been one of the favorable materials used to modify the working electrode surface due to its high electrical conductivity, high surface area, and biocompatibility. Hence, the composite between TiO_2-sol and G has become a promising material for electrode surface modification in an electrochemical sensor.

The first part aims to focus on developing the enzymatic biosensor based on TiO_2-sol/G nanocomposite modified Ni foam electrode to provide a novel device for lactate detection. Furthermore, this proposed system will be applied for the determination of lactate in biological samples.

1.1.2 Non-enzymatic electrochemical sensors

Although the enzymatic electrochemical sensors provide high selectivity but it suffer from some limitations such as poor storage stability, enzyme inactivation, high-cost, and complicated operation. These limitations stimulate the development of non-enzymatic electrochemical sensor with simple modification procedure, low cost, and good stability. Non-enzymatic electrochemical sensors have been widely used for determining the presence of biological marker, such as creatinine.

Creatinine is one of the most important biomarkers for diagnosis of kidney function and monitoring severity of kidney disease; its level generally maintains a range of 40-150 μM in blood serum, but can exceed 1000 μM in certain medical conditions [5]. Recently, there have been report that transition metal ions can chelate with creatinine to form a soluble creatinine-metal complex owing to several donor groups in the main tautomeric form of creatinine, such as Ag(1), Zn(II), Cd(II), Hg(II), Co(II), Cu(II) and Fe(III) [6]. The utilization of this property is used for the quantitative determination of creatinine. Among all, copper (II) oxide (CuO) is an

alternative material to improve the sensitivity of electrochemical sensor of creatinine owing to its large specific surface area, low-cost, non-toxicity, and electro-catalytic activity. The chelating ability of CuO with creatinine has been investigated via the formation of a soluble cupric-creatinine complex on the copper electrode and the oxidative current of creatinine has also been generated using amperometry [7]. Hence, CuO is a promising material to apply in electrode modification for creatinine detection via a soluble cupric-creatinine complex. To improve the electron transfer rate and catalytic activity of the modified electrode for creatinine, an ionic liquids (ILs) are applied as a modifier to enhance electrode performance in electrochemical measurement. They offers electro-catalytic ability, high ionic conductivity, wide electrochemical windows, and good biocompatibility; leading to fast signal responses, excellent electrochemical behavior, and remarkably increased electron-transfer rate of the sensor.

Another approach to improve the sensitivity of the electrochemical system is through the use of carbon-based material. Graphene is a highly desirable carbon-based material to use as a promising catalyst support in electrochemical sensing due to its unique structure and electrical properties which improve the conductivity of the modified electrode. Graphene-films modified on electrodes are usually prepared by drop-casting a graphene suspension obtained from chemical reduction of graphene oxide (GO) solution. The chemical process often employs hazardous chemicals (e.g. hydrazine or $NaBH_4$) as reducing agents or uses a high temperature treatment and the as-prepared graphene tends to form irreversible agglomerates via strong π-π stacking and Van der Waals interactions, which affects the reproducibility of sensors. A green method of preparing graphene by electrochemical reduction of GO under the mild condition is preferred [8]. This method can be more desirable than other graphene preparation techniques because of its simple instrumental setup, ease of fabrication, and lack of toxic reagents. The electrochemically reduced graphene oxide (ERGO) also offers a formation of stable film on the electrode surface without the further treatment.

To obtain a selective, rapid, disposable and low-cost device for creatinine detection, the CuO/IL/ERGO has been modified onto SPCE coupled with a paper

based analytical device (PAD). However, the precise dispensing of CuO/IL composite to the working electrode is a key requirement for the success of this approach. The current electrode modification is limited to techniques such as, simple drop-casting [9], electropolymerization [10], electrospining [11], electrospraying [12], or spin-coating [13], all of these have significantly low precision or accuracy in solution dispensing and volume control. Thermal inkjet based solution dispensing has been used for deposition of assay for microfluidic system. This technique generated accurate, reproducible, and high-throughput results for the application of dispensing compound in well plate platforms [14]. The HP D300 dispenser is able to precisely deposit droplets of material in the picoliter to microliter range, which can prepare an ultra-thin film on the surface substrate. In this work, we report the first use of HP dispenser in modification of the nanomaterial on PADs to detect creatinine.

In the second part, we developed a novel electrochemical sensor using a disposable paper-based device coupled with an inkjet dispensing technique for non-enzymatic sensing of creatinine. This system was fabricated by using a HP D300 dispenser to deliver the CuO/IL composite onto ERGO modified SPCEs coupled with PADs. The modified electrode has been thoroughly characterized and tested with the physiological inferences. The performance of this device was optimized and then applied to the determination of creatinine concentration in a complex biological fluid (*e.g.*, human serum).

1.2   Objectives

- To develop an enzyme-based biosensor using titanium sol-graphene nanocomposite modified nickel foam electrode surface

- To develop a non-enzymatic sensor using copper oxide-ionic liquid composite and reduced graphene oxide modified electrode on a paper-based analytical device

- To apply the proposed sensors for the detection of target analytes in biological fluid samples

1.3 Scope of research

This study is focusing on the development of novel electrochemical sensors based on metal oxides and graphene modified electrodes, then apply as devices for sensitive and low-cost point-of-care measurement of the required level of biomarkers in biological samples.

CHAPTER II

THEORY AND LITERATURE REVIEW

Biomedical markers are biomolecules which can be used as an indicator for evaluating organs dysfunction and health status of patients in a clinical field. Traditional instruments in hospital laboratory have some disadvantages such as expensiveness. Therefore, qualitative determination of biomarkers level in body fluids is very crucial.

2.1 Biosensors

There are many definitions of the term biosensor in the literatures [15-17], it is mostly defined as "an analytical device which combines a sensitive biological element with a properly physical transducer to convert a biological response into a measurable signal proportional in strength to the concentration of chemical species in biological samples". Biosensors can be broadly classified in function of bio-receptors and/or the principles of signal transduction used for the detection. Fig 2.1. Shows the general scheme of a biosensor, the bio-receptors specifically bind to the target analytes onto an interface where a specific biological element is immobilized, then the biological response is generated and picked up by the transducer. The transducer converts the biological signal to an electronic signal which is amplified by a detector circuit using the suitable reference and sent for processing by a computer software to be converted to a meaningful physical factors describing the process being investigated; finally, the resulting data is presented through a display to the human operator. According to the high specificity and selectivity of biosensors, the first biosensor is developed in 1962 for glucose determination by Clack and Lyons [18]. Since then, biosensor technology has arisen as an interesting alternative to traditional methods that can be applied for several applications in a wide range of fields such as medical diagnostics, environmental monitoring, food safety, and point of care testing. This technology has undergone important growth in recent years and it has been facing challenges, for example reducing the required sample volume for analysis, improving sensor sensitivity and selectivity in order to determine extremely low concentrations of analyte in real samples, also developing miniaturized,

noninvasive, and integrated devices [19]. However, the use of an electrochemical technique incorporated with biosensors can overcome these challenges because this technique provides a portable-filed based size used for a small volume sample, quantitative and qualitative analysis, and high sensitivity of the electrochemical transducer. Thus, the electrochemical technique has been received more attention in the development of biosensors.
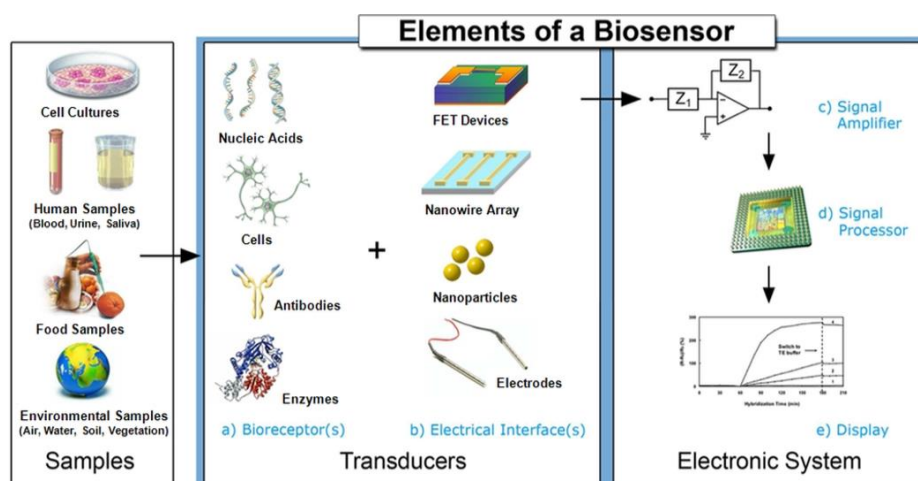
Fig. 1 Schematic of a typical biosensor [20]

2.2 Electrochemical biosensors

Electrochemical sensing technique is widely employed in many proposed and commercialized devices because it provides high sensitivity of transducer, both qualitative and quantitative analysis, and cost effectiveness [21]. The basic principle of electrochemical biosensor is based on an oxidation or reduction process of the immobilized biomolecule and target analyte producing or consuming electrons, which affects a measurable electrical signal presented in current or potential values [21, 22]. The produced electrochemical signals are quantitatively related to concentrations of analyte presented in real sample. The electrochemical system usually consists of a reference electrode (RE), a counter or auxiliary electrode (CE) and a working electrode (WE). The RE is commonly made from Ag/AgCl and kept at a distance from the reaction site to maintain a stable potential, while the CE provides

a connection to an electronic solution leading to input potential applied into the WE in order to complete the circuit and allow charge to flow [23].
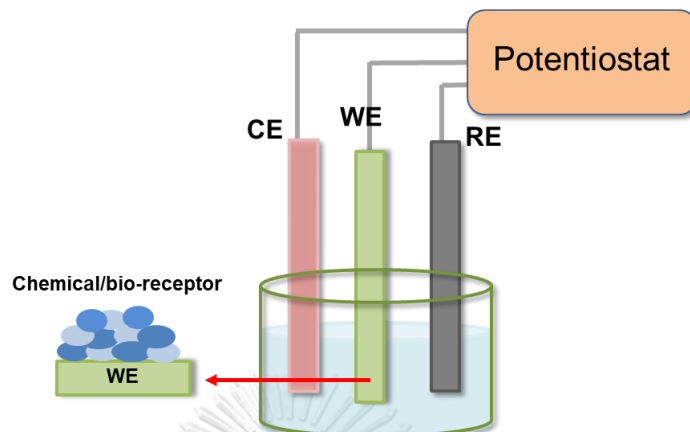
Fig. 2.2 Schematic diagram of the electrochemical cell

Cyclic voltammetry and amperometry are among the electrochemical detection techniques that often integrated with biosensing applications, their fundamental principles are summarized below,

2.2.1 Cyclic voltammetry (CV)

CV is an electrochemical technique which measures the currents that established in an electrochemical cell to obtain a general information of the behavior of an electrochemical system, it is typically used to study a thermodynamic of redox process, including the kinetic of electron transfer and couple chemical reactions or adsorption process [24]. In addition, this technique is commonly used for characterization of a new electrode [25], it could be used to initially characterize the electrode to observe the electrochemical behaviors in a wide scanning window and the interference of other reactions in this system [26]. The potential is applied to the working electrode with the triangular potential waveform and the resulting applied potential produces an excitation signal (Fig. 2.3a). The electrochemical result is obtained as a cyclic voltammogram by measuring the current at the working electrode during the potential scans, as shown in Fig. 2.3b, the CV results from a single electron in reduction and oxidation [27].
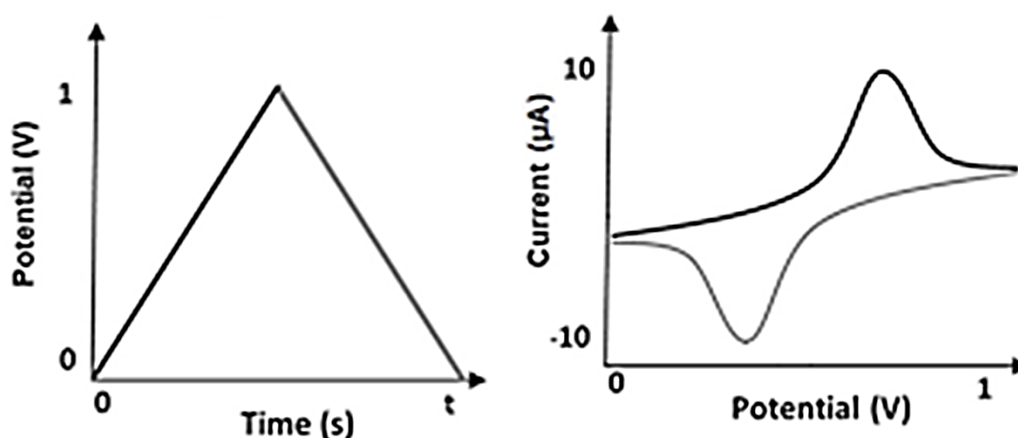
Fig. 2.3 A triangular potential waveform (a) and cyclic voltammogram of a reversible redox process (b) [28]

2.2.2 Amperometry

Amperometry is a method of electrochemical analysis measuring of the resulting current after a constant potential is applied to the working electrode and the measurable current is linearly dependent upon the concentration of analyte. This technique is highly quantitative and it provides excellent detection limits, good linear range, and reproducibility [29]. Selectivity is achieved by a sensible way of the detection potential, in which the optimal detection potential is normally determined by using hydrodynamic voltammetry [30]. The amperometric sensing is often used in the biosensor applications for various research fields. For example, the enzyme-based sensors for glucose detection, in which the enzyme glucose oxidase catalyzes the oxidation reaction of glucose to gluconic acid, where two electrons are produced per a glucose molecule. These electrons reduce the working electrode [31]. This technique is also employed in non-enzymatic based sensor for the determination of metal ion presented in the aqueous solution [32].

In this dissertation, we focused on the development of electrochemical biosensors in enzymatic and non-enzymatic systems for medical testing applications, the basic theory of each of these system are presented below.

2.3 Enzymatic-based electrochemical biosensor

An enzyme-based biosensor has achieved a great technological relevance in the last decades because it provides selective interaction with their target substrates, which have high catalytic activity for the detection. At the same time, the enzyme-coupled electrochemical technique converts a biological response into readable and quantified signals by an electro-active species (e.g. H2O2) from the enzymatic oxidation reaction, which either consumes oxygen (e.g. all oxidase) or produces hydrogen peroxide to generate electron (e-) according to Equation (1) and (2).

$$\text{Substrate} + O_2 \xrightarrow{\text{Enzyme}} \text{Product} + H_2O_2 \qquad (1)$$

$$H_2O_2 \longrightarrow O_2 + 2H^+ + 2e^- \qquad (2)$$
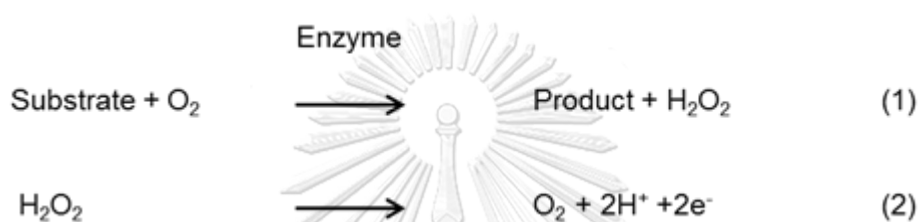
This electronic signal correlates to the concentration of analyte in the samples (*e.g. body fluids, cell cultures, and food samples*). A change in electrode potential can also be used as a measurable current in potentiometric sensors. Eventually, a signal processor connects to transducer collects, amplifiers, then displays as the output signal [33], as shown in Figure 2.4.
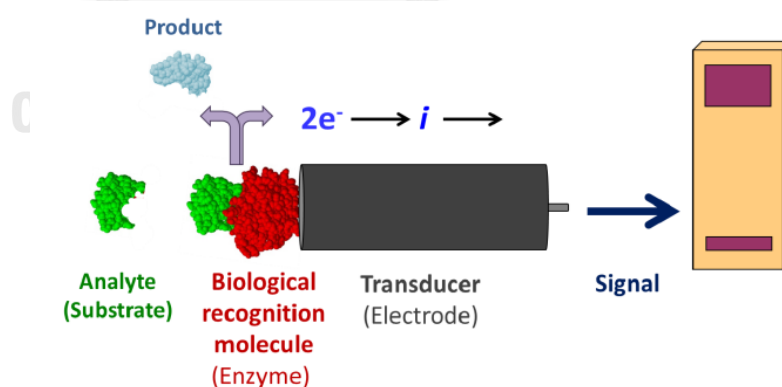
Fig. 2.4 A typical enzymatic-based electrochemical biosensor [34]

In the electrochemical detection, the WE represents the most important component in this system because it is an interface architecture where a specific bio-receptor take place and generate a signal. Thus, the WE should possess high specific

surface area, electrical conductivity, and stability allowing for increased interaction between immobilized biomolecule and analyte, enhanced sensitivity, and improved long term usage of sensors. To develop the suitable electrode, the materials used for the electrode modification is very important for enhancing the electrochemical performances of sensor.

2.3.1 Nanomaterials for electrode modification in the enzymatic biosensor

For the design of enzymatic electrodes, the primary concern for selection of an electrode material is usually based upon the electrical conductivity and material hardness [35]. Moreover, the architecture and surface area of support material are essential for the electrode modification and enzyme immobilization. Since a high surface volume to ratio and a large surface area of electrode is capable to allow the entrapment of great amount of enzyme leading to the promotion of mass transportation and enhancement of interaction between enzymes and target anaytes. Also, the sensor can express the high-performance sensing system and reduce relatively response times for the detection of biomarkers in the real samples.

2.3.2 Nickel foam (Ni foam)

Ni foam is a porous material, which have attracted much attention in the scientific applications owing to its high electrical conductivity, high mass transfer ability, and its three-dimensional (3D) cross-linked grid structure, which can provide a high specific surface area and high porosity. The open-pore architecture of Ni foam offers distinctive physical and chemical characteristics in interacting with atoms, ions, and molecules on its surface and along its porous networks [36]. Additionally, Ni foam has shown the great advantages over nanoparticles-modified electrodes in term of commercial availability and easy-to-scale up production because of its high sensitivity, excellent mechanical strength, and low toxicity [37]. Thus, it is considerable to be the ideal platform material to immobilize enzymes or other biomolecules for using as electrochemical sensors [38].

To date, the electrochemical sensor based on a modified nickel foam electrode has been rarely reported. To the best of our knowledge, Lu *et al*. [39] recently reported the first use of commercially available 3D porous Ni foam as a novel electrochemical sensing support for glucose detection. The demonstrated linear range and limit of detection (LOD) for glucose were 0.05-7.35 nM and 2.2 µM, respectively. The application of this glucose sensor was successfully performed in human blood serum.

Akhtar *et al*. [40] developed the sensing system based on a 3D open pore Ni foam electrode functionalized with hemoglobin (Hb) for detection of H_2O_2. The finding of this research reported that Hb could maintain its biological activity and effective electronic connections for 15 days after immobilization. In 2015, Akhtar *et al*. studied the development of a simple H_2O_2 sensor based on 3D porous Ni form electrode functionalized with cytochrome c (Cyt c) as an electron transfer-mediating layer between active center of Ni foam and H_2O_2 (Fig. 2.5). The steps of the proposed sensor fabrication are shown in Figure 3. The linear response with a detection limit was 2×10^{-7} M and sensitivity was 1.95 µAmM^{-1}. The resulting electrode showed long-term stability at 4 °C in a sealed system for 21 days and the sensing response efficiency was 97%.
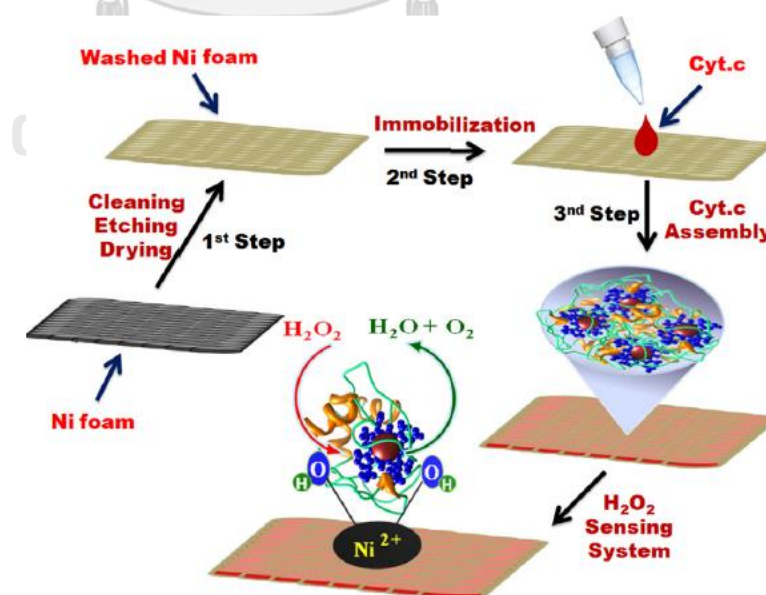
Fig. 2.5 The immobilization of Cyt c on the Ni foam electrode surface [41]

2.3.3 Titanium dioxide (TiO$_2$ sol)

For creation of a robust enzymatic biosensor, the immobilized enzymes must be stable enough to retain the long-life bioactivity of the enzyme for proper operational stability of sensor. Metal oxide (e.g. TiO$_2$, ZrO$_2$, ZnO$_2$) synthesized by sol-gel process or colloidal suspension has attracted great interest as a promising interface for enzyme immobilization and biosensor development. Although until now there are many types of metal oxide material, which have also been used for this purpose [42]. TiO$_2$-sol is an alternative material to utilize for improving the stability of sensor owing to the superior properties, such as excellent biocompatibility, environmentally friendly, and frequently proposed as prospective interface for the immobilizing enzyme. Moreover, titanium is able to form coordination bonds with amine and carboxyl groups of enzyme and maintain the enzyme-catalytic activity [42].

Yu *et al.* [43] reported the TiO$_2$ sol-gel applications for the entrapment of Hb and mimetic peroxidase to construct a novel biosensor for H$_2$O$_2$. The sol-gel matrix offers a biocompatible microenvironment for maintaining the native structure and activity of the entrapped Hb, also very low mass transport barrier to the substrates. This sol-gel is very efficient for preventing leakage of the Hb out of the electrode, resulting in a long-term stability for 80 days with the currents response at 89%. The linear range for H$_2$O$_2$ determination was 5 x10^{-7} to 5.4 x 10^{-5} M with a detection limit of 1.2 x 10^{-7} M.

Xu *et al.* [44] developed a novel H$_2$O$_2$ biosensor based on immobilization horseradish peroxidase (HRP) in TiO$_2$ sol-gel matrix on an electropolymerized phenazine methosulfate (PMS) modified a glassy carbon electrode. TiO$_2$ sol-gel was a promising substrate for immobilizing enzyme because it has high surface area for enzyme loading and good compatibility conducing to retain biological activity of enzyme to a large extent. The sensor stability was 80% of its original activity after two months of operation.

Kochana et al. [45] proposed the electrode modification based on incorporation of Meldola's Blue (redox mediator) with multi-walled carbon nanotubes and Nafion into a TiO$_2$ sol-gel modified graphite electrode. This composite

was used to immobilize alcohol dehydrogenase (ADH) for determination of ethanol. Operational stability was shown with currents values at 97% after one week storage at 4 °C. This biosensor showed linear range from 0.05 to 1.1 mmol/L and limit of detection of 25 µmol/L.

Tasviri *et al.* [46] investigated the synthesis of amine functionalized TiO_2-coat multiwalled carbon nanotubes (CNTs) using sol-gel route. They have reported that the nanocomposite was used to immobilize glucose oxidase (GOx) to detect glucose. The TiO_2 sol-gel can prevent catalytic activity of the enzyme, which indicated by the peak currents remained at 97% after two months of storage.

2.3.4 Graphene

A carbon based nanomaterial is one of the most common used as an ideal matrix to develop sensitivity of electrode for biosensor because of its advance physical and electrochemical possession, such as wide anodic potential range, chemical inertness and low residue current. In addition, carbon based matrixes can enhance fast response time of biosensor and they can be fabricated in different configurations. These features make them suitable for using in electrode modification. G is introduced as an emerging carbon based nanomaterial, which has received much popularity due to its unique electrical, thermal, mechanical, optical and electrochemical properties. G-based electrodes have exhibited greater performance than other carbon based electrodes in term of electro-catalytic activity and electric conductivity. Remarkably, with its useful advantages, G has been used as a substance to combine various kinds of functional materials to prepare as a nanocomposite material for electrode modification [47]. Therefore, TiO_2-sol/G nanocomposites have attracted a great deal of interest and stimulated increasing in the biosensor application.

Jang *et al.* [48] developed a novel glucose biosensor based on the adsorption of glucose oxidase modified TiO_2 colloidal-G nanocomposite electrode. The TiO_2-G composite showed better catalytic performance for glucose redox than a G or a TiO_2 electrocatalyst. The electrochemical response of the glucose biosensor was linear against concentration of glucose ranging from 0 to 8 mM.

Recently, Casero *et al.* [49] examined bionanocomposite composed of TiO_2 colloidal, G, and lactate oxidase modified glassy carbon electrode for lactate determination. Compared to a sensor without TiO_2-colloidal, the sensor exhibited higher sensitivity (6.0 μM mM^{-1}), a better detection limit (0.6 μM), and a wider linear response (2.0 μM to 0.4 mM).

According to these literature reviews, the development of a new and simple device to detect a target analyte with a selective reaction using TiO_2-sol/G composite for electrode modification is required. Coupling the use of TiO_2-sol and G is very attractive to improve the biosensor performances, which will provide a long life stability of enzyme while increasing electrochemical conductivity of the sensor.

2.3.5 Lactate detection

Lactate detection plays an important role in healthcare and medical diagnosis because lactate is a key metabolite of anaerobic metabolic pathway and it significantly increases in the human body when the energy demands or liver and kidney functional failure [50]. When this condition is combined with the vital organ dysfunctions, the patient will develop severe sepsis [3, 4]. A normal blood lactate level is in range from 0.5-1 mmol/L and the level > 4 mmol/L is defined as acidosis acid [51], but it can rise up to 25 mmol/L during the intense exertion [52]. Thus, lactate level in patient's blood can act as an alarm signal for severity of illness and may also be used to develop the diagnosis and treatment for various diseases. However, traditional techniques commonly used for lactate detection, such as high performance liquid chromatography (HPLC) [53], colorimetric test [54], chemiluminescence [55], and magnetic resonance spectroscopy [56] still have some limitations including complicated operation and expensive equipment. Hence, development of lactate sensor by using an electrochemical technique has received more interest owing to its high sensitivity and more cost effective than conventional techniques [57].

2.4 Non-enzymatic electrochemical sensor

Although the enzymatic sensors possess high selectivity but suffer from limitations such as instability, complicated modification procedures, and critical micro-environmental factors. Such limitations stimulate the development of non-enzymatic electrochemical sensors with simple fabrication and good stability. Enzyme-free electrochemical sensors have been widely used for determining compounds in diverse field of applications, such as biomedical analysis [58], food control quality [59], and environmental safety [60].

Kim *et al.* [61] developed a sensor by using NiO and Ni(OH)$_2$ modified glassy carbon electrodes for non-enzymatic detection of lactate. The analytical results revealed that the sensor had high selectivity and sensitivity, as well as low detection limit of 0.53 mM.

Shen *et al.* [62] fabricated a novel electrode by using a gold foam for non-enzymatic sensing of glucose. Amperometric response of the modified electrode indicated excellent catalytic activity in glucose oxidation, with a linear response in the range from 0.5 µM to 12 mM, and a limit of detection of 0.14 µM.

In particular, the determination of biomarkers which involve the multiple enzymes used in the specific reactions leading to complicated processes for sensor fabrication. Thus, the non-enzymatic system is attractive alternatives to develop the electrochemical-based sensor for determination of biological compounds in real samples.

2.4.1 Creatinine detection

Creatinine is one of the most important biomarkers for diagnosis of kidney function and monitoring severity of kidney disease; its level generally maintains a range of 40-150 µM in blood serum, but can exceed 1000 µM in certain medical conditions [5]. Conventional clinical methods for creatinine detection involve either spectrophotometry by Jaffe reaction [63] or an enzymatic method (usually electrochemical sensing) using multi-enzymes [64]. These methods have many disadvantages. Spectrophotometry has been commonly used in clinical laboratories for creatinine determination based on colorimetric detection of Jaffe reaction via the

complex of creatinine and picrate [65]. Although this methods is simple, it non-specific and non-selective because molecules in human biological fluids, such as ascorbic acid, uric acid, urea, glucose, and others interfere with this technique [66]. To enhance the specificity of the system, an enzymatic electrochemical method has been established using three enzymes, consisting of creatininase, creatinase, and sarcosine oxidase [67]. The assay is constructed by immobilization of the enzymes on the electrode surface and the enzymatic detection of creatinine is achieved using CV or amperometry to monitoring an electro-active product (*i.e.,* hydrogen peroxide) generated from the enzymatic reaction [68, 69].

Yadav *et al*. [70] developed a creatinine biosensor by immobilization of multi enzymes, including creatininase, creatinase, and sarcosine oxidase on iron oxide nanoparticles/chitosan-g-polyaniline modified Pt electrode. The sensor showed a linear range from 1.0 to 800.0 μM with sensitivity of 3.9 μA μM $^{-1}$ cm $^{-2}$, and limit of detection of 1.0 μM for the creatinine detection.

Serafin *et al.* [71] studied the electrochemical biosensor for creatinine based on the immobilization of creatininase, creatinase and sarcosine oxidase onto a ferrocene/horseradish peroxidase/gold nanoparticles/multi-walled carbon nanotubes/Teflon composite electrode. This sensor was constructed with many steps and complicated processes, showing the analytical results with a linear range from 0.003–1.0 mM and limit of detection of 0.1 μM for the creatinine detection in human serum.

Nonetheless, the enzymatic system suffers from poor storage stability, ease of enzyme inactivation, high-cost, and complex operation [72]. Therefore, the development of simple, low-cost, selective, and rapid measurement of creatinine is highly desired in clinical applications.

2.4.2 Disposal paper-based analytical devices (PADs)

Development of a device for sensitive, reliable and low-cost point-of-care measurement of disease biomarkers for early stage screening and healthcare evaluation is a significant challenge. At present, cellulose filter paper has received great attention and is widely applied for microfluidic sensor construction because of

its high porosity, large surface area, and hydrophilic properties [73]. The material provides several advantages compared to traditional substrates (*i.e.,* glass, ceramic, and polymer), such as inexpressiveness, disposability, and biodegradability [74]. Also, paper-based analysis requires only small sample volume and reagents which make it suitable for point of care application [75]. The paper-based analytical device (PAD) has been integrated with an electrochemical technique to develop easy-to-use, rapid, and highly sensitive analytical platform. Moreover, it can simultaneously produce qualitative and quantitative results making it is an ideal device for bimolecular detection in biological fluids. [76, 77].

2.4.3 Nanomaterials for the electrode modification in the non-enzymatic detection

2.4.3.1 Copper oxide (CuO)

Recently, transition metals and metal oxides has received increasing attention as modifier due to the ability to promote electron transfer reactions at low potential, outstanding electrocatalytic activity, good stability and low cost [78, 79]. The transition metal ions can chelate with creatinine to form a soluble creatinine-metal complex owing to several donor groups in the main tautomeric form of creatinine [80]. The utilization of this property is proposed for the quantitative determination of creatinine.

Raveendran *et al.* [81] developed a disposable non-enzymatic sensor utilizing the formation of copper creatinine complex via electrodepositing copper on screen printed carbon electrodes (SPCE), as shown in Fig. 2.7. This sensor has been presented with a stable response and low detection limit of 0.0746 µM and a linear rang of 6 to 378 µM for creatinine.
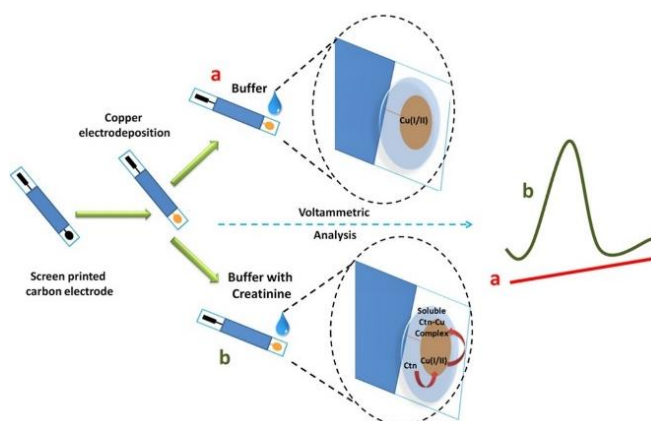
Fig. 2.6 Schematic diagram of the fabrication and analytical measurement of a non-enzyamtic sensor based on electrodepositing copper on SPCE [81]

Chen *et al.* [7] investigated a chelating property of copper metal and copper oxide with creatinine via the formation of a soluble cupric-creatinine complex on the copper electrode. The oxidative current of creatinine has also been generated using amperometry showing a low detection limit of 6.8 µg/dL in a linear range from 25 mg/dL to 1.5 µg/dL.

CuO is a p-type transition metal oxide with a narrow band gap that has been effectively used in fabrication of electrical devices due to its large specific surface area, low-cost, non- toxicity, and electro-catalytic activity [82]. Pint *et al.* [83] fabricated a simple and highly reproducible electrode based on CuO, graphite particles, and ionic liquid for the non-enzymatic determination of hydrogen peroxide. The high catalytic activity of the CuO resulted in the modified electrode with attractive properties in analytical performance, showing a wide linear range of 1.0 µM to 2.5 mM and detection limit of 0.5 µM for the determination of hydrogen peroxide in real samples. Nia *et al.* [84] reported the application of CuO with polypyrrol nanofiber and reduced graphene oxide for the non-enzymatic detection of glucose. The sensor exhibited a linear range of 0.1-100 mM with a low detection limit of 0.03 µM. Hence, CuO is a promising material to apply in electrode modification for creatinine detection via a soluble cupric-creatinine complex.

2.4.3.2 Ionic liquid

To improve the electron transfer rate and catalytic activity of the modified electrode for creatinine, an ionic liquid (IL) is applied as a modifier to enhance electrode performances in electrochemical measurements [85]. ILs are either organic salts or a mixture of salts, which act as a charged transferring bridge [86]. It offers electro-catalytic ability, high ionic conductivity, wide electrochemical windows, and good biocompatibility, leading to fast signal responses, excellent electrochemical behavior, and remarkably increased electron-transfer rate of the sensor.

Naeim *et al*. [87] prepared a non-enzymatic glucose sensor based on IL dispersed bimetallic Ni/Pd nanoparticles on reduced graphene oxide modified glassy carbon electrodes. The electrochemical measurements revealed that the modified electrode directly catalyzed glucose oxidase and displayed current responses with a linear range from 0.2 μM to 10 mM and detection limit of 0.03 μM.

Li *et al.* [88] described a non-enzymatic electrochemical sensor for uric acid. It is based on a carbon nanotube/IL paste electrode modified with poly(β-cyclodextrin) via electro-polymerization. The electrochemical measurements of uric acid was examined by CV and linear sweep voltammetry. The current response of uric acid is linear in the 0.6 to 400 μM and in the 0.4 to 1.0 mM concentration ranges, and the detection limit is 0.3 μM.

2.4.3.3 Reduced graphene oxide (RGO)

Another approach to improve the sensitivity of the electrochemical system is through the use of carbon-based materials [89]. Graphene is a highly desirable carbon-based material to use in electrochemical sensing due to its unique structure and electrical properties which improve the conductivity of the modified electrode [89]. Graphene-films modified on electrodes are usually prepared by drop-casting a graphene suspension obtained from chemical reduction of graphene oxide (GO) solution [90]. The chemical process often employs hazardous chemicals (*e.g.* hydrazine or $NaBH_4$) as reducing agents or uses a high temperature treatment [91]. The chemicals may also leave some residual epoxide groups on the reduced GO sheet leading to loss in electron mobility [92]. The as-prepared graphene tends to

form irreversible agglomerates via strong **π-π** stacking and Van der Waals interactions, which affects the reproducibility of sensors [93]. A green method of preparing graphene by electrochemical reduction of GO under mild condition is preferred [94].

Mutyala *et al.* [95] proposed a green procedure for high quality graphene synthesis using the electrochemical reduction of graphene oxide. The electrochemically reduced graphene oxide (ERGO) was employed to develop a non-enzymatic hydrogen peroxide sensor, which exhibited high sensitivity, selectivity, and finite limit of detection for H_2O_2 sensing at low potential.

Jian *et al.* [96] developed a high performance sensor based on gold nanoparticles (AuNPs) deposited ERGO modified SPCE for nitrite detection. The superior electrocatalysis of ERGO/AuNPs composite for sensing nitrite was attributed to synergistic effects of ERGO sheets and AuNPs. The sensor presented excellent properties for the detection of nitrite, including a low oxidation potential at 0.65 V, wide linear range from 1 to 6000 μM, high sensitivity of 0.3048 μA $μM^{-1}$ cm^{-2}, low detection limit of 0.13 μM (S/N = 3), and great selectivity.

This method can be more desirable than other graphene preparation techniques because of its simple instrumental setup, ease of fabrication, and lack of toxic reagents. The ERGO also offers a formation of stable film on the electrode surface without any further treatment [8].

2.4.4 Thermal ink-jet technique

To obtain a selective, rapid, disposable and low-cost device for creatinine detection, the CuO/IL/ERGO has been modified onto SPCE coupled with a PAD in this work. However, the precise dispensing of CuO/IL composite to the working electrode is a key requirement for the success of this approach. The current electrode modification is limited to techniques such as simple drop-casting [9], electropolymerization , electrospining [10, 11], electrospraying [12], or spin-coating [13], all of these have significantly low precision or accuracy in solution dispensing and volume control. Thermal inkjet based solution dispensing has been used for deposition of assay for microfluidic systems [97, 98]. This technique generated

accurate, reproducible, and high-throughput results for application of dispensing compound in well plate platforms [99]. The HP D300 dispenser (Fig. 2.7) is able to precisely deposit droplets of material in the picoliter to microliter range, which can prepare an ultra-thin film onto the surface substrate [14, 99]; however, it has been limited to aqueous or organic assays in liquid form. Thus, the HP-300 was utilized in the modification of the nanomaterials on PADs to detect creatinine for the first time.
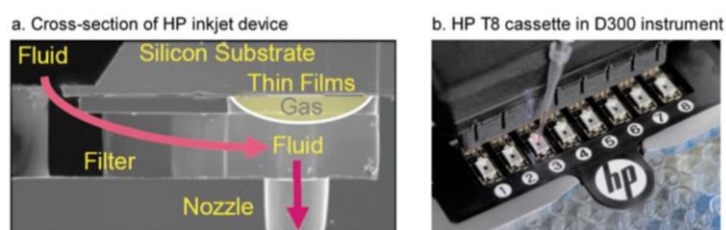
Fig. 2.7 (a) Cross-sectional micrograph of fluidic architecture depicting gas drive bubble formation. (b) HP dispense head array with one of eight dispense heads being filled with a compound dropped on the HP D300 digital dispenser [99].

CHAPTER III

METHODOLOGY

3.1   Chemical and reagent

Part I: Development of the enzymatic biosensor

3.1.1 Open-cell Ni foam samples (size 0.2 cm × 1 cm × 2 cm; density 0.075 g/cm^3) (Surface Coatings Technology for Metals and Materials Research Unit, (Bangkok, Thailand))

3.1.2 Hydrogen peroxide (H_2O_2), (30%, v/v) (Sigma Chemical Co. (St. Louis, MO, USA))

3.1.3 Hydrochloric acid (HCl) (Sigma Chemical Co. (St. Louis, MO, USA))

3.1.4 Titanium diisopropoxide bis-(acetylacetonate) or TIAA (75% wt in isopropanol) (Sigma Chemical Co. (St. Louis, MO, USA))

3.1.5 Lactate oxidase (LOx) (EC 1.1.3.2 from *Aerococus viridans*) lyophyilized powder containing 31 Unit mg^{-1} (Sigma Chemical Co. (St. Louis, MO, USA))

3.1.6 Isopropanol (Univar Chemical Co (Illinois, USA))

3.1.7 Ethanol (Merck (Darmstadi, Germany))

3.1.8 1, 3-propanediol (98% wt) (ACROS organics (Morris plains, NJ, USA))

3.1.9 Conductive graphene dispersion (Graphene Supermarket (New York, USA)).

3.1.10 Potassium hydrogen phosphate (K_2HPO_4) (Carlo Erba Reagenti-SDS (Van de Reuil, France))

3.1.11 Sodium dihydrogenphosphate (NaH_2PO_4) (Carlo Erba Reagenti-SDS (Van de Reuil, France))

3.1.12 D-(+)-glucose anhydrous (Carlo Erba Reagenti-SDS (Van de Reuil, France))

3.1.13 Dopamine (DA) (Wako Pure Chemical Industries, Ltd. (Osaka, Japan))

3.1.14 Ascorbic acid (AA) (Wako Pure Chemical Industries, Ltd. (Osaka, Japan))

3.1.15 Sodium phosphate monobasic (NaH_2PO_4) (Sigma-Aldrich (St. Louis, MO, USA))

3.1.16 Dibasic potassium phosphate (K_2HPO_4) (Sigma-Aldrich (St. Louis, MO, USA))

3.1.17 Commercial rabbit serum (Thermo Fisher Scientific (Waltham, MA USA)).

Part II: Development of the non-enzymatic biosensor

3.1.18 Carbon ink (the Gwent group (Torfaen, UK))

3.1.19 Silver/silver chloride ink (the Gwent group (Torfaen, UK))

3.1.20 Aqueous graphene oxide (GO) (Graphene Supermarket (New York, USA)).

3.1.21 D-(+)-glucose (Mallinckrodt (Staines, UK))

3.1.22 Sodium dihydrogen phosphate monohydrate ($NaH_2PO_4 \cdot H_2O$) (Mallinckrodt (Staines, UK))

3.1.23 Trichloroacetic acid (TCA)) (Mallinckrodt (Staines, UK))

3.1.24 Disodium hydrogen phosphate heptahydrate ($Na_2HPO_4 \cdot 7H_2O$) (Mallinckrodt (Staines, UK))

3.1.25 Copper oxide (CuO) nanopowder (US Research Nanomaterials, Inc. (Texas, USA)). 3.1.26 Ascorbic acid (Macron Fine Chemicals^{TM} (Pennsylvania, USA))

3.1.27 1-Butyl-2, 3-dimethylimidazolium tetrafluoroborate (IL) (Sigma–Aldrich (Buchs, Switzerland))

3.1.28 Filter paper grade no.1 (58 cm × 60 cm) (Sigma–Aldrich (Buchs, Switzerland))

3.1.29 Uric acid (Sigma–Aldrich (Buchs, Switzerland))

3.1.30 Urea (Sigma–Aldrich (Buchs, Switzerland))

3.1.30 Potassium hexacyanoferrate(III) ($K_3[Fe(CN)_6]$) (Sigma–Aldrich (Buchs, Switzerland))

3.1.31 N, N-dimethylformamide (DMF) (Merck (Darmstadt, Germany))

3.1.32 Creatinine (Alfa Aesar (Massachusetts, USA))

3.1.33 Human serum (Excellence Center for Critical Care Nephrology, King Chulalongkorn Memorial Hospital (Bangkok, Thailand))

3.2 Equipment and instrument

3.2.1 Screen-printing block (Chaiyaboon Co., Ltd. (Bangkok, Thailand))

3.2.2 CHI1240B potentiostat/galvanostat (CH Instruments, Inc., USA)

3.2.3 HP D300 digital dispenser (HP Inc., Oregon, USA)

3.2.4 Fourier Transform Raman Spectroscopy (FT-Raman; Perkin Elmer, Spectrum GX)

3.2.5   Fourier transform infrared spectroscopy (FTIR) (PerkinElmer Spectrum One LabX, USA)

3.2.6   FEI Quanta 600F scanning electron microscope (SEM) (Oregon, USA)

3.2.7   JEM-6400 from scanning electron microscope (SEM) (Japan Electron Optics Laboratory, Japan)

3.2.8   Energy-dispersive X-ray (EDX) (PerkinElmer Spectrum One LabX, USA)

3.2.9   JEM 2100 transmission electron microscope (TEM) (Japan Electron Optics Laboratory, Japan)

3.2.10 X-ray photoelectron spectra (XPS) (Kratos Analytical Axis UltraDLD, USA)

Part I: Development of the enzymatic biosensor

3.3   Preparation of the modified Ni foam electrode for enzymatic biosensor
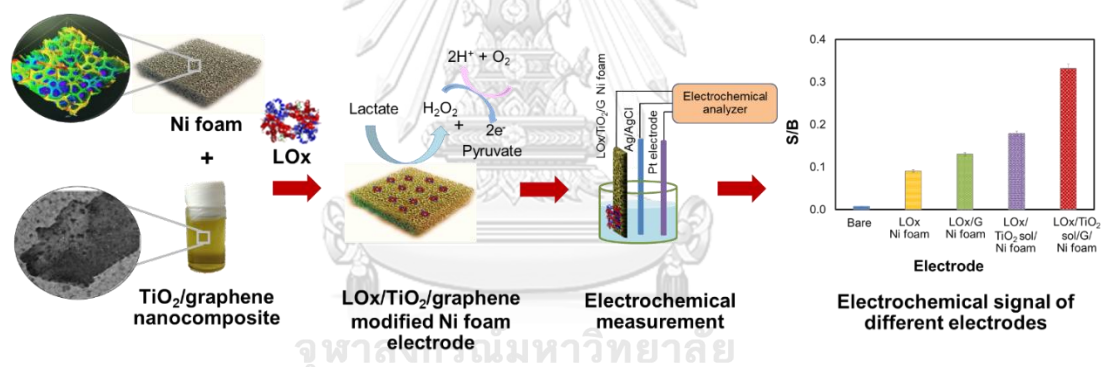
Fig. 3.1 Schematic representation of the preparation and analysis for the enzymatic lactate biosensor based on the LOx immobilized on TiO_2 sol/graphene modified Ni foam electrode for measurement of lactate.

3.3.1   Synthesis of TiO_2 sol/graphene nanocomposite

TiO_2 sol/graphene nanocomposite was synthesized by hydrolysis and condensation of titanium alkoxides and the method was slightly modified from our previous reports [100, 101]. For the synthesis process, 1.5 mg mL^{-1} (consisting of 23% wt) conductive graphene dispersion was added into a vigorously stirred mixture solution of 0.025 mole TIAA and 0.025 mole 1, 3-propanediol in a round bottom flask at a room temperature of 30 ±2 °C. The mixed solution was refluxed at 85 °C for 60

minutes with continuous stirring by a magnetic stirrer. Then, the obtained solution was TiO_2/graphene nanocomposite solution. Following a reflux process, the nanocomposite was distilled at 55 ° C until no liquid remained. The solution was left to cool down to a room temperature, and diluted with isopropanol. The as prepared nanocomposite was characterized by transmission scanning electron microscopy.

3.3.2   Modification of Ni foam electrode surface

An open-cell Ni foam was cut into small pieces of dimension 1 cm × 2 cm × 1 mm. they were cleaned using 0.05 M hydrochloric acid (HCl) in an ultrasonicator for 30 minutes, and were then thoroughly washed with ethanol and deionized water for 15 minutes each. The obtained nanocomposite was coated onto the Ni foam electrode surface by immersing in the nanocomposite solution (10× diluted in isopropanol) for 1 minute, then allowed to dry at room temperature and stored in a desiccator. After being air-dried, the modified Ni foam electrode was washed with PB, then a specific amount of enzyme was immobilized on the modified Ni foam electrode surface, which was kept overnight at 4 °C for immobilization process. The resulting electrode was washed 3 or 4 times by PB to remove any weakly bound materials and stored at 4 °C until it was used.

3.3.3   Characterization of the nanocomposites and modified electrode

The morphology of TiO_2 sol and TiO_2 sol/graphene nanocomposites was investigated by transmission scanning electron microscopy using JEM 2100 microscope (Japan Electron Optics Laboratory, Japan) at an acceleration voltage of 100 kV and a magnification of 6,000×. The characteristic peaks of the as-prepared TiO_2 sol/graphene were evaluated by fourier transform infrared spectroscopy (FTIR; PerkinElmer Spectrum One LabX, USA), fourier Transform Raman Spectroscopy (FT-Raman; Perkin Elmer, Spectrum GX), and X-ray photoelectron spectra (XPS; Kratos Analytical Axis UltraDLD, USA). The morphology of a Ni foam and a LOx/TiO_2 sol/graphene modified Ni foam electrode was investigated by scanning electron microscopy (SEM; model JEM-6400 from Japan Electron Optics Laboratory, Japan). The microscope was operated at an acceleration voltage of 15.0 kV at a working

distance of 6.8 mm with a 50× and 1,500× magnification. The chemical composition was analyzed by energy-dispersive X-ray (EDX) microanalysis incorporated in the SEM instrument. Grahpene, TiO_2 sol and TiO_2 sol/graphene nanocomposite samples for FT-IR measurements were prepared by allowing of 100 µL of the corresponding stock dispersion to air-dry on a metal plate substrate surface.

3.3.4 Electrochemical measurement

Cyclic voltammetric measurement was carried out in an electrochemical cell with 4 mL analyte so in a circular chamber of 2.0 cm diameter and 1.5 cm height. In all H_2O_2 detection experiments, the potential of the cell was scanned from 0.0 to +0.8 V at a scan rate of 50 mV s^{-1}. Amperometric measurements were performed by placing the Ni foam electrode on a filter paper (1 cm × 2 cm), which was put onto a working zone of screen-printed electrodes, whereby a screen-printed method of carbon ink and Ag/AgCl ink was prepared on polyvinyl chloride substrate [102]. Amperometry was conducted to optimize the detection potential using H_2O_2 in PB at a TiO_2/graphene modified Ni foam electrode at different potentials in a range from 0.0 to +1.0 V for a fixed duration. The H_2O_2 oxidation current (S) to the background current (B) was used to obtain signal-to-background (S/B) ratios [76]. Amperometric lactate detection at a LOx/TiO_2 sol/graphene modified Ni foam electrode was conducted at an optimized potential. Then, the anodic current was recorded at steady state for 180 s. All measurements were conducted at room temperature of 30 ±2 °C.

Part II: Development of the non-enzymatic biosensor

3.4 Preparation of the modified electrode for non-enzymatic biosensor
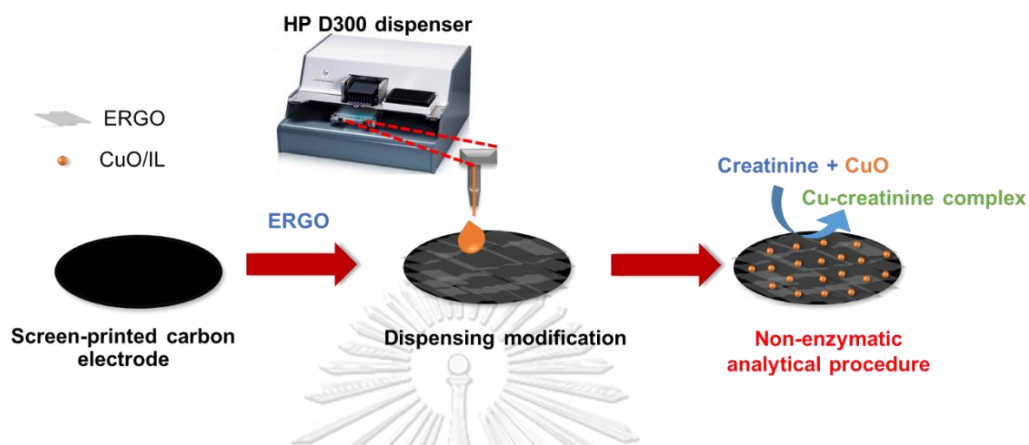
Fig. 3.2 Schematic representation of the preparation and analytical procedure for the non-enzymatic creatinine biosensor based on the CuO/IL composite dispensed electrochemically reduce graphene oxide modified SPCE on a PAD.

3.4.1 Fabrication of PAD

PADs were fabricated from Whatman no. 1 filter paper (Camlab, UK) using a wax printing method according to previous reports [76, 103]. To describe the method briefly, the patterned paper-based sensor was designed by a graphic program (Adobe Illustrator) and then printed onto filter paper using a wax printer (Xerox ColorQube 8570, Japan). Next, the as-prepared paper based sensor was heated on a hot plate at 175 °C for 40s to melt the wax. The area covered with wax was hydrophobic, and the area without wax was hydrophilic. To construct the three electrode system on the PADs, a working electrode (WE, area = 0.07 cm2) and a counter electrode (CE) were screen-printed in-house using carbon ink. Silver/silver chloride (Ag|AgCl) ink was used as a pseudo-reference electrode (RE) and conductive pad. The sensor was allowed to dry at 55 °C for 1 h.

3.4.2 Preparation of the modified electrode

The ERGO modification was initially performed on the PAD using a previously described cyclic voltammetry technique [104]. The GO solution (6.2 mg mL^{-1}) was

diluted with 0.1 M phosphate buffer (PB) pH 6 to adjust the final concentration of 90% (v/v) GO. 100 μL of this solution was then pipetted onto the electrode surface, and potential was applied in the range of +0.1 to -1.5 V with a scan rate of 50 mV s^{-1} for 16 cycles. The modified electrode was then rinsed twice with deionized water.

The CuO/IL composite was prepared by dispersing 5 mg of CuO nanopowder in 1 mL of DMF, then adding 300 μL of IL solution (10 mg mL^{-1}) into the dispersion, followed by sonication for 1 hour. To selectively dispense CuO/IL composite suspension on the working electrode of the PAD, the SPCE was placed on the platen of an HP D300 digital dispenser programmed using HP bio pattern software to define the deposition location and parameters. CuO/IL suspension was then loaded into an HP D300 cartridge and 400 nL was dispensed in 2 layers onto the working electrode area. For comparison, a drop-cast CuO/IL modified ERGO/SPCE was prepared by placing the composite solution onto the working electrode, and dried at room temperature and atmospheric pressure.

3.4.3   Electrochemical measurement

The unmodified (bare ERGO/SPCE) and CuO/IL modified electrodes were characterized by CV using a standard three-electrode system fabricated on a paper-based sensor. Electrochemical detection was conducted in a solution containing 0.5 mM creatinine in 0.1 M PB pH 7.4 over the range of potentials of -1.0 to +1.0 V with a scan rate of 50 mv s^{-1}. Amperometry was conducted to optimize the detection potential using creatinine in PB solution on a CuO/IL/ERGO/SPCE at different potentials in a range of -0.4 to +0.3 V for a fixed time duration. The creatinine oxidation current (S) to the background current (B) was used to obtain signal-to-background (S/B) ratios. Amperometric creatinine detection on CuO/IL/ERGO/SPCE electrode was carried out at an optimized potential and the anodic current was recorded at 5 s. All measurements were conducted at the room temperature.

3.4.4   Preparation of protein in the human serum

To obtain reliable results, the human serum was pretreated using the TCA method to precipitate the protein [105]. Aliquots of 250 μL from each of human

serum samples were added to individual microcentrifuge tubes, and 250 μL of 10% (W/V) TCA was added to each tube. The resulting mixture was centrifuged for 10 min at 6000 rpm at 4 °C and the supernatant was kept for further analysis. All samples were analyzed by amperometry on the multiple individual paper-based sensors.

CHAPTER IV
RESULTS AND DISCUSSION

Part I: Development of the enzymatic biosensor
4.1 Characterisation of TiO$_2$ sol/graphene nanocomposites prepared by sol-gel method

4.1.1 TEM characterization

In this study, TiO$_2$ sol/graphene nanocomposites were prepared by a sol-gel method slightly modified from our previous reports [100, 101]. Two images of a TiO$_2$ sol and a TiO$_2$ sol/graphene nanocomposite are shown in Fig. 4.1a and b, respectively, indicating that the nanocomposite was visually a darker yellow homogenous solution compared to TiO$_2$ sol. The transmission electron micrographs of graphene, TiO$_2$ sol nanoparticles, and TiO$_2$ sol/graphene nanocomposite are shown in Fig. 4.2a, which reveals a thin, transparent graphene layer with sharp corner, while that in Fig. 4.2b shows that TiO$_2$ sol nanoparticles are uniformly spherical-shaped with a size distribution in a range of 50-150 nm without agglomeration. According to Fig. 4.2c, the nanoparticles of TiO$_2$ were well dispersed on the surface of a two-dimensional graphene sheet as displayed in the large black sheet.
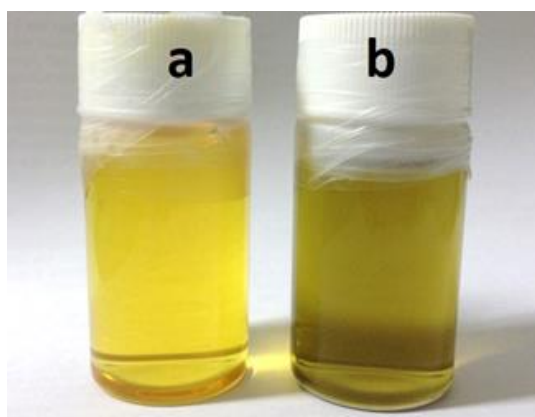
Fig. 4.1 (a) Photographs of TiO$_2$ sol and (b) TiO$_2$ sol/graphene nanocomposite
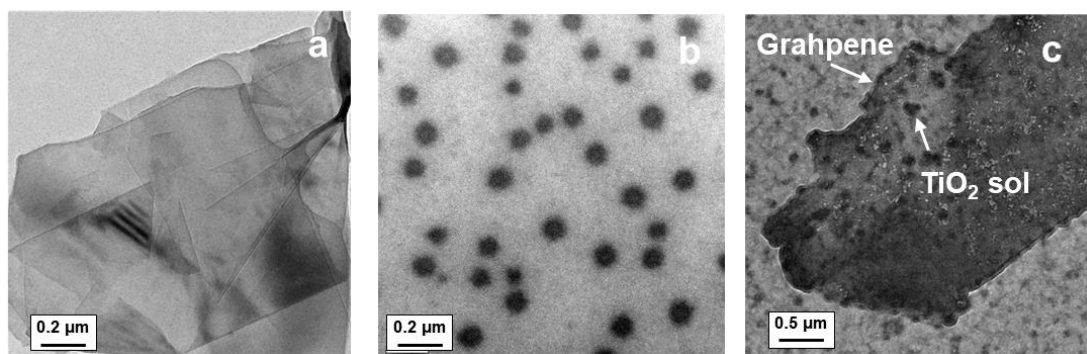
Fig. 4.2 (a) Transmission electron micrographs of graphene dispersion, (b) TiO_2 sol nanoparticles synthesized by sol-gel method, and (c) TiO_2 sol/graphene nanocomposite solution

4.1.2 FT-IR characterization

FT-IR was used to verify the successful incorporation of graphene in TiO_2 sol and the results are shown in Fig. 4.3. A comparison of the spectrum of graphene (Fig. 4.3a) and TiO_2 sol/graphene (Fig. 4.3b) shows the presence of characteristic vibration of Ti-O-Ti at 717 cm^{-1} [106], which is not appear in a spectrum of pure graphene (Fig. 4.3a) but similar to the spectrum of pure TiO_2 (Fig. 4.3c) [107, 108]. The band at 1042 cm^{-1} in TiO_2 sol/graphene and was ascribed to the stretching vibration of C-OH [109]. The absorption peak at 1391 cm^{-1} was attributed to the bond vibration of Ti-OH [106]. Also, the broadband is near 3420 cm^{-1} appeared in TiO_2 sol/graphene (Fig. 4.3b) is assigned to the presence of hydroxyl groups of TiO_2 [106] and also to an interaction of hydrogen bonding between the hydroxyl groups on the surface of titanium oxide [106].
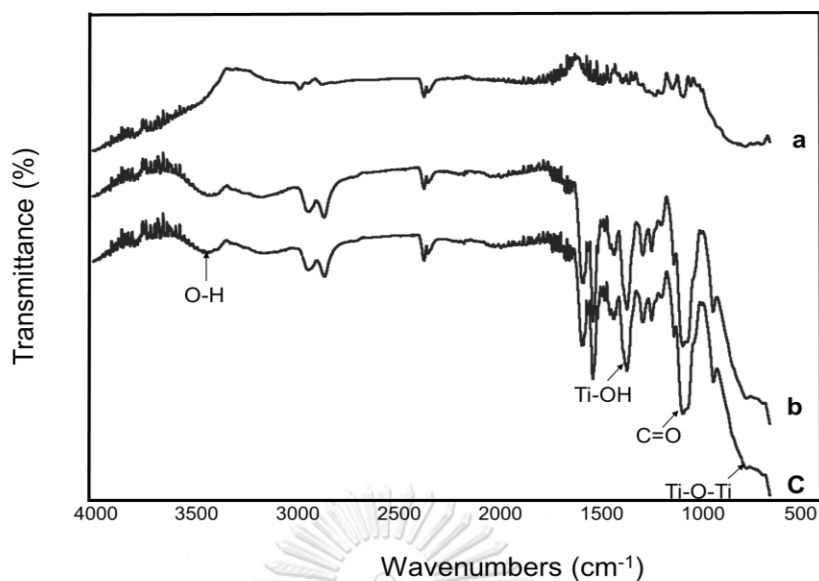
Fig. 4.3 (a) FT-IR spectra of graphene, (b) TiO_2 sol/graphene nanocomposites, and (c) TiO_2 sol

4.1.3 FTIR-Raman characterization

Raman spectra of graphene, TiO_2 sol, and TiO_2 sol/graphene nanocomposite are shown in Fig. 4.4 to confirm the successful preparation of TiO_2 sol/graphene nanocomposite. The spectrum of graphene displays a D band at 1360 cm^{-1} and a G band at 1580 cm^{-1} (Fig. 4.4a) [110], and the spectrum of TiO_2 sol/graphene also contains both D and G bands (Fig. 4.4c). Moreover, the weak 2D peak at 2700 cm^{-1} in the TiO_2 sol/graphene nanocomposite corresponds to the 2D peak of graphene, which is absent in spectrum of TiO_2 sol (Fig. 4.4b) [111]. Thus, the formation of TiO_2 sol/grahpene nanocomposite has been confirmed via Raman spectroscopy [107].
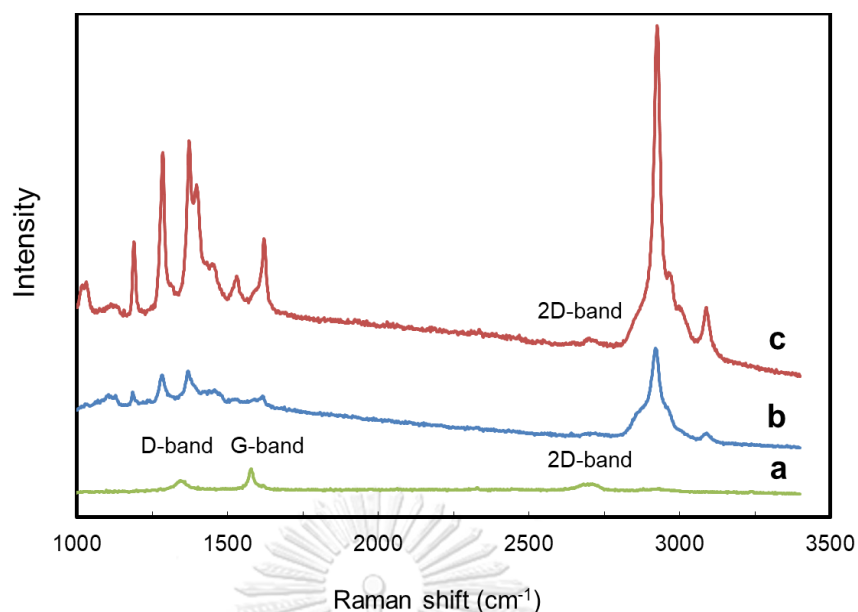
Fig. 4.4 (a) Raman spectra of graphene, (b) TiO_2 sol, and (c) TiO_2/graphene nanocomposite

4.1.4 XPS characterization

The formation of TiO_2 sol/graphene was also confirmed by XPS. Fig. 4.5a shows the X-ray photoelectron spectrum of TiO_2 sol and TiO_2 sol/graphene nanocomposite in the Ti 2p3/2 and Ti 2p1/2 binding energy regions. As for the pure TiO_2, Ti 2p3/2 and Ti 2p1/2 spin-orbital splitting photoelectrons are located at binding energies of 455.9 and 461.8 eV, respectively, giving rise to a peak separation of 5.9 eV, which is the same result reported by Erdem *et al*. [112]. The O 1s spectrum of TiO_2 sol and TiO_2 sol/graphene is shown in Fig.4.5b, a peak for TiO_2 sol was observed at 528.4 eV and the board peak of the TiO_2 sol/graphene can be fitted into two symmetric peaks at 529.2 and 533.3 eV arising from Ti-O-Ti and Ti-O-C bond, respectively, displaying a covalent bond connection between graphene and TiO_2 [113]. After the formation of TiO_2/graphene, a shift from 455.8 to 456.3 eV and 461.8 to 462.4 eV in Ti 2p, also 528.4 to 529.2 eV in O 1s binding energies was observed in X-ray photoelectron spectrum of TiO_2 sol/graphene. All these shifts were induced by a change of the chemical state or coordination environment [114]. In addition, C 1s spectrum of TiO_2 sol/graphene nanocomposite is shown in Fig. 4.5c. Deconvolution of C 1s peak in X-ray photoelectron spectrum presents the carbon bonds of C-C

(284.5 eV), C-O (286.1 eV), and -COOH (288.3 eV). The minor peak corresponds to small amount of residue oxygenate groups on graphene sheet, which are favorable to maintain a good dispersion of the nanoparticles [115]. It is possible to form O=C-O-Ti bonds through esterification of -OH groups on TiO_2 and oxygenate groups on graphene surface. [114]
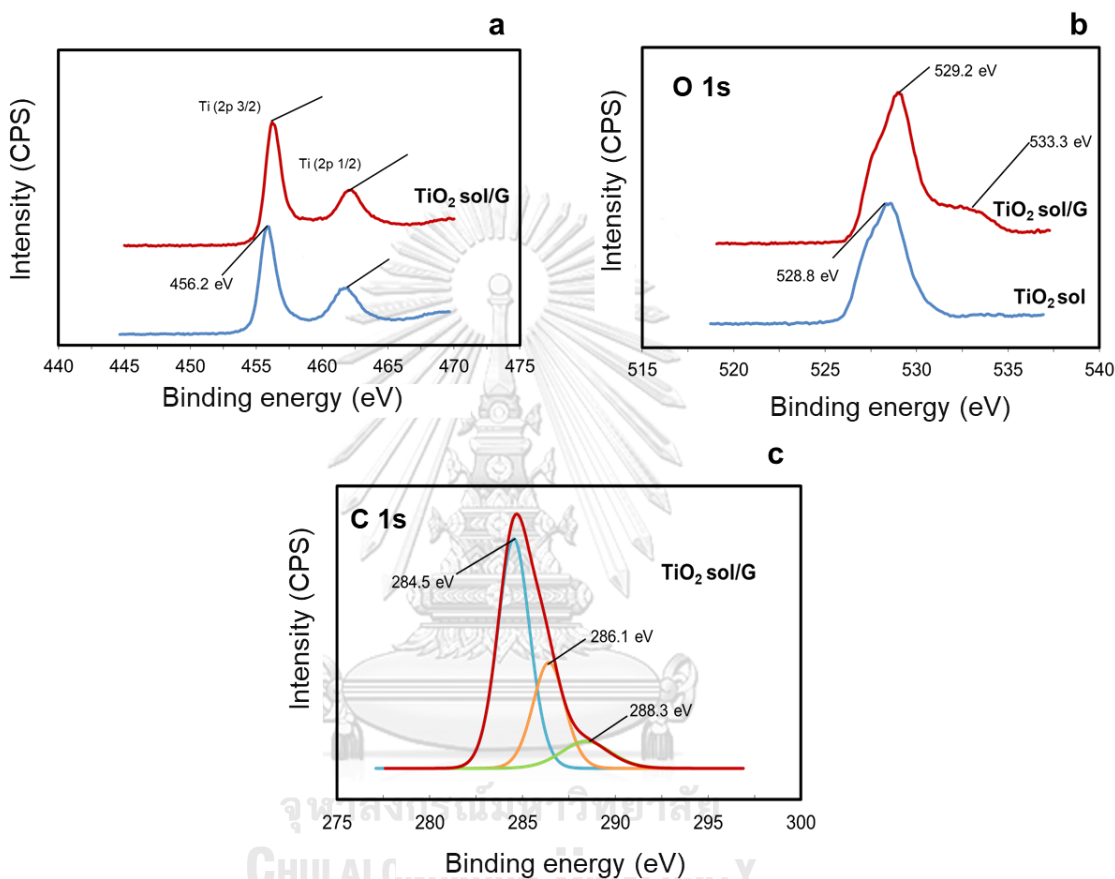
Fig. 4.5 (a) The X-ray photoelectron spectra of Ti 2p and (b) O 1s for TiO_2 sol and TiO_2 sol/graphene. (c) The C 1s X-ray photoelectron spectra of TiO_2 sol/graphene

4.2 Microstructures of modified Ni foam electrode

The as-prepared TiO_2 sol and TiO_2 sol/graphene nanocomposites were coated on a Ni foam for 1 minute. The morphologies of Ni foam and modified Ni foam electrodes were examined by SEM. The scanning electron micrographs of Ni foam substrate before modification (Fig. 4.6a) shows that Ni foam is a 3D cross-linked network architecture with an average pore size of 300-500 μm. The higher magnification of scanning electron micrograph exhibits the rough surface with the

grain nodule of Ni (Fig. 4.6b) as confirmed by SEM-EDX (Fig. 4.6e) and this feature has also been observed in a previous report Akhtar *et al*. [41]. The 3D porous structure of Ni foam possesses high porosity and high specific surface area leading to enhanced accessibility of analytes to closely interact at the electrode surfaces to produce an improved sensor sensitivity [116, 117]. The presence of TiO_2 sol/grahpene nanocomposites on Ni foam surface after modification is verified by Fig. 4.6c, indicating that Ni foam surface is completely coated by the as-prepared nanocomposites. Although there are some micro cracks observed on the surface, Ni substrate surface was entirely coated by the nanocomposites and this was observed in a previous report [118]. Scanning electron micrograph-EDX was used to identify the composition of TiO_2 sol/graphene nanocomposite on the Ni foam surface (Fig. 4.6f). The nanocomposite mainly consisted of Ti, Ni, and C elements, which confirms that TiO_2 sol/graphene nanocomposite was successfully deposited onto Ni foam surface. As shown in Fig. 4.6d, an scanning electron micrograph shows a dimly rougher surface compared to that depicted in Fig. 4.6c because of the nonconductive property of LOx enzyme immobilized on the surface of Ni foam [119]. Overall, scanning electron micrograph results clearly verify the successful modification of LOx/TiO_2 sol/graphene onto the open-cell 3D Ni foam electrode.
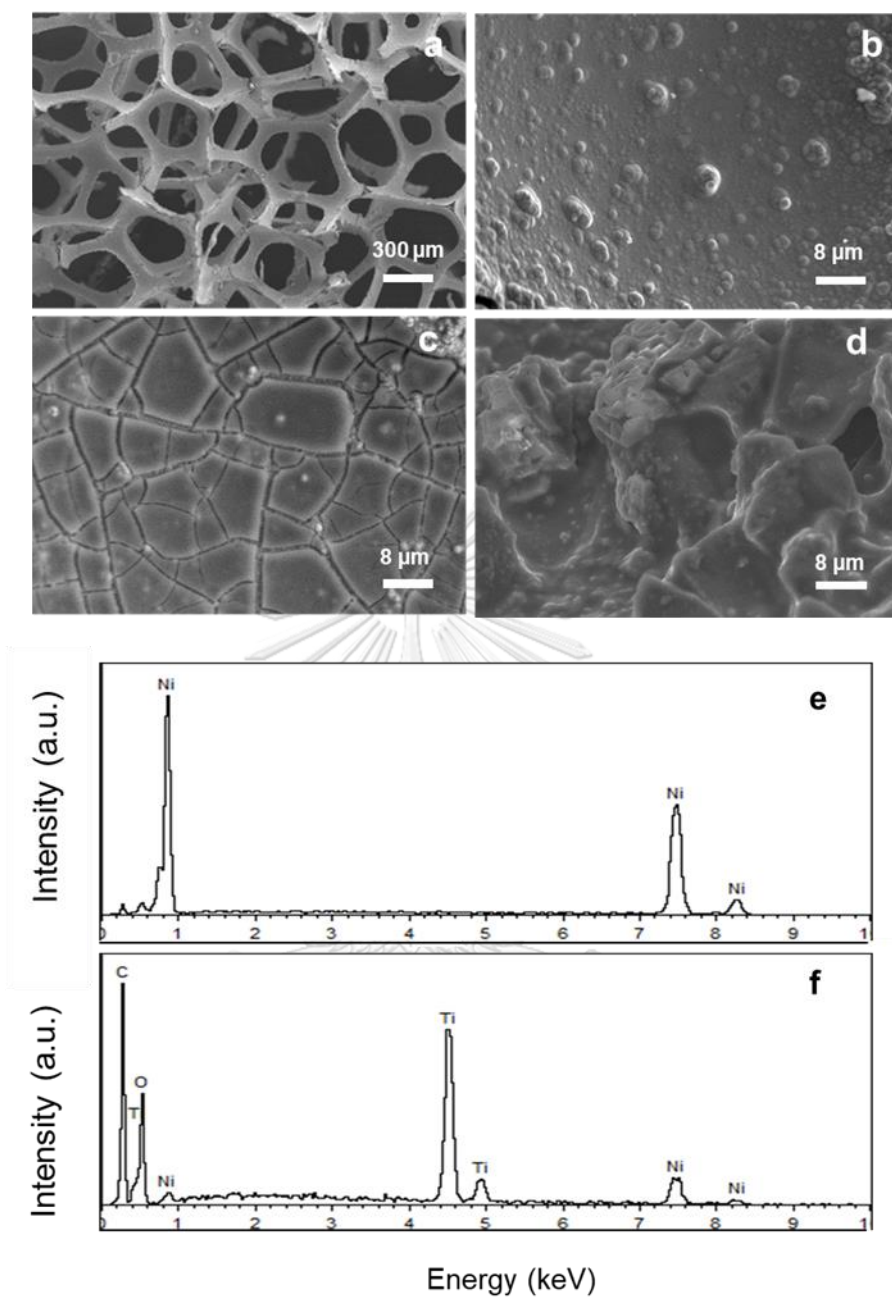
Fig.4.6 (a) Scanning electron micrograph of unmodified Ni foam (50x); (b) highly magnified micrograph of Ni foam (1,500x); (c) TiO$_2$ sol/graphene/ modified on Ni foam (1,500x); (d) LOx/TiO$_2$ sol/grahpene modified on Ni foam (1,500x); (e) EDX micrograph of Ni foam and (f) EDX micrograph of TiO$_2$ sol/graphene modified Ni foam

4.3 Application of the modified Ni foam for enzymatic electrochemical biosensor

4.3.1. H_2O_2 detection

4.3.1.1 Electrochemical characterization of the modified electrode

To find the optimal conditions of Ni foam surface modification as a novel working electrode in an enzymatic electrochemical biosensor, a standard H_2O_2 solution was initially tested using CV. In this study, the electrochemical responses measured at unmodified Ni foam, TiO_2 sol/graphene nanocomposite modified Ni foam, TiO_2 sol modified Ni foam, and graphene modified Ni foam are presented in Fig. 4.7. The cyclic voltammograms show that the anodic current signal of H_2O_2 measured at graphene-modified Ni foam electrode (green line) is higher than the others (Fig. 4.7a); however, the background current is also high (light blue line) as shown in an inset of Fig. 4.7b. Meanwhile, the current response of TiO_2/graphene modified Ni foam in the presence and absence of H_2O_2 is shown in Fig. 4.7b and Fig. 4.8, suggesting that it is more distinguishable from the background current than graphene-modified Ni foam electrode (inset Fig. 4.7b) and other electrodes (Fig. 4.8), but the anodic peak current is not clearly shown in the cyclic voltammogram which is similar to a shape of current signal reported in a previous study [76], who detected cholesterol via H_2O_2 generated from a reaction of cholesterol oxidase using graphene/polyvinylpyrrolidone/ polyaniline nanocomposite paper-based biosensor. Due to the high background current from the cyclic voltammogram and the effect of applied potential on the electrochemical sensing performances, Chaiyo *et al*. [103] have employed hydrodynamic voltammetry to optimise a detection potential in a quiescent system for electrochemical detection, also used S/B ratios instead of currents only to investigate the current response from glucose detection by using a cobalt phthalocyanine/ionic liquid/graphene composite paper-based sensor. Hence, hydrodynamic voltammetry was applied to select an optimal potential for electrochemical detection in this work, conducted by Section 2.6 (Fig. 4.9).
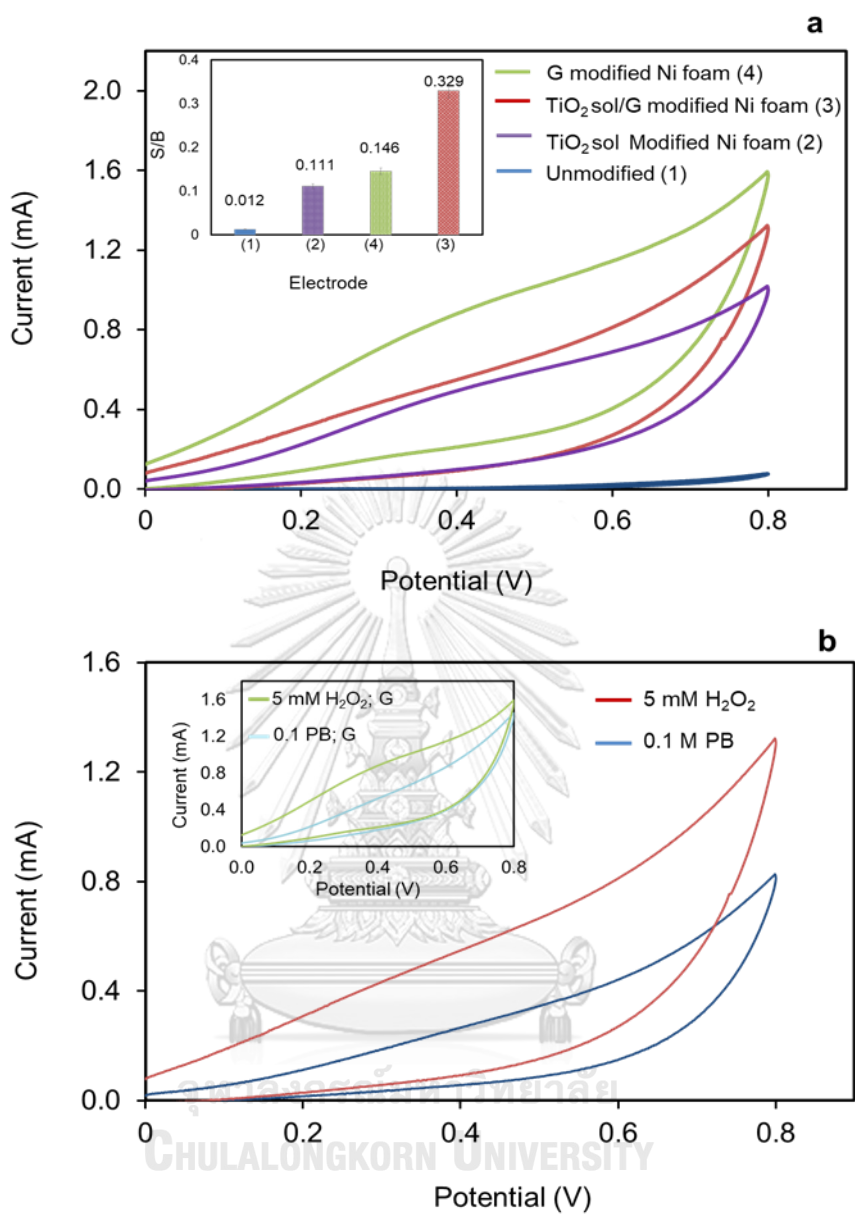
Fig. 4.7 (a) Cyclic voltammograms of 5.0 mM H_2O_2 in 0.1 M PB measured on different working electrodes with a scan rate of 50 mV s^{-1}; (b) cyclic voltammograms of TiO_2/graphene modified Ni foam measured in the absence and presence of 1.0 mM H_2O_2 at scan rate of 50 mVs^{-1}. G: graphene
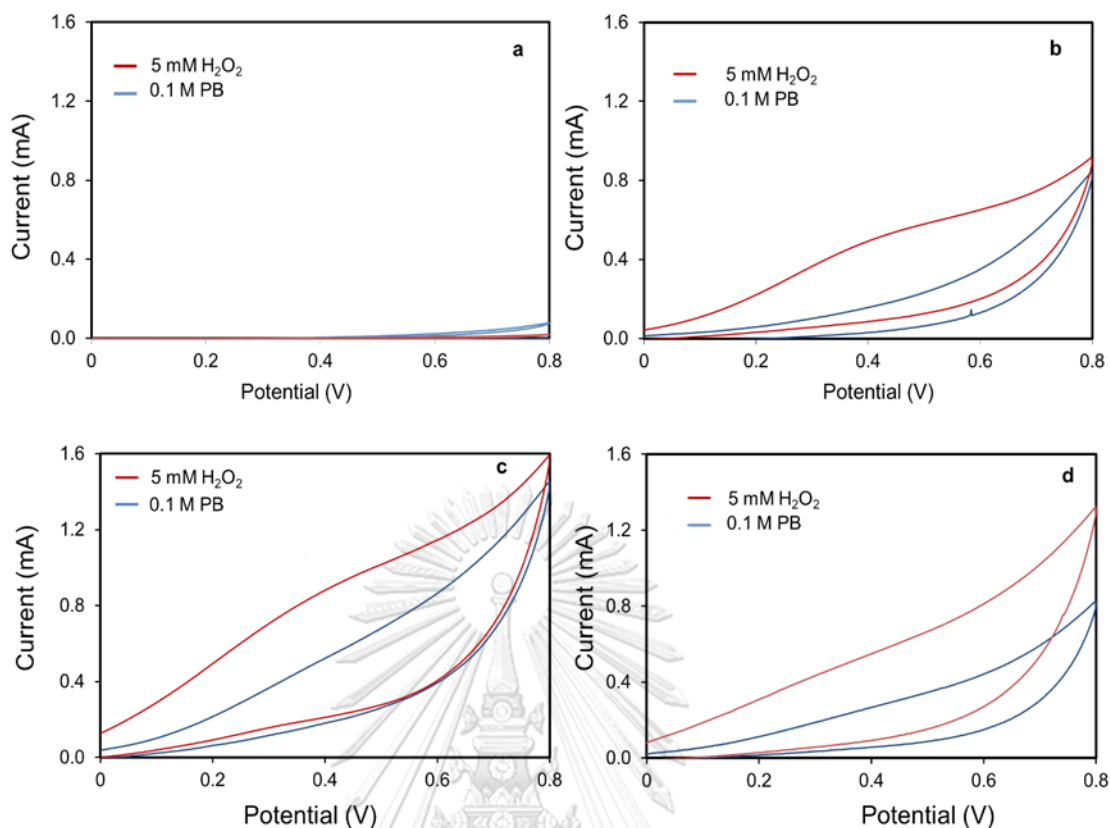
Fig. 4.8 (a) Cyclic voltammograms of 5 mM H_2O_2 and blank (0.1 M PB buffer solution) using unmodified Ni foam electrode, (b) TiO_2 sol modified Ni foam electrode, (c) graphene modified Ni foam electrode, and (d) TiO_2 sol/graphene modified Ni foam electrode

4.3.1.2 Study of the detection potential for the modified electrode

According to the hydrodynamic voltammogram, S/B was investigated instead of current signal (Fig. 4.9b) because the anodic current of H_2O_2 significantly increased as the applied voltage increased (blue line) while the current of background also increased (green line) as seen in Fig. 4.9a. At an applied potential of +0.5 V (Ag/AgCl), which is a minimal applied potential that can differentiate the current signal from background signal. Moreover, this low potential is also likely to minimize interferences during lactate detection in real-life samples [120]. Hence, +0.5 V was selected as a detection potential for all electrochemical detections. The S/B values determined from different working electrodes are presented in an inset of Fig. 4.7a. The S/B value measured on TiO_2 sol/graphene/Ni foam electrode (0.33 mA) is

approximately 28 times higher than an unmodified Ni foam electrode (0.012 mA), indicating this modified Ni foam might be a promising electrode for an enzymatic electrochemical biosensor, such as lactate detection via tracking on generated H_2O_2, which is an electroactive product generated from an enzymatic reaction.
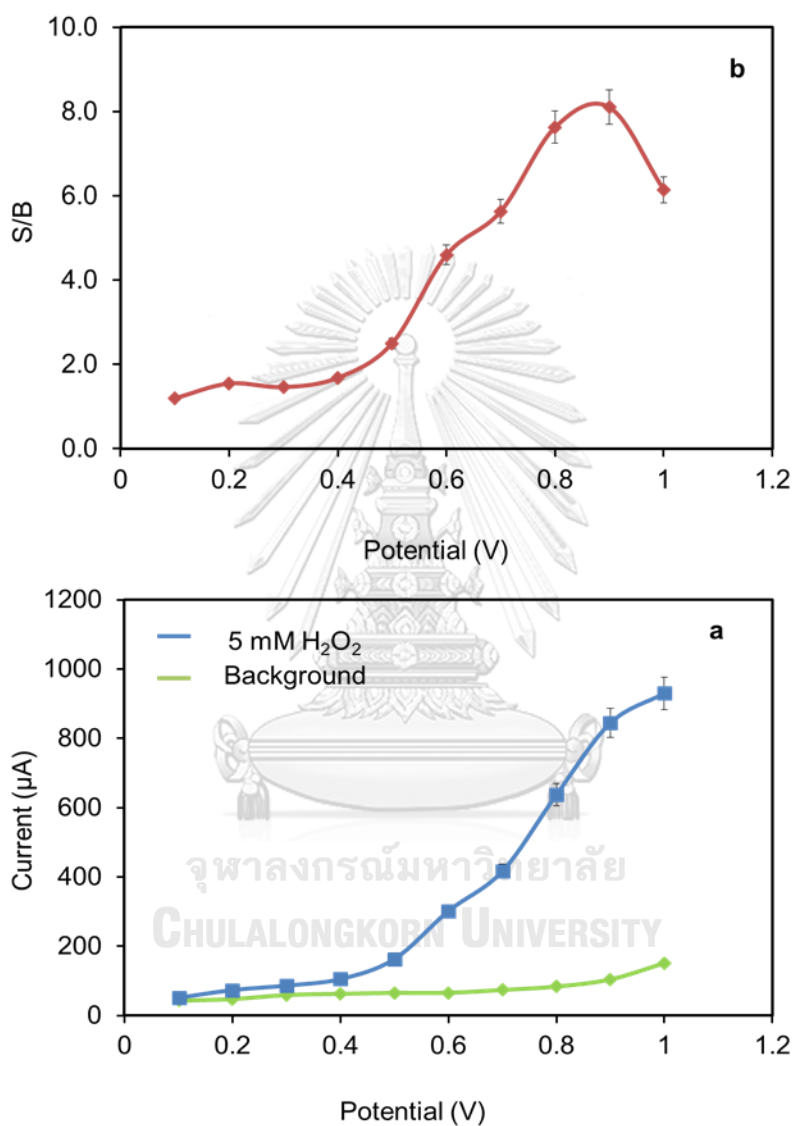
Fig. 4.9 (a) Amperometric current responses of 5 mM H_2O_2 (blue line) and background (green line) in 0.1 M PB solution pH 7.0 at a 180 s sampling time measured on a TiO_2 sol/graphene/ modified Ni foam electrode and (b) hydrodynamic voltammogram of S/B extracted from the data in Fig. 4.9a

4.3.1.3 Study of TiO$_2$ sol/graphene concentration for the electrode modification

Furthermore, the optimal concentration of TiO$_2$ sol and graphene used for preparation of TiO$_2$ sol/graphene nanocomposites were investigated by CV of 5 mM H$_2$O$_2$ at a TiO$_2$ modified electrodes and TiO$_2$ sol/graphene modified electrodes. The results are presented in Fig. 4.10, showing the S/B value of an optimal TiO$_2$ and graphene concentration derived from cyclic voltammograms (inset of Fig. 4.10). In our experiment, 0 to 16 mg mL^{-1} TiO$_2$ sol was used in preparing a TiO$_2$/graphene nanocomposite. As shown in Fig. 4.10a, an optimal TiO$_2$ sol concentration is found to be 8 mg mL^{-1}. At this TiO$_2$ sol concentration, the amount of graphene was varied (Fig. 4.10b) and 1.5 mg mL^{-1} is an optimal concentration. Thus, a suitable mass ratio of TiO$_2$ sol to graphene is 5:1. This ratio provided the highest S/B values toward H$_2$O$_2$ detection; therefore, these concentrations were selected to prepare TiO$_2$ sol/graphene nanocomposites for all further experiments.
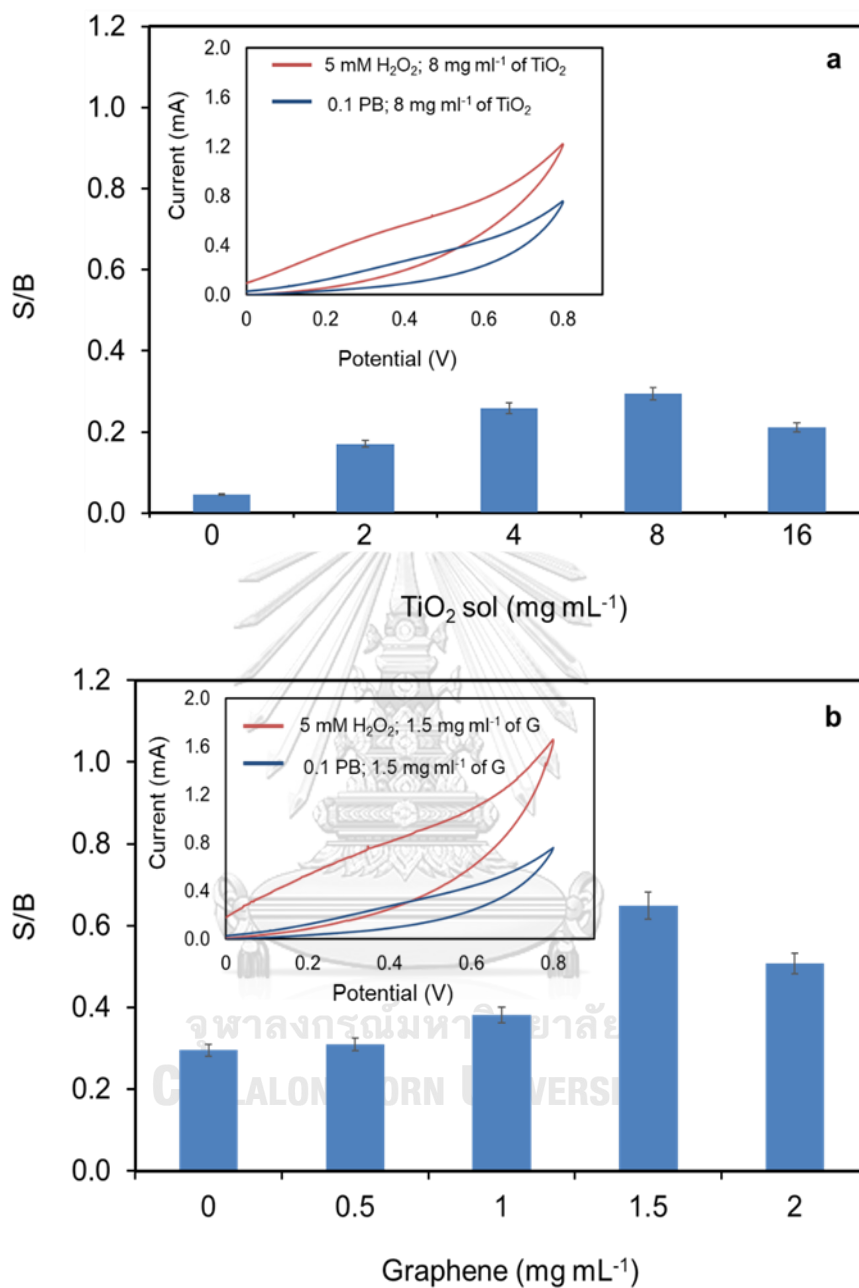
Fig. 4.10 (a) Optimization of TiO_2 sol and (b) graphene concentration used to prepare TiO_2 sol/graphene nanocomposites for Ni foam electrode surface modification towards 5 mM H_2O_2 in PB pH 7 at scan rate 50 mVs^{-1} using CV (Note: assuming molecular weight of TiO_2 sol is equal to TiO_2 nanoparticles as the characterization results of TiO_2 sol).

4.3.2 Lactate detection

4.3.2.1 Electrochemical characterization for the lactate detection

To evaluate the ability of TiO_2 sol/graphene modified Ni foam electrode for an enzyme based electrochemical biosensor application, detection of lactate through H_2O_2 generated from enzymatic reaction between lactate and LOx are shown in Equation (1) and (2). A lactate level higher than 1.5 mM in patient's blood generally indicates the hyperlactatemia or lactic acidosis [51], which will lead to severe sepsis and septic shock [52]. Thus, 1.5 mM lactate is selected for testing electrochemical performances of our platform.

$$\text{Lactate} + O_2 \xrightarrow{\text{LOx}} \text{Pyruvate} + H_2O_2 \quad\quad (1)$$

$$H_2O_2 \longrightarrow O_2 + 2H^+ + 2e^- \quad\quad (2)$$
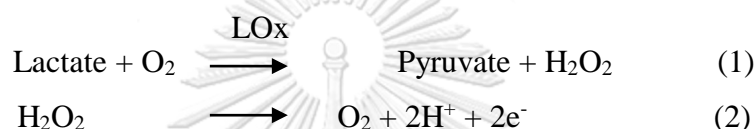
Thus, LOx was immobilized on a modified electrode before CV of 1.5 mM lactate in 0.1 M PB (pH 7.4) was conducted to primarily test the ability of this electrode toward lactate. The same experiment was also conducted at an unmodified Ni foam electrode. All results obtained are shown in Fig. 4.11a. It was obvious that anodic current signal of lactate measured on LOx/TiO_2 sol/graphene modified Ni foam electrode (red line) is higher than an unmodified electrode (blue line) and this modified electrode showed a drastic increase of S/B value ($\sim$ 47 times) compared with an unmodified Ni foam electrode as shown in Fig. 4.11b. This result verifies that the combination of TiO_2 sol/graphene nanocomposite on Ni foam increased the electrochemical conductivity of Ni foam electrode. Moreover, the high porosity of Ni foam accelerated the electron transfer of analyte molecules at the electrode/electrolyte interface, leading to enhanced sensitivity of the sensor.
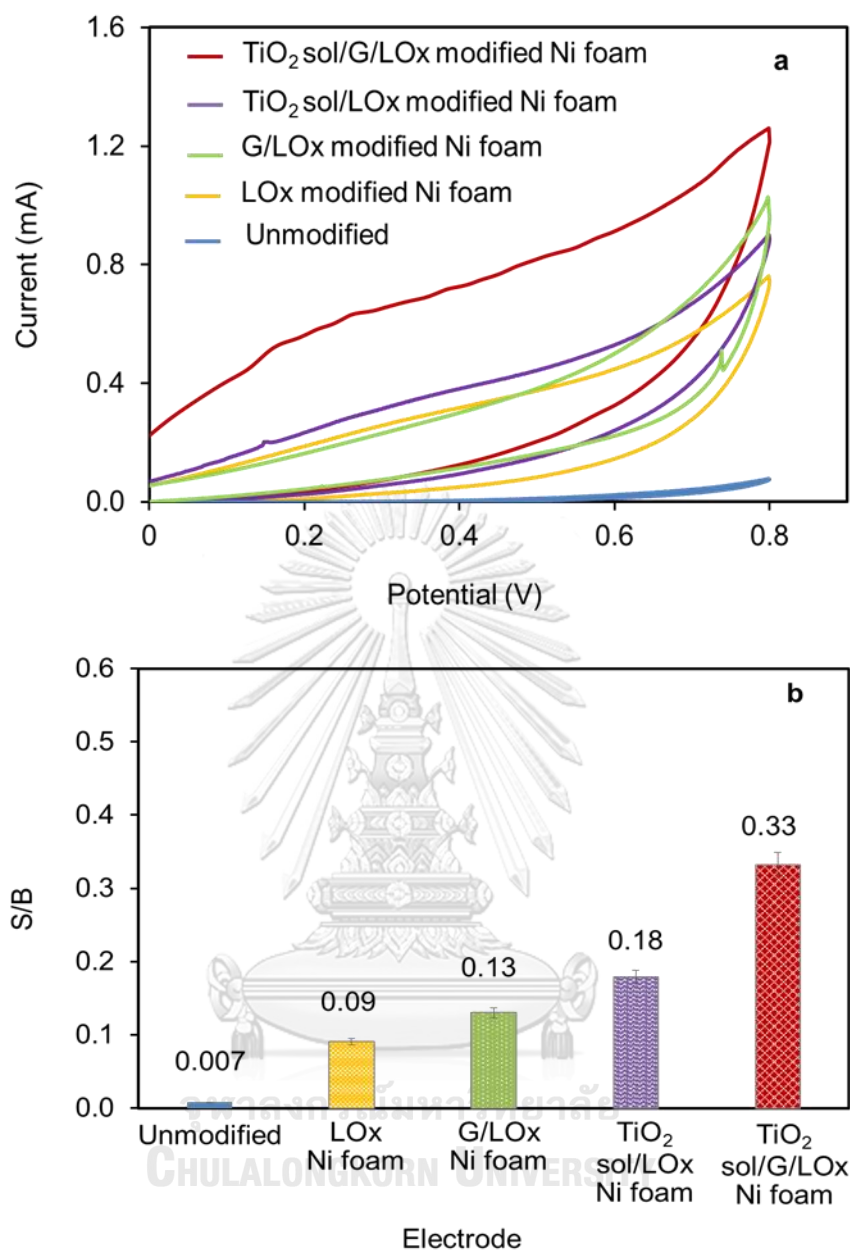
Fig. 4.11 (a) Cyclic voltammograms of 1.5 mM lactate in 0.1 M PB measured on different working electrodes with a scan rate of 50 mV s^{-1}; (b) signal-to-background current (S/B) extracted from the data in Fig. 4.11a. G: graphene.

> *4.3.2.2 Study of analytical performances of the modified Ni foam*
> *electrode*

To examine the analytical performance of LOx/TiO$_2$ sol/graphene modified Ni foam electrode, it was used to measure lactate at different concentrations by using amperometry (Fig. 4.12a) and the amperometric current responses recorded at

steady state current at 180 s was used to construct a calibration plot for the lactate. The LOx/TiO$_2$ sol/graphene modified Ni form electrode shows a linear region over the range of 50 µM to 10 mM with a correlation coefficient of 0.9974 as shown in Fig. 4.12b. Based on the linear range, the limit of detection (LOD) and limit of quantitation (LOQ) were found to be 0.019 mM and 0.06 mM, respectively. LOD was estimated as the concentrations that yielded a signal at 3 times higher than the standard deviation of a blank (n=5) [75]. The proposed sensor has lower detection limit for lactate compared to 0.1 mM reported by Suman *et al.* [121], who detected lactate by immobilizing LOx onto polyaniline-co-fluoroaniline films deposited on indium tin oxide (ITO) coated glass plate, and 0.05 mM reported by Park *et al.* [122], who detected lactate by immobilizing LOx onto osmium polymer sol-gel modified glassy carbon electrode. Normally, the level of total blood lactate in human ranges from 0.5 to 1.5 mM at rest [51]. Hence, this information confirms that TiO$_2$ sol/graphene/Ni foam could be a novel working electrode utilized for sensitive detection of H$_2$O$_2$ generated by an enzymatic reaction. This system might be an alternative way for developing of sensor to detect a biomarker for the preliminary diagnosis.
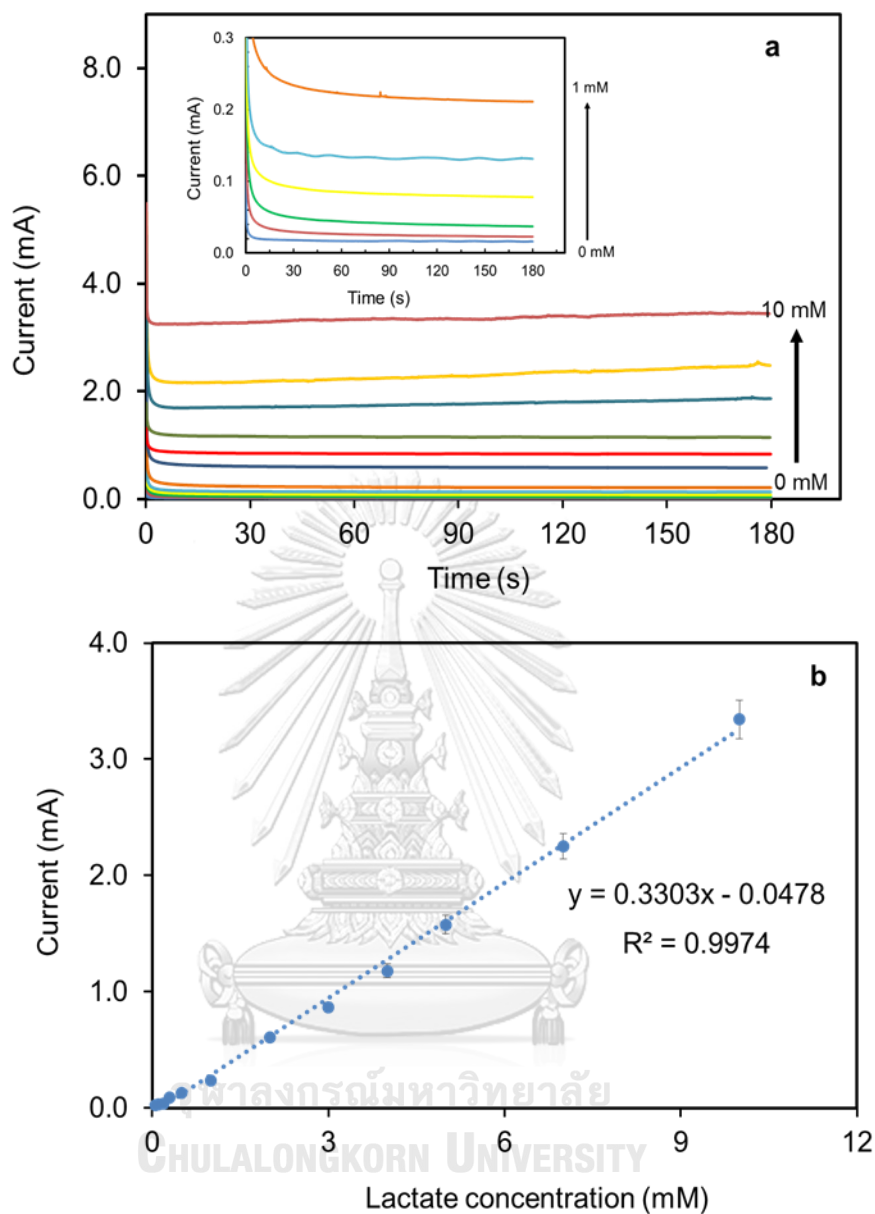
Fig. 4.12 (a) Amperometry measurements recorded on a LOx/TiO$_2$/graphene/Ni foam electrode with different concentrations (from 0.0 to 2.0 mM) and (b) a calibration plot for lactate detection constructed from the signal measurements presented in a (E = +0.5 V, pH 7.4).

4.3.2.3 Study of reproducibility and stability for the lactate detection

To investigate electrode-to-electrode reproducibility, five different LOx/TiO$_2$ sol/graphene/Ni foam electrodes were used to detect 0.5 mM lactate by

amperometry and the relative standard deviation (RSD) was founded to be 2.2%. The response of five amperometric measurements toward 0.5 mM lactate on the modified electrode yielded reproducible responses with a 3.4% RSD (Fig. 4.13a). To evaluate the stability of this sensor, the LOx/TiO$_2$ sol/graphene/Ni foam electrodes were stored in the sealed system at 4 °C for 8 days and the storage electrode retained the current response towards 0.5 mM lactate in PB (0.1 M) up to 91% of its initial response (Fig. 4.13b), verifying that the good stability of this electrode, which is caused by the enzymatic preservation property of TiO$_2$ sol within TiO$_2$ sol/graphene nanocomposites [123], while using Ni foam electrode without nanocomposite immobilized with LOx, the current response decreased to less than 50% of original signal within 24 hr. after immobilization.
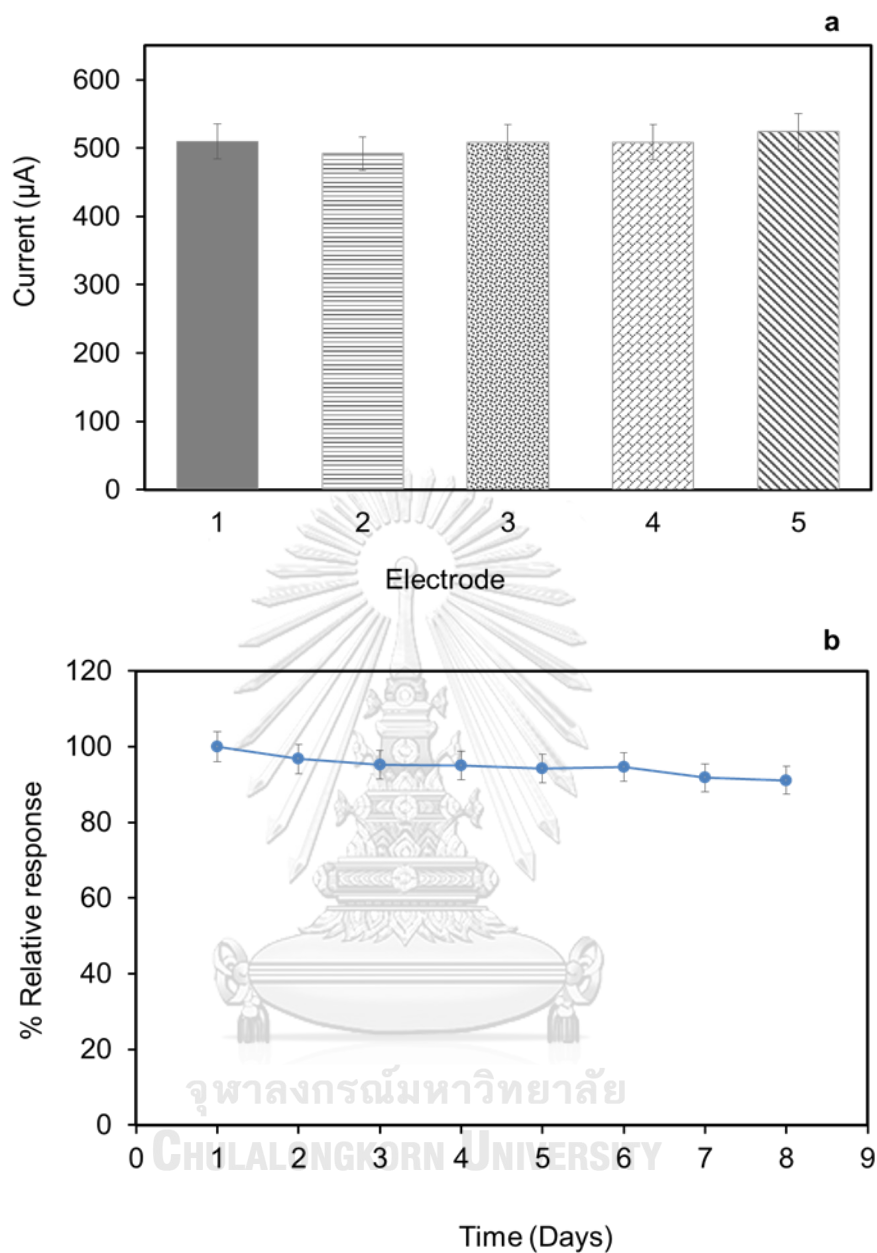
Fig. 4.13 (a) Amperometric responses of five different LOx/TiO$_2$ sol/graphene/Ni foam electrodes toward 0.5 mM lactate at 0.5 V (*vs*. Ag/AgCl) and (b) stability testing of LOx/TiO$_2$ sol/graphene/Ni foam electrode for continuous lactate detection for 8 consecutive days at 0.50 V (*vs*. Ag/Ag/Cl)

In addition, the effect of TiO$_2$ sol on electrode stability was studied to confirm that TiO$_2$ sol can retain the immobilized LOx on the modified Ni foam electrode as shown in Fig. 4.14. The results show that LOx/TiO$_2$ sol modified Ni foam

electrode used retain the electrode stability more than 90% of the initial sensitivity in 8 days continuous test for measurement of 0.5 mM lactate (Fig. 4.14a), suggesting that LOx has favorable long-term stability with TiO_2 sol. Nonetheless, the obtained current response of LOx/TiO_2 sol modified Ni foam electrode is lower than LOx/TiO_2 sol/graphene modified Ni foam electrode toward lactate analysis for 8 consecutive days as shown in Fig. 4.14b. This verify that graphene significantly improves the electrochemical sensitivity of electrode while TiO_2 sol preserves the activity of LOx and increases the electrode stability.
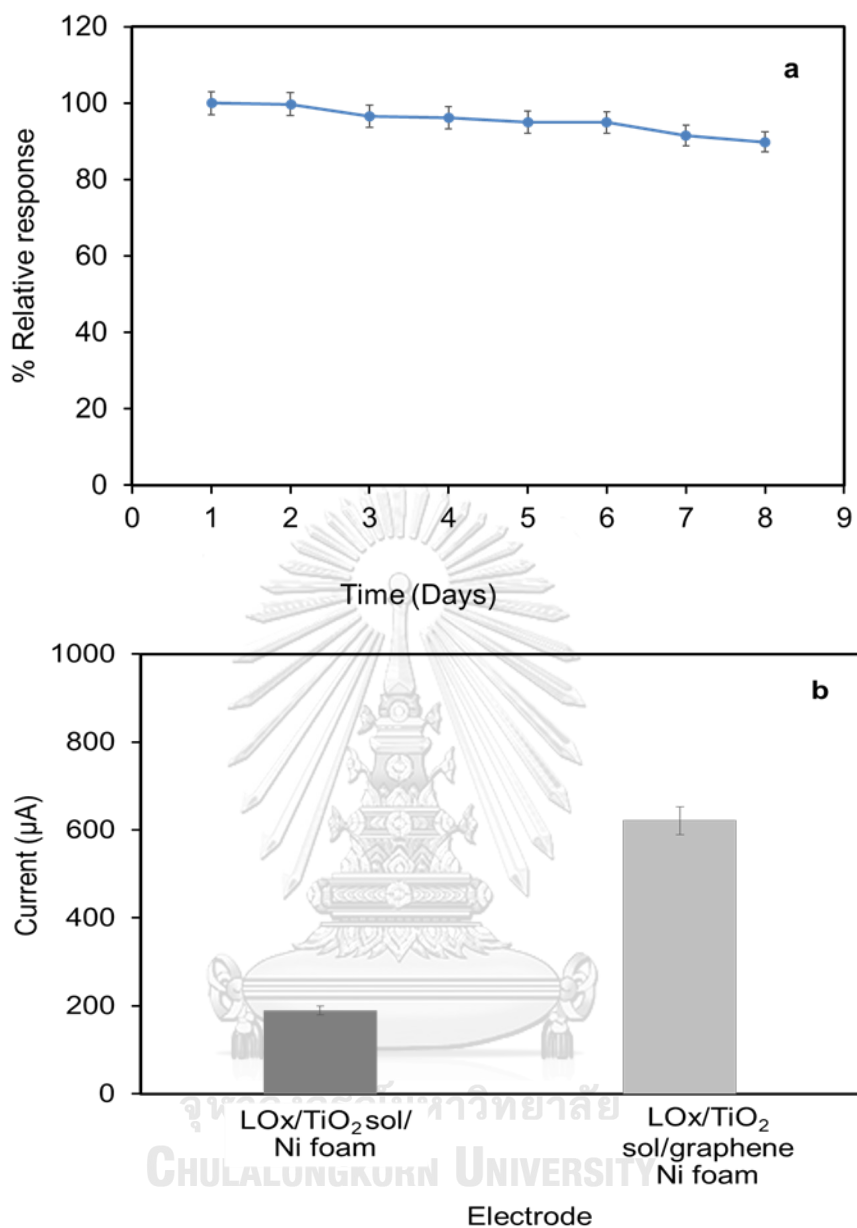
Fig. 4.14 (a) Stability test of TiO$_2$ sol modified Ni foam electrode for continuous lactate detection for 8 consecutive days and (b) amperometric response of TiO$_2$ sol/LOx modified Ni foam comparing with TiO$_2$ sol/graphene/LOx modified Ni foam obtained from studying the electrodes stability measured of 500 μM lactate for 8 days.

4.3.2.4 Study of selective determination of lactate

　　　　To test the selectivity of the LOx/TiO$_2$ sol/graphene Ni foam electrode, the modified electrode was used to determine lactate via amperometric measurements in the presence of the common electrochemical interfering species, such as AA, DA, and glucose. These compounds were investigated using the highest anticipated concentration of AA (80 μM), DA (50 μM), and glucose (5 mM) in a normal serum [75, 124] that lactate concentration was fixed at 1.5 mM. The results of the interference study are listed in Table 4.1. The influence of AA, DA, and glucose on the lactate response was little under the testing conditions. Moreover, The LOx/TiO$_2$ sol/graphene Ni foam electrode exhibited a high selectivity because the graphene-based composite materials have lowered the overvoltage potential for the oxidation of H$_2$O$_2$ [125]. This could be possible that the interference effects were eliminated from the electroactive species above [126].

Table 4.1 The response of LOx/TiO$_2$ sol/G/ Ni foam biosensor toward lactate and its interfering species [a] (n = 3)

	Lactate	Lactate + AA	Lactate + DA	Lactate + Glu
Current[a] (mA)	0.252 ± 0.024	0.252 ± 0.028	0.262 ± 0.033	0.261 ± 0.040
Relative response (%)	100	100	103	104

4.3.2.5 Detection of lactate in a real sample

In order to evaluate the utilization of the proposed system, the measurement of lactate in a commercial rabbit serum was studied using a standard addition method. A blank serum is commonly used for the determination of the accuracy and validation of a new diagnostic assay. For the sample preparation, different concentrations of lactate (0.50, 1.00, 3.00, and 5.00 mM) were spiked into 20 µL of the serum, which was filtered to remove the proteins and then diluted to 800 µL with 0.1 M PB (pH 7.4). The results are listed in Table 4.2, indicating that the current responses depended on the lactate concentration.

Table 4. 2 Determination of lactate in a rabbit serum (n = 3)

Lactate concentration (mM)		% Recovery	% RSD
Added	Found		
0.50	0.52 ± 0.02	104.0	0.8
1.00	1.03 ± 0.04	102.1	1.2
3.00	3.04 ± 0.20	101.5	0.7
5.00	5.09 ± 0.42	101.8	0.6

An acceptable linearity with a correlation coefficient (R^2) of 0.9994 (n = 3) was accomplished (Fig. 4.15). The percentage of recoveries were found in the range of 101.5 to 104.0% and 0.6 to1.2 %RSD, verifying that this promising system is highly accurate.
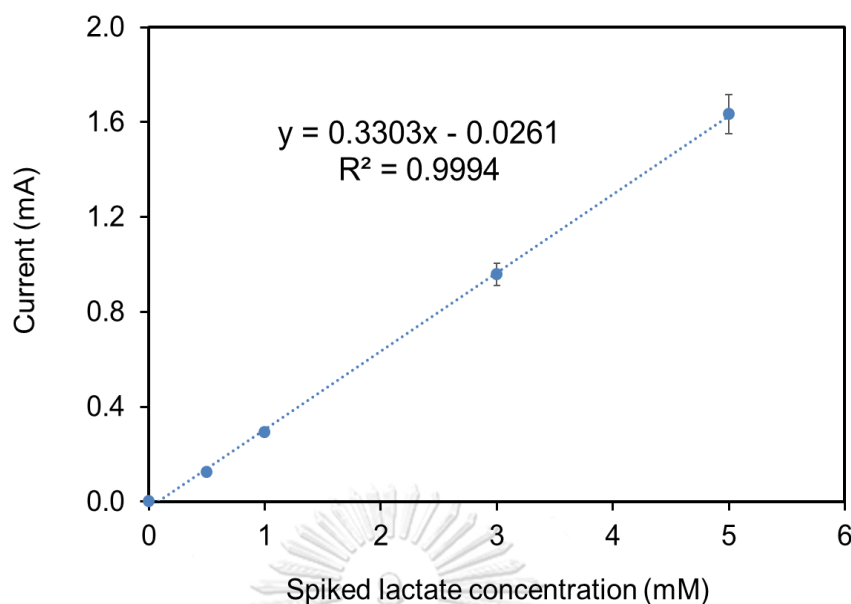
Fig. 4.15 A calibration plot between amperometric current response and lactate concentration spiked in a commercial serum; applied potential at +0.5 V

Part II: Development of the non-enzymatic sensor

4.4 Paper-based analytical sensor for the non-enzymatic detection of creatinine

4.4.1 SEM characterization of the prepared electrodes

The morphologies of unmodified and modified electrodes were characterized by SEM as shown in Fig. 4.16. The surface of the unmodified SPCE is dominated by isolated and irregularly shaped graphite flakes, which form the separated layers (Fig. 4.16a). The SEM micrograph of ERGO/SPCE shows wrinkle, smooth and thin sheet was completely covered on the modified electrode surface (Fig. 4.16b). This indicates the successful reduction of graphene oxide on the surface. Also, CuO nanocrystals are completely deposited on the ERGO sheet modified SPCE (Fig. 4.16c). The result from energy-dispersive X-ray with SEM (EDX-SEM) of CuO/IL/ERGO/SPCE shows the signal of carbon, oxygen, calcium, chloride, and copper, confirming the successful modification of CuO/IL/ERGO on SPCE (Fig. 4.16d).
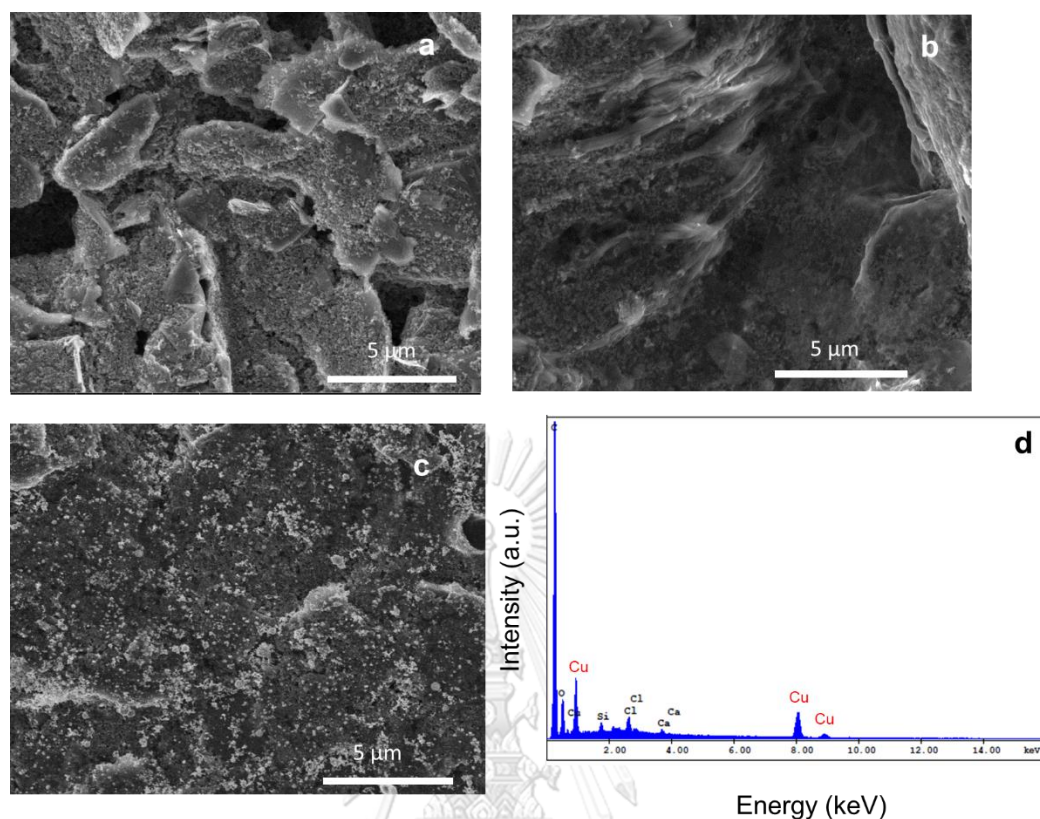
Fig. 4.16 (a) SEM micrograph of SPCE, (b) ERGO/SPCE, (c) CuO/IL/ERGO/SPCE at 15,000X magnification, and (d) EDX-SEM micrograph of CuO/IL/ERGO/SPCE.

The use of HP D300 dispenser for electrode surface modification can improve the dispersion of CuO/IL, which is observed from the electrode surface as shown in Fig. 4.17. The features of drop-casting and dispensing electrode are clearly different. There are some aggregated particles and clusters of CuO/IL on the drop-casting electrode surface while the electrode prepared by dispensing is composed of the greater distribution of uniform CuO/IL particles on the electrode surface resulting in enhancement of specific surface area, sensitivity and reproducibility of the sensor.
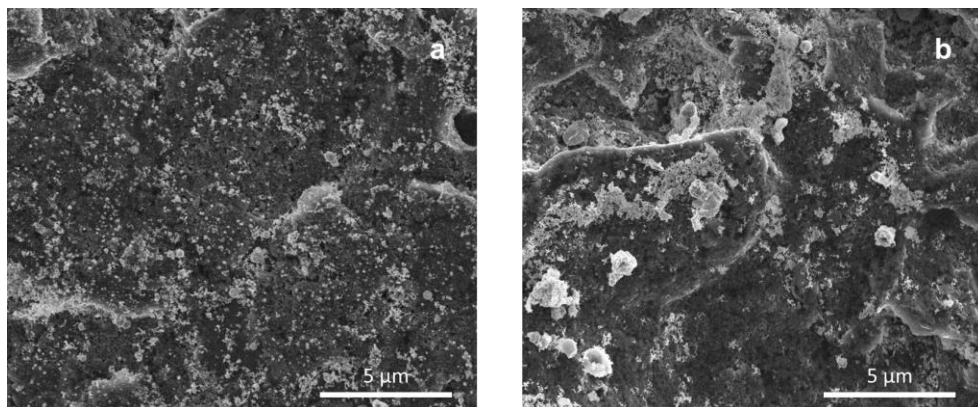
Fig. 4.17 (a) SEM micrographs of CuO/IL/ERGO/SPCE obtained from dispensing and (b) drop-casting method at 0.8 µL of CuO/IL.

4.4.2   Electrochemical characterization of the modified electrode

The clinically relevant range for serum creatinine in healthy humans is 0.5 mg/dL to 1.2 mg/dL (about 0.060 mM to 0.110 mM). Since the creatinine values differ greatly with variations in muscle mass, individual measurements have far less value than trends, giving serial measurements far more diagnostic utility and justifying the development of simple, low-cost methods for distributed measurement. Our goal was the development of a sensor that can indicate the presence of creatinine at levels above the clinically "normal" range.

CV was utilized to determine the utility of CuO/IL/ERGO/SPCE modified PADs for the detection of creatinine. The modified electrodes were examined in 0.1 M PB (pH 7.4) containing 0.5 mM creatinine, a value indicative of compromised kidney health. Fig. 4.18a shows the cyclic voltammogram obtained from an unmodified SPCE electrode on the PAD, measured in 0.1 mM PB (pH 7.4) with and without creatinine. Here, it is observed that there is no faradic current in the present of creatinine. In contrast, the cyclic voltammogram in Fig. 4.18b obtained from a CuO/SPCE shows a significant anodic current generated in the presence of creatinine (pink line) at -0.1 V compared to the background (black line). The oxidation peaks are attributed to the copper undergoes electrochemical oxidation during applying the potential, the generated cupric ions chelate with the creatinine in the solution and form a soluble copper-creatinine complex. The increase of peak current of creatinine after increasing

of creatinine concentration due to the increased dissolution of copper as copper-creatinine complex. Thus, CuO/IL/ERGO/SPCE can be applied for non-enzymatic electrochemical detection of creatinine. [81, 127].

Fig. 4.18c depicts cyclic voltammetry responses for the electrochemical oxidation of 0.5 mM creatinine obtained on an unmodified SPCE device, a CuO/IL device, a CuO/IL/SPCE device, a CuO/ERGO/SPCE device, and a full-complement CuO/IL/ERGO/SPCE paper electroanalytical device. The results show that the presence of CuO on the modified electrode generates a sensitive oxidation peak for creatinine (pink line) when compared to the unmodified SPCE device (yellow line): CuO is an effective copper ion source and facilitates formation of a copper-creatinine complex [7], enabling a strong electrocatalytic oxidation of creatinine. An increase in oxidative current from creatinine is observed upon incorporating IL in the CuO/IL composite modified electrode, while the oxidative current peaks are shifted cathodically (light blue and red lines). The anodic peak potential measured on the CuO/IL and CuO/IL/ERGO/SPCE devices are decreased by 30 mV relative to CuO/SPCE, and by 60 mV when compared to the peak potentials measured using the CuO/ERGO/SPCE device, attributed to the presence of IL on the modified electrode enhances the promotion of electron transfer, a strong electrocatalytic effect, and the high ionic conductivity of IL, which decreases the oxidation potential and response time for the measured oxidation of creatinine. A marked increase of the oxidative current from creatinine is noticed when ERGO is integrated into the modified electrode (green line). This significant improvement may be ascribed to the excellent electrical conductivity of ERGO.
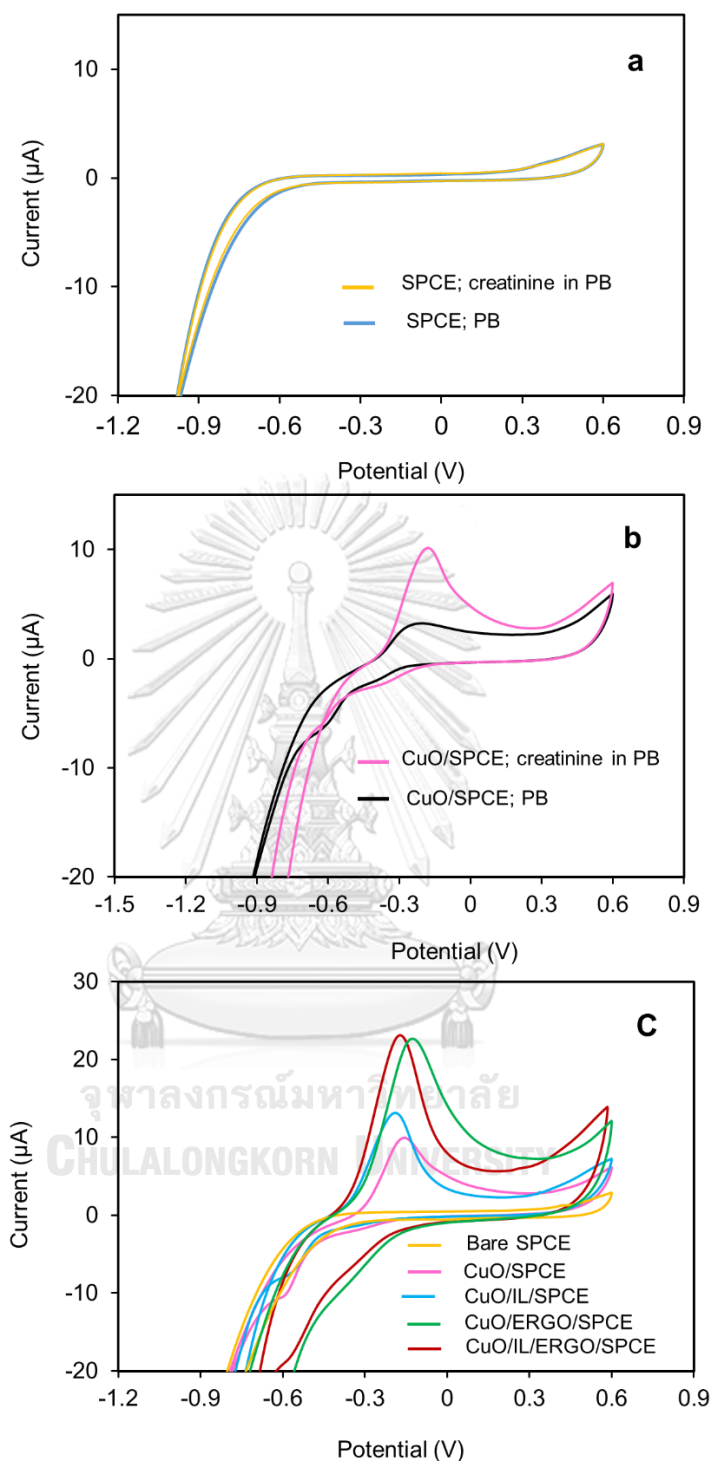
Fig. 4.18 (a) Cyclic voltammograms of a SPCE, (b) CuO/IL/ERGO/SPCE measured in PB (pH 7.4) with and without 0.5 mM creatinine, and cyclic voltammogram of a SPCE, and (c) four modified electrodes in PB (pH 7.4) with 0.5 mM creatinine at a scan rate of 50 mV s^{-1}.

Although the intensity of oxidation current on CuO/IL/ERGO/SPCE is not significantly higher than CuO/IL/ERGO; however, S/B ratio was investigated to optimize the modified electrode, as shown in Fig. 4.19. This result exhibits the S/B value of CuO/IL/ERGO/SPCE is the highest compared to others verifying that the integration of CuO/IL/ERGO/SPCE working electrodes into electrochemical PADs enhances the electrocatalytic activity, rate of electron transfer, and electrical conductivity of the electrode (red line). Therefore, CuO/IL/ERGO/SPCE modified electrode improves the overall performances of the device.
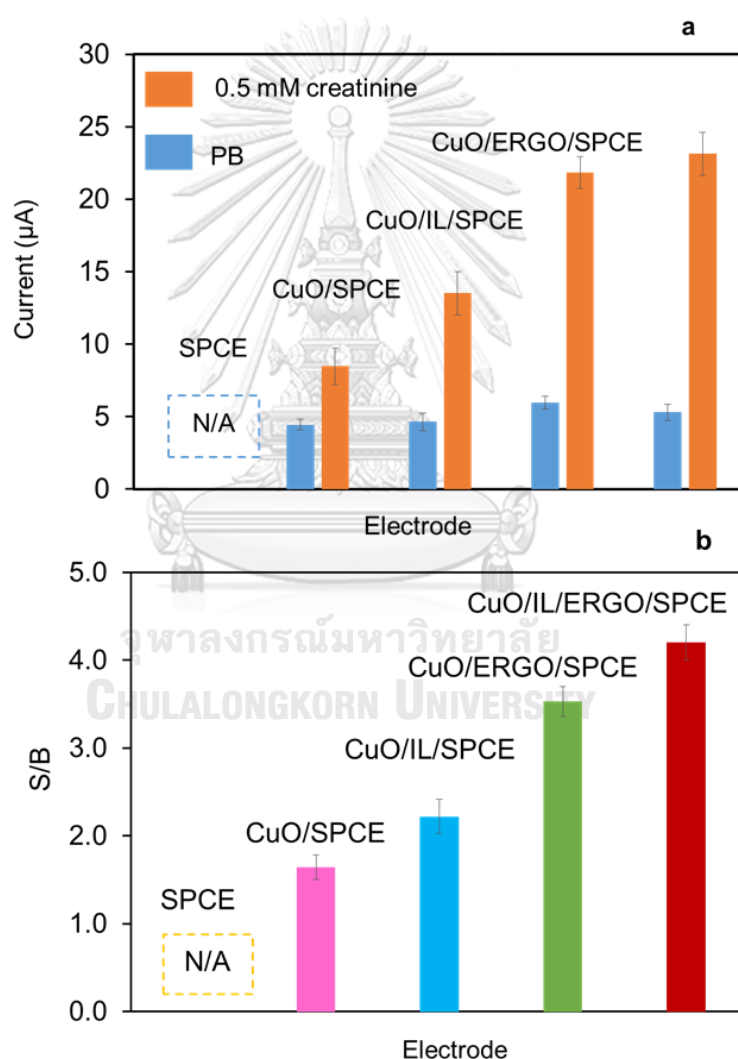
Fig. 4.19 (a) The oxidation current responses of modified electrodes compared to background and (b) signal-to-background current (S/B) ratio extracted from the data in (a). N/A: no detection peak.

Moreover, CuO/IL/ERGO/SPCE electrodes produced using the inkjet deposition approach generated a higher oxidative current for creatinine than those produced via drop-casting; in addition, the inkjet prepared electrodes yielded superior reproducibility (Fig. 4.20). The HP D300 dispenser-produced devices had a more uniform dispersion of CuO/IL particles, which in turn gave rise to their superior performances.
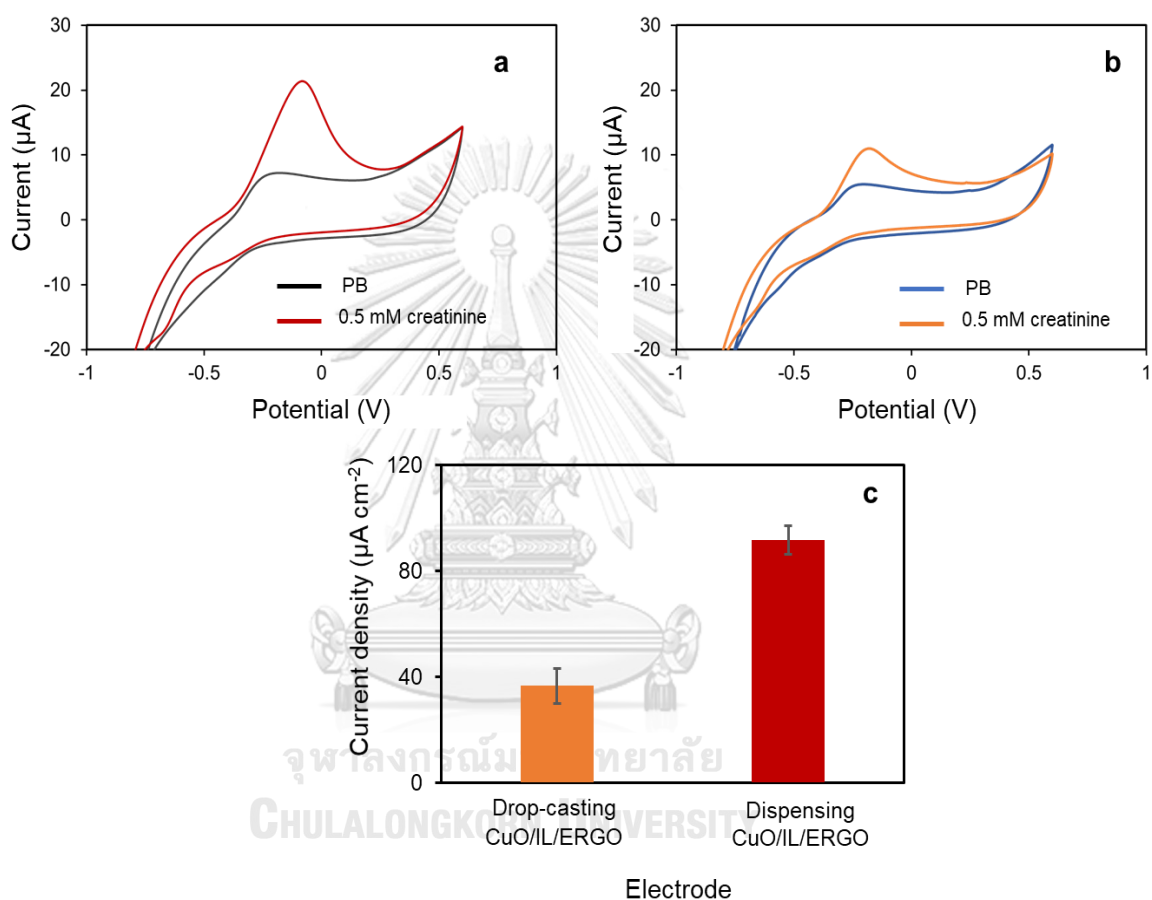
Fig. 4.20 (a) Cyclic voltammograms of CuO/IL/ERGO/SPCE obtained by drop-casting and (b) inkjet dispensing measured in 0.1 PB (pH 7.4) with and without 0.5 mM creatinine at a scan rate of 50 mv s^{-1}, and (c) current response extracted from the data.

4.5 Optimization of experiment parameters

4.5.1 Effect of GO concentration and number of reduction cycles

The modification of electrode using electrochemical reduction of GO can control the thickness and size of the produced ERGO by varying the electrochemical parameter and GO concentration [128]. The amount of GO loading and number of reduction cycle were the crucial factors in the electrode surface modification for the creatinine detection. The effect of GO loading and number of reduction cycles on the current response of creatinine were examined by CV. As shown in Fig. 4.21a, the current response increases remarkably upon the increase of GO concentration from 0 to 0.9 mg mL^{-1}, indicating that the surface concentration of GO greatly increases and accumulates on the electrode, which results in the higher current response of creatinine. However, the current response tends to decrease with GO concentrations above 0.9 mg mL^{-1}, which is likely caused by generated multiple layer of graphene on the electrode surface, making it to have similar characteristic to graphite [104]. Therefore, 0.9 mg mL^{-1} of GO was selected to modify the electrode and the optimal number of reduction cycle was chosen to be 16 cycles (Fig. 4.21b). The current response gradually decreased with more cycles, the decreased signal could be attributed to the agglomeration of generated ERGO, which leads to the lower rate of electron transfer between the analytes and the electrode surface.
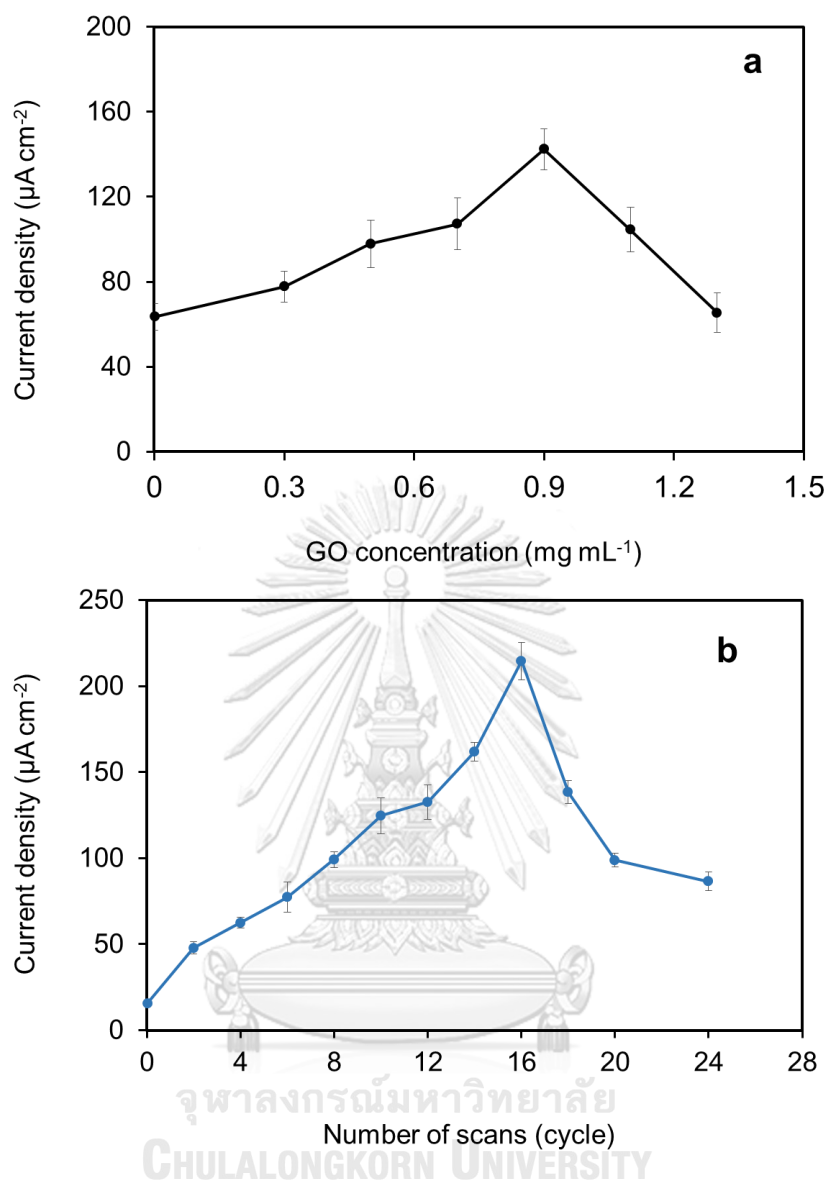
Fig. 4.21 (a) Influence of GO concentration and (b) number of reduction cycles on the current signal of creatinine (0.5 mM) in 0.1 M PB of pH 7.4.

4.5.2. Effect of CuO, IL concentration, CuO/IL loading volume, and number of dispensing layers

To study the effect of the amount of CuO and IL on the current response of creatinine, various electrodes were fabricated by dispensing different concentrations of CuO in a fixed concentration of IL, and dispensing different concentrations of IL with a fixed concentration of CuO. These modified electrodes were investigated by detecting 0.5 mM of creatinine in PB (pH 7.4) using CV. Fig. 4.22a shows the CuO

concentration is varied from 0.5 to 10 mg mL^{-1} and Fig. 4.22b shows the IL concentration is varied from 0 to 10 mg mL^{-1}. The current signal of creatinine is compared for these ranges of CuO and IL concentrations. It is found that 5 mg ml^{-1} of CuO concentration and 3 mg mL^{-1} of IL concentration produce the maximum current response and there is no improvement in current signals with further increase in CuO and IL concentration. Thus, 5 mg mL^{-1} of CuO and 3 mg mL^{-1} of IL concentration was considered as the optimal condition for the modification of the electrode. To obtain the suitable condition of dispensing CuO/IL for detection of creatinine, the loading volume of CuO/IL and number of dispensing layers were also examined by CV. Fig. 4.22c and d shows the current responses of 0.5 mM creatinine at different loading volume of CuO/IL and number of dispensing layers. The current responses remarkably rise with increase in the CuO/IL volume from 0.1 to 0.4 µL and the number of layers from 1 to 2 layers, but the current responses decrease thereafter.
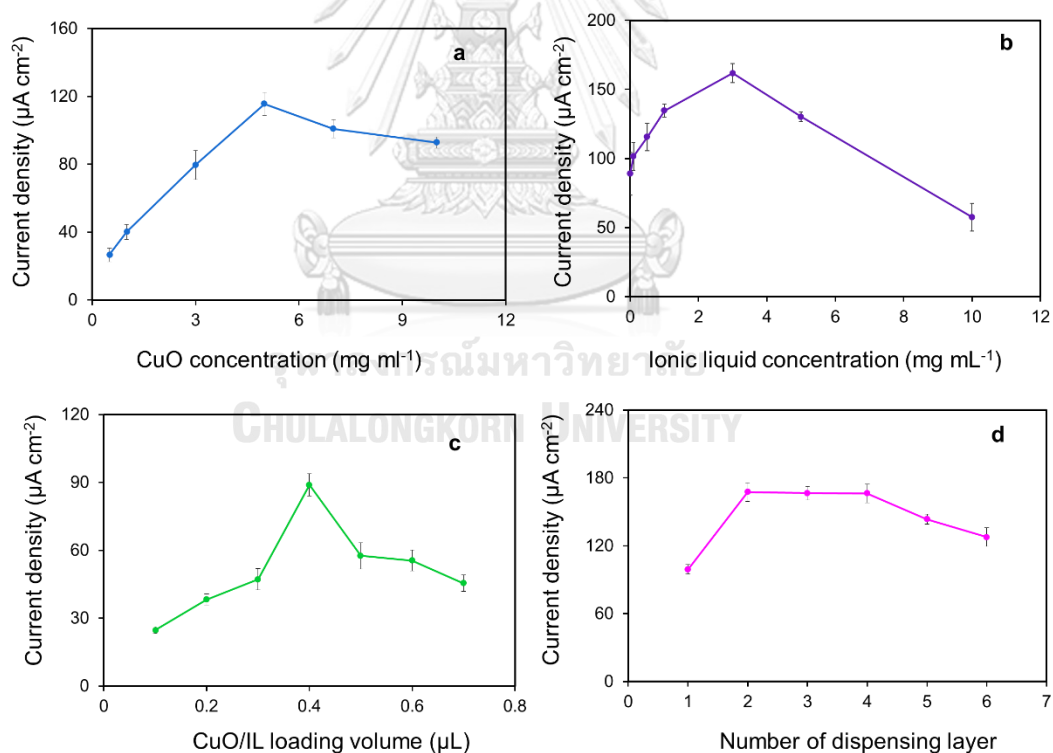
Fig. 4.22 (a) The influence of CuO concentration, (b) IL concentration, (c) CuO/IL composite dispensing volume, and (d) number of dispensing layer on the current signal of 0.5 mM creatinine in 0.1 M PB of pH 7.4.

The decrease in current signals of creatinine could be due to the formation of thick CuO/IL particles, which affect to electrical conductivity. Some evidences of the increased number in dispensing layers of CuO/IL was observed under SEM (Fig. 4.23). Considering the loading volume of CuO/IL was achieved at 0.4 µL by dispensing of 2 layers.
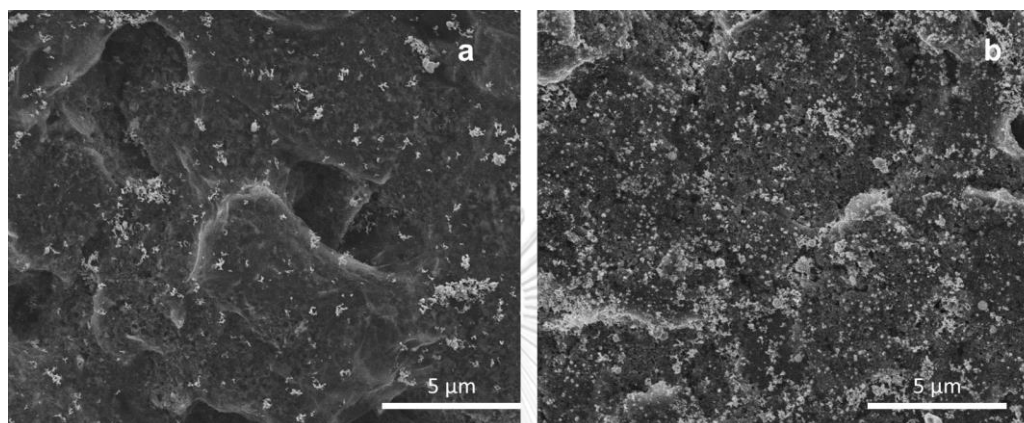
Fig. 4.23 SEM micrographs of CuO/IL/ERGO/SPCE obtained by inkjet dispensing at 0.4 µL of CuO/IL in (a) 1st layer and (b) 2nd layers.

4.5.3. Effect of applied voltage

Amperometry was employed for the quantitative determination of creatinine because it is a very convenient, simple and fast technique which can be easily implemented in portable devices. The response signal can be read much faster than with equilibrium-based techniques. In general, the applied voltage has an effect on the sensing performance of an electrochemical sensor, thus the applied potential was optimized in a quiescent system for electrochemical detection. After optimization, the current response of creatinine in PB (S) to the current response of PB (B) was used to obtain signal-to-background (S/B) ratios, which was used to investigate the current responses from creatinine detection as shown in Fig. 4.24. As the result, the S/B ratio evaluated at -0.1 V provides a maximum value for creatinine. Therefore, applied potential of -0.1 V was chosen for further amperometric detection.
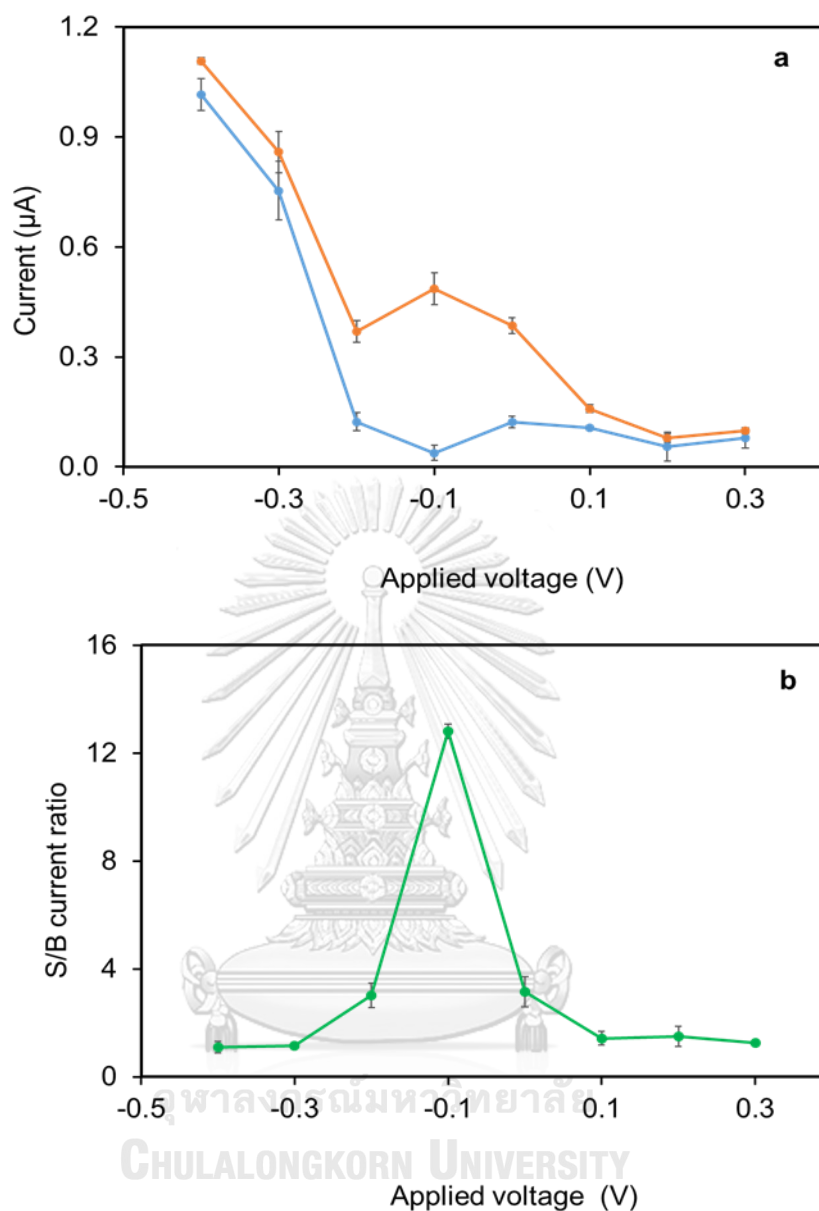
Fig. 4.24 (a) Amperometric current response of PB with 0.5 mM creatinine (orange line) and (b) PB without 0.5 mM creatinine (blue line) for 5 s sampling time. S/B current ratios (green line) extracted from the data in (a).

4.6 Analytical performance of the CuO/IL/ERGO/SPCE on PADs

4.6.1 Ampermetric measurements of creatinine

After obtaining the optimum condition of CuO/IL/ERGO/SPCE, the quantification of creatinine at various concentration in 0.1 M PB (pH 7.4) was

conducted by amperometry at a fixed potential of -0.1 V (vs. Ag/AgCl) and the calibration plot for creatinine was constructed using amperometric current responses at 5 s. As shown in Fig. 4.25a, the current response increases as a function of the creatinine concentration, and the modified electrode shows a linear trend over the range of 0.01 mM to 2 mM with a correlation coefficient of 0.99 (Fig. 4.25b). Based on the linear range, the limit of detection and limit of quantitation were found to be 0.22 μM and 0.74 μM, respectively. The detection limit was calculated as the concentrations which provided the signal at 3 times the standard deviation of blank (n=5). The analytical performances of the proposed system offer a wider linear range and lower detection limit than other electrodes published in creatinine detections, as shown in Table 1.

จุฬาลงกรณ์มหาวิทยาลัย

CHULALONGKORN UNIVERSITY
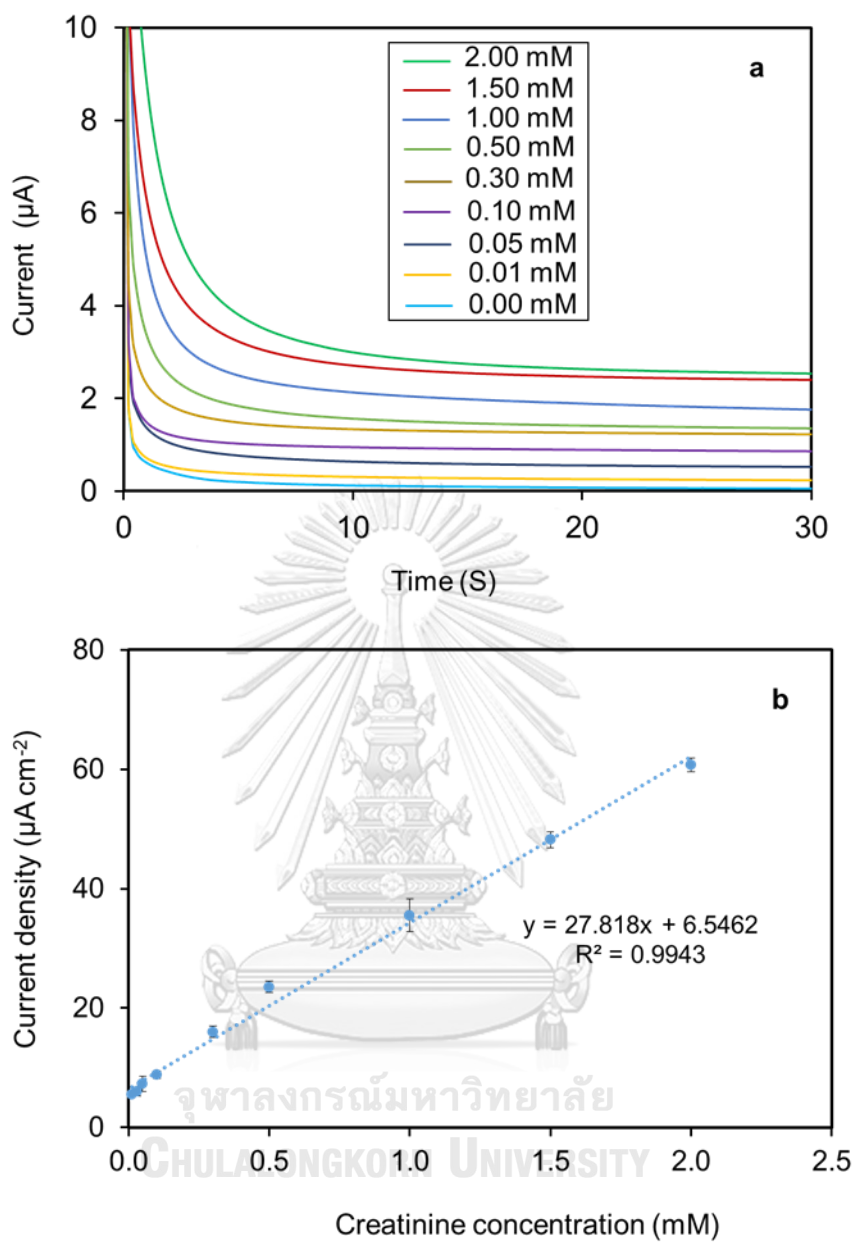
Fig. 4.25 (a) Amperometry measurements recorded on CuO/IL/ERGO/SPCE with different concentrations (from 0.0 to 2.0 mM) in 0.1 M PB (pH 7.4) at a fixed potential of -0.1 vs Ag/AgCl for 30 s and (b) calibration plot for creatinine detection constructed from the signal measurements presented in (a).

Table 4.3 Comparison of analytical performances between the developed and previously reported electrode in creatinine detection methods.

Working electrode	Linear range (µM)	LOD (µM)	Reference
GCE (based on Jaffe's reaction)	1-80	0.4	[129]
EPPG (based on Jaffe's reaction)	0-6000	720	[130]
ZnO-NPs/CHIT/c-MWCNT/PANI/Pt electrode (enzymatic)	10-650	0.5	[67]
Fe_3O_4-NPs/CHIT/g-PANI (enzymatic)	1-800	1.0	[131]
Pt/SPCE (enzymatic)	8-180	-	[132]
Cu/Cu electrode (non-enzymatic)	-	0.6	[7]
SPCE (non-enzymatic)	370-3600	8.6	[133]
CuO/IL/ERGO (non-enzymatic)	0.01-2000	0.2	This work

GCE: glassy carbon electrode; EPPG: edge plane pyrolytic graphite; CHIT: chitosan; c-MWCNT: carboxylated multiwall carbon nanotube; PANI: polyaniline; SPCE: screen printed-carbon electrode.

4.6.2 Interference study

The selectivity is a crucial factor in the fabrication of the sensor for practical applications. The common interfering molecules in biological samples such as glucose, uric acid, urea, and ascorbic acid were tested by injecting at physiological concentration in human serum (glucose- 6 mM, uric acid- 125 µM, urea- 6 mM, and

ascorbic 125 µM) in the presence of 100 µM creatinine. The current responses of creatinine oxidation are insignificantly changed and found to be free from these interferences (Fig. 4.26). The result indicates that the CuO/IL/ERGO/SPCE on PAD is selective for the detection of creatinine in the presence of potentially active interfering compounds.
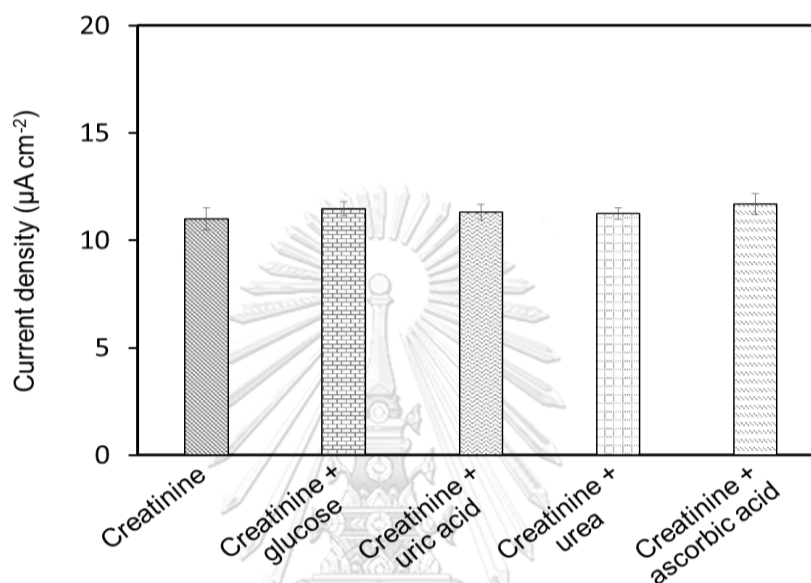
Fig. 4.26 Anodic current responses of the CuO/IL/ERGO/SPCE on PAD sensors in the presence of 0.1 mM creatinine and different interfering compounds at physiological concentrations.

4.6.3 Study of repeatability and reproducibility

The repeatability of the CuO/IL/ERGO/SPCE modified PADs was studied by examining the performance of a single electrode for five repetitive measurements of 0.5 mM of creatinine in PB solution (pH 7.4) using amperometry. It is found that the dispensing electrode shows a relative standard deviation (RSD) of 2.1%, which is lower than the drop-casting electrode (3.0%). The fabrication reproducibility of the modified electrode was investigated by measuring the amperometric response from five different electrodes to 0.5 mM creatinine. The modified electrode obtained from drop-casting has an RSD value at 6.1% while the RSD value of the electrode prepared by dispensing is found to be at 3.8% with approximately 5 times higher current response (Fig. 4.27). The results indicate that the utilization of dispensing

technique not only remarkably minimizes electrode-to-electrode deviation but also enhances the oxidative current for creatinine detection.
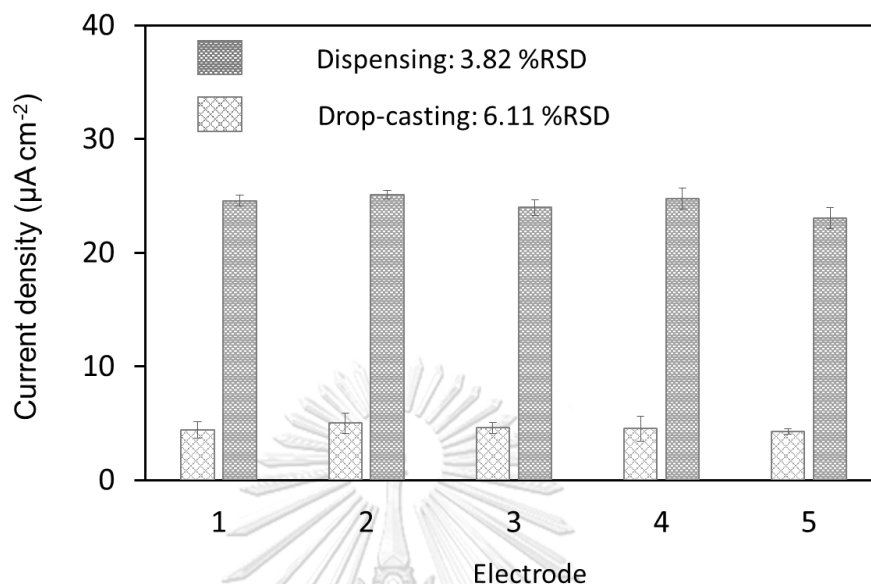
Fig. 4.27 Amperometric current response for five different CuO/IL/ERGO/SPCEs obtained by drop-casting (bars on the left) and inkjet dispensing (bars on right), measured for 0.5 μM creatinine at -0.1 V (vs. Ag/AgCl).

4.6.4 Real sample analysis

In order to demonstrate the practical utility of the sensor, the CuO/IL/ERGO modified paper-based device was applied to the quantification of creatinine in human serum using the standard addition method. Prior to sample analysis, the human serum was prepared using the TCA method as described in Section 2.6, it was then analyzed on three independently prepared electrodes using amperometry. Table 2 shows the creatinine determination results from six different human serum samples and the results are corresponded well with the measurements obtained by immunoturbidimetric assay used in a standard hospital laboratory (Chemistry Analyser COBAS INTEGA® 400 plus).

Table 4.4 Determination of creatinine in human serum samples (n=3).

Sample	Measured by the hospital-used instrument (µM)	Measured by The developed sensor (µM)	RSD (%, n=3)	Accuracy (%)
1	62.76	63.19 ± 3.00	4.74	100.70
2	74.26	73.79 ± 1.16	1.58	99.38
3	77.80	77.10 ± 2.30	2.96	100.27
4	97.24	98.35 ± 2.85	3.01	101.15
5	116.70	114.37 ± 2.80	2.45	98.00
6	137.90	137.00 ± 1.59	1.16	99.35
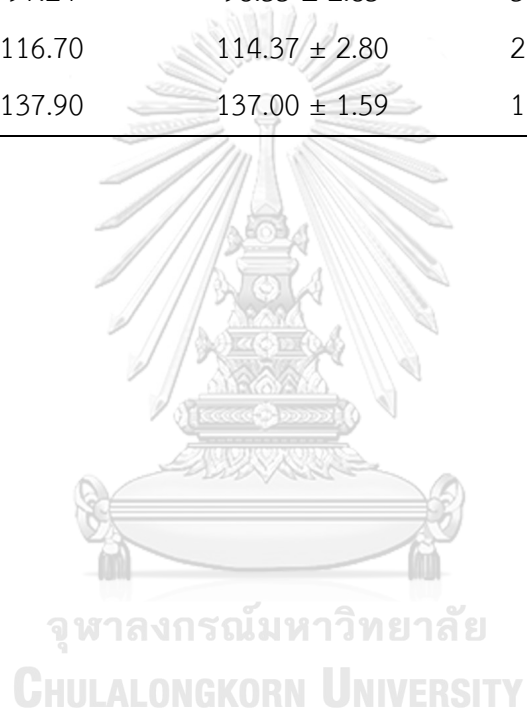
CHAPTER V

CONCLUSION

In this study, the electrochemical sensors were successfully developed and applied for the enzymatic lactate detection and non-enzymatic creatinine detection in biological fluids that can be concluded as following:

Part I: Development of the enzymatic biosensor

An electrochemical sensor based on nickel foam electrode modified by titanium dioxide sol/graphene nanocomposite and lactate oxidase (LOx) has been successfully developed for the sensing of lactate. TiO_2 sol/graphene nanocomposite was synthesized by a sol-gel method and the as-prepared nanocomposite was coated on a 3D porous Ni foam surface. After immobilizing LOx on the surface, the electrode was applied for the detection of H_2O_2 and lactate. The as-prepared nanocomposite and the modified Ni foam were characterized by fourier transform infrared spectroscopy (FT-IR), transmission electron microscopy (TEM) and scanning electron microscopy (SEM) verifying the well intercalation of graphene within TiO_2 sol and then such material was coated on Ni foam surface. Comparing with an unmodified Ni foam, TiO_2 sol/graphene modified Ni foam showed a drastic increase in current response signal (28-fold) towards H_2O_2 suggesting a potential application of this system for a sensitive electrochemical sensor. Then, LOx was immobilized onto the modified electrode for lactate sensor via H_2O_2 detection. The existence of graphene within the nanocomposite drastically increased the sensor sensitivity towards H_2O_2 detection compare to an unmodified Ni foam electrode, while the presence of TiO_2 sol improved graphene dispersion within the nanocomposite and maintained LOx activity allowing for long-term usage. Under the optimal conditions, a wide linear range of 50 µM to 10 mM with a detection limit of 19 µM was obtained for lactate without interfering effect from ascorbic acid, dopamine, and glucose. This platform was sensitive enough for early diagnosis of severe sepsis and septic shock via the detection of concerned lactate level. In addition, the proposed biosensor can significantly improve the current response signal for lactate sensor with high

reproducibility and high stability (RSD < 5%). Ultimately, this system was successfully applied to lactate detection in a biofluidic sample. The results showed the potential of the sensor as an alternative tool for early diagnosis of severe sepsis or septic shock.

Part II: Development of the non-enzymatic sensor

A novel PAD for non-enzymatic creatinine detection based on CuO/IL/ERGO modified paper-based device was successfully developed. The device was fabricated using a HP D300 for dispensing a copper oxide and ionic liquid composite onto an electrochemically reduced graphene modified screen-printed carbon electrode (CuO/IL/ERGO/SPCE) on a PAD. The modified electrode was characterized by electrochemical and microscopic techniques. The electrochemical detection of creatinine was based on the formation of a soluble copper-creatinine complex on the SPCE using amperometry at a constant potential. Experiment results showed that the dispensing technique provided an increased distribution of CuO/IL composite and improved sensitivity and reproducibility of the sensor towards creatinine compared with drop-casting. Under the optimized conditions, PAD exhibited catalytic response towards creatinine in a wide linear range from 0.01 to 2.0 mM and a low detection limit of 0.22 µM (S/N =3). The common physiological interferences were found to have a negligible or minimal effect. In addition, this system was effectively performed in a practical application for the determination of creatinine in human serum. This novel PAD could be an alternative device for screening creatinine in clinical diagnosis to evaluate kidney function of patients.

As summarized above, the sensors could be alternative tools for screening lactate and creatinine level in medical diagnosis, non-hospital point-of-care testing, including home healthcare settings which would benefit to treat the patients and improve the quality of life.

REFERENCES

[1]   F. Alam, S. RoyChoudhury, A.H. Jalal, Y. Umasankar, S. Forouzanfar, N. Akter, S. Bhansali and N. Pala, Lactate biosensing: The emerging point-of-care and personal health monitoring. Biosensors and Bioelectronics, 117 (2018). p. 818-829.

[2]   A. Uzunoglu and L.A. Stanciu, Novel CeO2–CuO-decorated enzymatic lactate biosensors operating in low oxygen environments. Analytica Chimica Acta, 909 (2016). p. 121-128.

[3]   D.C. Angus, W.T. Linde-Zwirble, J. Lidicker, G. Clermont, J. Carcillo and M.R. Pinsky, Epidemiology of severe sepsis in the United States: analysis of incidence, outcome, and associated costs of care. Critical care medicine, 29 (2001). (7): p. 1303-1310.

[4]   R.A. Fowler, M. Hill-Popper, J. Stasinos, C. Petrou, G.D. Sanders and A.M. Garber, Cost-effectiveness of recombinant human activated protein C and the influence of severity of illness in the treatment of patients with severe sepsis. Journal of critical care, 18 (2003). (3): p. 181-191.

[5]   U. Lad, S. Khokhar and G.M. Kale, *Electrochemical creatinine biosensors*. 2008, ACS Publications.

[6]   V. Kumar, S. Hebbar, R. Kalam, S. Panwar, S. Prasad, S. Srikanta, P. Krishnaswamy and N. Bhat, Creatinine-iron complex and its use in electrochemical measurement of urine creatinine. IEEE Sensors Journal, 18 (2017). (2): p. 830-836.

[7]   C.-H. Chen and M.S. Lin, A novel structural specific creatinine sensing scheme for the determination of the urine creatinine. Biosensors and Bioelectronics, 31 (2012). (1): p. 90-94.

[8]   J. Ping, Y. Wang, Y. Ying and J. Wu, Application of electrochemically reduced graphene oxide on screen-printed ion-selective electrode. Analytical chemistry, 84 (2012). (7): p. 3473-3479.

[9]   C.W. Foster, J. Pillay, J.P. Metters and C.E. Banks, Cobalt phthalocyanine modified electrodes utilised in electroanalysis: Nano-structured modified

electrodes vs. bulk modified screen-printed electrodes. Sensors, 14 (2014). (11): p. 21905-21922.

[10] P. Najafisayar and M. Bahrololoom, The effect of pulse electropolymerization on the electrochemical properties of polythiophene films. Electrochimica Acta, 114 (2013). p. 462-473.

[11] D. Ariyanayagamkumarappa and I. Zhitomirsky, Electropolymerization of polypyrrole films on stainless steel substrates for electrodes of electrochemical supercapacitors. Synthetic Metals, 162 (2012). (9-10): p. 868-872.

[12] S.Y. Chae, G. Rahman and O.-s. Joo, Elucidation of the structural and charge separation properties of titanium-doped hematite films deposited by electrospray method for photoelectrochemical water oxidation. Electrochimica Acta, 297 (2019). p. 784-793.

[13] J.C. Arrebola, A. Caballero, L. Hernán, M. Melero, J. Morales and E.R. Castellón, Electrochemical properties of LiNi0. 5Mn1. 5O4 films prepared by spin-coating deposition. Journal of power sources, 162 (2006). (1): p. 606-613.

[14] J. Nielsen, M. Day, C. Dudenhoefer, H. Paris, K.F. Peters, D. Thomas, K. Ward and J. Yu. *Thermal inkjet system to enable picoliter dispense of pharmaceutical compounds*. in *NIP & Digital Fabrication Conference*. 2011. Society for Imaging Science and Technology.

[15] A. Turner, I. Karube and G.S. Wilson, Biosensors: fundamentals and applications. 1987: Oxford university press.

[16] D.R. Thevenot, K. Toth, R.A. Durst and G.S. Wilson, Electrochemical biosensors: recommended definitions and classification. Pure and applied chemistry, 71 (1999). (12): p. 2333-2348.

[17] J.D. Newman and S.J. Setford, Enzymatic biosensors. Molecular Biotechnology, 32 (2006). (3): p. 249-268.

[18] L.C. Clark Jr and C. Lyons, Electrode systems for continuous monitoring in cardiovascular surgery. Annals of the New York Academy of sciences, 102 (1962). (1): p. 29-45.

[19] S. Carrara, S. Ghoreishizadeh, J. Olivo, I. Taurino, C. Baj-Rossi, A. Cavallini, M. Op de Beeck, C. Dehollain, W. Burleson and F.G. Moussy, Fully integrated biochip

platforms for advanced healthcare. Sensors, 12 (2012). (8): p. 11013-11060.

[20]   C.R. Lowe, Biosensors. Trends in biotechnology, 2 (1984). (3): p. 59-65.

[21]   X. Zhang, H. Ju and J. Wang, Electrochemical sensors, biosensors and their biomedical applications. 2011: Academic Press.

[22]   D.R. Thévenot, K. Toth, R.A. Durst and G.S. Wilson, Electrochemical biosensors: recommended definitions and classification. Analytical Letters, 34 (2001). (5): p. 635-659.

[23]   D. Grieshaber, R. MacKenzie, J. Vörös and E. Reimhult, Electrochemical biosensors-sensor principles and architectures. Sensors, 8 (2008). (3): p. 1400-1458.

[24]   A. Padwa, Comprehensive heterocyclic chemistry III. Katritzky, AR, (2008). p. 1-105.

[25]   S. Brahim, D. Narinesingh and A. Guiseppi-Elie, Amperometric determination of cholesterol in serum using a biosensor of cholesterol oxidase contained within a polypyrrole–hydrogel membrane. Analytica chimica acta, 448 (2001). (1-2): p. 27-36.

[26]   S. Mundinamani and M. Rabinal, Cyclic voltammetric studies on the role of electrode, electrode surface modification and electrolyte solution of an electrochemical cell. J. Appl. Chem, 7 (2014). p. 45-52.

[27]   P.T. Kissinger and W.R. Heineman, Cyclic voltammetry. Journal of Chemical Education, 60 (1983). (9): p. 702.

[28]   A.J. Bard and L.R. Faulkner, Fundamentals and applications. Electrochemical Methods, 2 (2001). p. 482.

[29]   P.D. Voegel and R.P. Baldwin, Electrochemical detection in capillary electrophoresis. Electrophoresis, 18 (1997). (12‐13): p. 2267-2278.

[30]   A.J. Blasco and A. Escarpa, Electrochemical detection in capillary electrophoresis on microchips, in Comprehensive Analytical Chemistry. 2005, Elsevier. p. 703-758.

[31]   G.S. Wilson and Y. Hu, Enzyme-based biosensors for in vivo measurements. Chemical Reviews, 100 (2000). (7): p. 2693-2704.

[32]   V. Bhatt, Essentials of Coordination Chemistry: A Simplified Approach with 3D Visuals. 2015: Academic Press.

[33]   N.J. Ronkainen, H.B. Halsall and W.R. Heineman, Electrochemical biosensors. Chemical Society Reviews, 39 (2010). (5): p. 1747-1763.

[34]   W. Putzbach and N.J. Ronkainen, Immobilization techniques in the fabrication of nanomaterial-based electrochemical biosensors: A review. Sensors, 13 (2013). (4): p. 4811-4840.

[35]   A.K. Sarma, P. Vatsyayan, P. Goswami and S.D. Minteer, Recent advances in material science for developing enzyme electrodes. Biosensors and Bioelectronics, 24 (2009). (8): p. 2313-2322.

[36]   C. Yuan, L. Yang, L. Hou, L. Shen, X. Zhang and X.W. Lou, Growth of ultrathin mesoporous Co3O4 nanosheet arrays on Ni foam for high-performance electrochemical capacitors. Energy & Environmental Science, 5 (2012). (7): p. 7883-7887.

[37]   M. Khairy and S.A. El-Safty, Hemoproteins–nickel foam hybrids as effective supercapacitors. Chemical Communications, 50 (2014). (11): p. 1356-1358.

[38]   S.A. El-Safty, M. Shenashen and M. Khairy, Bioadsorption of proteins on large mesocage-shaped mesoporous alumina monoliths. Colloids and Surfaces B: Biointerfaces, 103 (2013). p. 288-297.

[39]   W. Lu, X. Qin, A.M. Asiri, A.O. Al-Youbi and X. Sun, Ni foam: a novel three-dimensional porous sensing platform for sensitive and selective nonenzymatic glucose detection. Analyst, 138 (2013). (2): p. 417-420.

[40]   N. Akhtar, S.A. El-Safty and M. Khairy, Simple and sensitive electrochemical sensor-based three-dimensional porous Ni-hemoglobin composite electrode. Chemosensors, 2 (2014). (4): p. 235-250.

[41]   N. Akhtar, S.A. El-Safty, M. Khairy and W.A. El-Said, Fabrication of a highly selective nonenzymatic amperometric sensor for hydrogen peroxide based on nickel foam/cytochrome c modified electrode. Sensors and Actuators B: Chemical, 207 (2015). p. 158-166.

[42]   M.M. Rahman, A. Ahammad, J.-H. Jin, S.J. Ahn and J.-J. Lee, A comprehensive review of glucose biosensors based on nanostructured metal-oxides. Sensors, 10

(2010). (5): p. 4855-4886.

[43]   J. Yu and H. Ju, Amperometric biosensor for hydrogen peroxide based on hemoglobin entrapped in titania sol–gel film. Analytica Chimica Acta, 486 (2003). (2): p. 209-216.

[44]   X. Xu, J. Zhao, D. Jiang, J. Kong, B. Liu and J. Deng, TiO2 sol-gel derived amperometric biosensor for H2O2 on the electropolymerized phenazine methosulfate modified electrode. Analytical and bioanalytical chemistry, 374 (2002). (7-8): p. 1261-1266.

[45]   J. Kochana and J. Adamski, Detection of NADH and ethanol at a graphite electrode modified with titania sol-gel/Meldola's Blue/MWCNT/Nafion nanocomposite film. Open Chemistry, 10 (2012). (1): p. 224-231.

[46]   M. Tasviri, H.-A. Rafiee-Pour, H. Ghourchian and M.R. Gholami, Amine functionalized TiO 2–carbon nanotube composite: synthesis, characterization and application to glucose biosensing. Applied Nanoscience, 1 (2011). (4): p. 189-195.

[47]   Y. Shao, J. Wang, H. Wu, J. Liu, I.A. Aksay and Y. Lin, Graphene based electrochemical sensors and biosensors: a review. Electroanalysis, 22 (2010). (10): p. 1027-1036.

[48]   H.D. Jang, S.K. Kim, H. Chang, K.-M. Roh, J.-W. Choi and J. Huang, A glucose biosensor based on TiO2–Graphene composite. Biosensors and Bioelectronics, 38 (2012). (1): p. 184-188.

[49]   E. Casero, C. Alonso, M.D. Petit-Domínguez, L. Vázquez, A.M. Parra-Alfambra, P. Merino, S. Álvarez-García, A. de Andrés, E. Suárez and F. Pariente, Lactate biosensor based on a bionanocomposite composed of titanium oxide nanoparticles, photocatalytically reduced graphene, and lactate oxidase. Microchimica Acta, 181 (2014). (1-2): p. 79-87.

[50]   J. Uribarri, M.S. Oh and H.J. Carroll, D-lactic acidosis: a review of clinical presentation, biochemical features, and pathophysiologic mechanisms. MEDICINE-BALTIMORE-, 77 (1998). p. 73-82.

[51]   G.J. Kost and M. McQueen, New whole blood analyzers and their impact on cardiac and critical care. Critical reviews in clinical laboratory sciences, 30 (1993).

(2): p. 153-202.

[52]   M.L. Goodwin, J.E. Harris, A. Hernández and L.B. Gladden, Blood lactate measurements and analysis during exercise: a guide for clinicians. Journal of diabetes science and technology, 1 (2007). (4): p. 558-569.

[53]   S.B. Barker and W.H. Summerson, The colorimetric determination of lactic acid in biological material. Journal of Biological Chemistry, 138 (1941). p. 535-554.

[54]   B. Heinemann, A rapid colorimetric method for the determination of lactic acid in milk. Journal of Dairy Science, 23 (1940). (10): p. 969-972.

[55]   F. Wu, Y. Huang and C. Huang, Chemiluminescence biosensor system for lactic acid using natural animal tissue as recognition element. Biosensors and Bioelectronics, 21 (2005). (3): p. 518-522.

[56]   J. Ren, A. Dean Sherry and C.R. Malloy, Noninvasive monitoring of lactate dynamics in human forearm muscle after exhaustive exercise by 1H‑magnetic resonance spectroscopy at 7 tesla. Magnetic resonance in medicine, 70 (2013). (3): p. 610-619.

[57]   N. Nikolaus and B. Strehlitz, Amperometric lactate biosensors and their application in (sports) medicine, for life quality and wellbeing. Microchimica Acta, 160 (2008). (1-2): p. 15-55.

[58]   L. Han, R. Liu, C. Li, H. Li, C. Li, G. Zhang and J. Yao, Controlled synthesis of double-shelled CeO 2 hollow spheres and enzyme-free electrochemical bio-sensing properties for uric acid. Journal of Materials Chemistry, 22 (2012). (33): p. 17079-17085.

[59]   Y. Haldorai, J.Y. Kim, A.E. Vilian, N.S. Heo, Y.S. Huh and Y.-K. Han, An enzyme-free electrochemical sensor based on reduced graphene oxide/Co3O4 nanospindle composite for sensitive detection of nitrite. Sensors and Actuators B: Chemical, 227 (2016). p. 92-99.

[60]   J. Zhou, Y. Zhao, J. Bao, D. Huo, H. Fa, X. Shen and C. Hou, One-step electrodeposition of Au-Pt bimetallic nanoparticles on MoS2 nanoflowers for hydrogen peroxide enzyme-free electrochemical sensor. Electrochimica Acta, 250 (2017). p. 152-158.

[61]   S. Kim, K. Kim, H.-J. Kim, H.-N. Lee, T.J. Park and Y.M. Park, Non-enzymatic electrochemical lactate sensing by NiO and Ni (OH) 2 electrodes: A mechanistic investigation. Electrochimica Acta, 276 (2018). p. 240-246.

[62]   N. Shen, H. Xu, W. Zhao, Y. Zhao and X. Zhang, Highly Responsive and Ultrasensitive Non-Enzymatic Electrochemical Glucose Sensor Based on Au Foam. Sensors, 19 (2019). (5): p. 1203.

[63]   T. Tsuchida and K. Yoda, Multi-enzyme membrane electrodes for determination of creatinine and creatine in serum. Clinical Chemistry, 29 (1983). (1): p. 51-55.

[64]   S. Yadav, A. Kumar and C. Pundir, Amperometric creatinine biosensor based on covalently coimmobilized enzymes onto carboxylated multiwalled carbon nanotubes/polyaniline composite film. Analytical biochemistry, 419 (2011). (2): p. 277-283.

[65]   H.H. Taussky, A procedure increasing the specificity of the Jaefe reaction for the determination of creatine and creatinine in urine and peasma. Clinica Chimica Acta, 1 (1956). (3): p. 210-224.

[66]   R. Vaishya, S. Arora, B. Singh and V. Mallika, Modification of Jaffe's kinetic method decreases bilirubin interference: A preliminary report. Indian Journal of clinical biochemistry, 25 (2010). (1): p. 64-66.

[67]   S. Yadav, R. Devi, A. Kumar and C. Pundir, Tri-enzyme functionalized ZnO-NPs/CHIT/c-MWCNT/PANI composite film for amperometric determination of creatinine. Biosensors and Bioelectronics, 28 (2011). (1): p. 64-70.

[68]   T. Osaka, S. Komaba and A. Amano, Highly sensitive microbiosensor for creatinine based on the combination of inactive polypyrrole with polyion complexes. Journal of the Electrochemical Society, 145 (1998). (2): p. 406-408.

[69]   M. Zhybak, V. Beni, M. Vagin, E. Dempsey, A. Turner and Y. Korpan, Creatinine and urea biosensors based on a novel ammonium ion-selective copper-polyaniline nano-composite. Biosensors and Bioelectronics, 77 (2016). p. 505-511.

[70]   S. Yadav, R. Devi, P. Bhar, S. Singhla and C. Pundir, Immobilization of creatininase, creatinase and sarcosine oxidase on iron oxide nanoparticles/chitosan-g-polyaniline modified Pt electrode for detection of

creatinine. Enzyme and microbial technology, 50 (2012). (4-5): p. 247-254.

[71] V. Serafín, P. Hernández, L. Agüí, P. Yáñez-Sedeño and J. Pingarrón, Electrochemical biosensor for creatinine based on the immobilization of creatininase, creatinase and sarcosine oxidase onto a ferrocene/horseradish peroxidase/gold nanoparticles/multi-walled carbon nanotubes/Teflon composite electrode. Electrochimica Acta, 97 (2013). p. 175-183.

[72] T. Yasukawa, Y. Kiba and F. Mizutani, A Dual Electrochemical Sensor Based on a Test-strip Assay for the Quantitative Determination of Albumin and Creatinine. Analytical Sciences, 31 (2015). (7): p. 583-589.

[73] A. Apilux, W. Dungchai, W. Siangproh, N. Praphairaksit, C.S. Henry and O. Chailapakul, Lab-on-paper with dual electrochemical/colorimetric detection for simultaneous determination of gold and iron. Analytical chemistry, 82 (2010). (5): p. 1727-1732.

[74] A.W. Martinez, S.T. Phillips, M.J. Butte and G.M. Whitesides, Patterned paper as a platform for inexpensive, low-volume, portable bioassays. Angewandte Chemie International Edition, 46 (2007). (8): p. 1318-1320.

[75] W. Dungchai, O. Chailapakul and C.S. Henry, Electrochemical detection for paper-based microfluidics. Analytical chemistry, 81 (2009). (14): p. 5821-5826.

[76] N. Ruecha, R. Rangkupan, N. Rodthongkum and O. Chailapakul, Novel paper-based cholesterol biosensor using graphene/polyvinylpyrrolidone/polyaniline nanocomposite. Biosensors and Bioelectronics, 52 (2014). p. 13-19.

[77] X. Li, C. Zhao and X. Liu, A paper-based microfluidic biosensor integrating zinc oxide nanowires for electrochemical glucose detection. Microsystems & Nanoengineering, 1 (2015). p. 15014.

[78] Y. Wang, S. Wang, L. Tao, Q. Min, J. Xiang, Q. Wang, J. Xie, Y. Yue, S. Wu and X. Li, A disposable electrochemical sensor for simultaneous determination of norepinephrine and serotonin in rat cerebrospinal fluid based on MWNTs-ZnO/chitosan composites modified screen-printed electrode. Biosensors and Bioelectronics, 65 (2015). p. 31-38.

[79] H. Beitollai, F. Garkani Nejad, S. Tajik, S. Jahani and P. Biparva, Voltammetric

determination of amitriptyline based on graphite screen printed electrode modified with a Copper Oxide nanoparticles. International Journal of Nano Dimension, 8 (2017). (3): p. 197-205.

[80]   M. Mitewa, Coordination properties of the bioligands creatinine and creatine in various reaction media. Coordination chemistry reviews, 140 (1995). p. 1-25.

[81]   J. Raveendran, P. Resmi, T. Ramachandran, B.G. Nair and T.S. Babu, Fabrication of a disposable non-enzymatic electrochemical creatinine sensor. Sensors and Actuators B: Chemical, 243 (2017). p. 589-595.

[82]   S. Reddy, B.K. Swamy and H. Jayadevappa, CuO nanoparticle sensor for the electrochemical determination of dopamine. Electrochimica Acta, 61 (2012). p. 78-86.

[83]   J. Ping, S. Ru, K. Fan, J. Wu and Y. Ying, Copper oxide nanoparticles and ionic liquid modified carbon electrode for the non-enzymatic electrochemical sensing of hydrogen peroxide. Microchimica Acta, 171 (2010). (1-2): p. 117-123.

[84]   P.M. Nia, W.P. Meng, F. Lorestani, M. Mahmoudian and Y. Alias, Electrodeposition of copper oxide/polypyrrole/reduced graphene oxide as a nonenzymatic glucose biosensor. Sensors and Actuators B: Chemical, 209 (2015). p. 100-108.

[85]   S. Chaiyo, E. Mehmeti, K. Žagar, W. Siangproh, O. Chailapakul and K. Kalcher, Electrochemical sensors for the simultaneous determination of zinc, cadmium and lead using a Nafion/ionic liquid/graphene composite modified screen-printed carbon electrode. Analytica chimica acta, 918 (2016). p. 26-34.

[86]   H. Xu, H.-Y. Xiong, Q.-X. Zeng, L. Jia, Y. Wang and S.-F. Wang, Direct electrochemistry and electrocatalysis of heme proteins immobilized in single-wall carbon nanotubes-surfactant films in room temperature ionic liquids. Electrochemistry Communications, 11 (2009). (2): p. 286-289.

[87]   H. Naeim, F. Kheiri, M. Sirousazar and A. Afghan, Ionic liquid/reduced graphene oxide/nickel-palladium nanoparticle hybrid synthesized for non-enzymatic electrochemical glucose sensing. Electrochimica Acta, 282 (2018). p. 137-146.

[88]   Y. Li, X. Zhai, H. Wang, X. Liu, L. Guo, X. Ji, L. Wang, H. Qiu and X. Liu, Non-enzymatic sensing of uric acid using a carbon nanotube ionic-liquid paste

electrode modified with poly (β-cyclodextrin). Microchimica Acta, 182 (2015). (11-12): p. 1877-1884.

[89]   J.S. Bunch, A.M. Van Der Zande, S.S. Verbridge, I.W. Frank, D.M. Tanenbaum, J.M. Parpia, H.G. Craighead and P.L. McEuen, Electromechanical resonators from graphene sheets. Science, 315 (2007). (5811): p. 490-493.

[90]   K.R. Ratinac, W. Yang, J.J. Gooding, P. Thordarson and F. Braet, Graphene and related materials in electrochemical sensing. Electroanalysis, 23 (2011). (4): p. 803-826.

[91]   H.C. Schniepp, J.-L. Li, M.J. McAllister, H. Sai, M. Herrera-Alonso, D.H. Adamson, R.K. Prud'homme, R. Car, D.A. Saville and I.A. Aksay, Functionalized single graphene sheets derived from splitting graphite oxide. The Journal of Physical Chemistry B, 110 (2006). (17): p. 8535-8539.

[92]   Z. Wang, X. Zhou, J. Zhang, F. Boey and H. Zhang, Direct electrochemical reduction of single-layer graphene oxide and subsequent functionalization with glucose oxidase. The Journal of Physical Chemistry C, 113 (2009). (32): p. 14071-14075.

[93]   Z. Wang, H. Wang, Z. Zhang, X. Yang and G. Liu, Sensitive electrochemical determination of trace cadmium on a stannum film/poly (p-aminobenzene sulfonic acid)/electrochemically reduced graphene composite modified electrode. Electrochimica Acta, 120 (2014). p. 140-146.

[94]   D. Li, M.B. Müller, S. Gilje, R.B. Kaner and G.G. Wallace, Processable aqueous dispersions of graphene nanosheets. Nature nanotechnology, 3 (2008). (2): p. 101.

[95]   S. Mutyala and J. Mathiyarasu, A reagentless non-enzymatic hydrogen peroxide sensor presented using electrochemically reduced graphene oxide modified glassy carbon electrode. Materials Science and Engineering: C, 69 (2016). p. 398-406.

[96]   J.-M. Jian, L. Fu, J. Ji, L. Lin, X. Guo and T.-L. Ren, Electrochemically reduced graphene oxide/gold nanoparticles composite modified screen-printed carbon electrode for effective electrocatalytic analysis of nitrite in foods. Sensors and

Actuators B: Chemical, 262 (2018). p. 125-136.

[97] G.C. Bandara, C.A. Heist and V.T. Remcho, Patterned polycaprolactone-filled glass microfiber microfluidic devices for total protein content analysis. Talanta, 176 (2018). p. 589-594.

[98] G.C. Bandara, C.A. Heist and V.T. Remcho, Chromatographic Separation and Visual Detection on Wicking Microfluidic Devices: Quantitation of Cu2+ in Surface, Ground, and Drinking Water. Analytical chemistry, 90 (2018). (4): p. 2594-2600.

[99] R.E. Jones, W. Zheng, J.C. McKew and C.Z. Chen, An alternative direct compound dispensing method using the HP D300 digital dispenser. Journal of laboratory automation, 18 (2013). (5): p. 367-374.

[100] N. Promphet, P. Rattanawaleedirojn and N. Rodthongkum, Electroless NiP-TiO2 sol-RGO: A smart coating for enhanced corrosion resistance and conductivity of steel. Surface and Coatings Technology, 325 (2017). p. 604-610.

[101] P. Rattanawaleedirojn, K. Saengkiettiyut, Y. Boonyongmaneerat, S. Sangsuk, N. Promphet and N. Rodthongkum, TiO 2 sol-embedded in electroless Ni–P coating: a novel approach for an ultra-sensitive sorbitol sensor. RSC Advances, 6 (2016). (73): p. 69261-69269.

[102] S. Jampasa, W. Wonsawat, N. Rodthongkum, W. Siangproh, P. Yanatatsaneejit, T. Vilaivan and O. Chailapakul, Electrochemical detection of human papillomavirus DNA type 16 using a pyrrolidinyl peptide nucleic acid probe immobilized on screen-printed carbon electrodes. Biosensors and Bioelectronics, 54 (2014). p. 428-434.

[103] S. Chaiyo, E. Mehmeti, W. Siangproh, T.L. Hoang, H.P. Nguyen, O. Chailapakul and K. Kalcher, Non-enzymatic electrochemical detection of glucose with a disposable paper-based sensor using a cobalt phthalocyanine–ionic liquid–graphene composite. Biosensors and Bioelectronics, 102 (2018). p. 113-120.

[104] S. Jampasa, W. Siangproh, K. Duangmal and O. Chailapakul, Electrochemically reduced graphene oxide-modified screen-printed carbon electrodes for a simple and highly sensitive electrochemical detection of synthetic colorants in beverages. Talanta, 160 (2016). p. 113-124.

[105] F. Bugamelli, C. Marcheselli, E. Barba and M. Raggi, Determination of l-dopa, carbidopa, 3-O-methyldopa and entacapone in human plasma by HPLC–ED. Journal of pharmaceutical and biomedical analysis, 54 (2011). (3): p. 562-567.

[106] G.D. Tarigh, F. Shemirani and N.S. Maz'hari, Fabrication of a reusable magnetic multi-walled carbon nanotube–TiO 2 nanocomposite by electrostatic adsorption: enhanced photodegradation of malachite green. RSC Advances, 5 (2015). (44): p. 35070-35079.

[107] R. Rahimi, S. Zargari and Z. Sadat Shojaei. *Photoelectrochemical investigation of TiO2-graphene nanocomposites*. in *Proceedings of the 18th International Electronic Conference on Synthetic Organic Chemistry, Basel, Switzerland*. 2014.

[108] M.-y. Duan, J. Li, G. Mele, C. Wang, X.-f. Lu, G. Vasapollo and F.-x. Zhang, Photocatalytic activity of novel tin porphyrin/TiO2 based composites. The Journal of Physical Chemistry C, 114 (2010). (17): p. 7857-7862.

[109] J.-J. Shim, Ionic liquid mediated synthesis of graphene–TiO2 hybrid and its photocatalytic activity. Materials Science and Engineering: B, 180 (2014). p. 38-45.

[110] Y.-p. Zhang, J.-j. Xu, Z.-h. Sun, C.-z. Li and C.-x. Pan, Preparation of graphene and TiO 2 layer by layer composite with highly photocatalytic efficiency. Progress in Natural Science: Materials International, 21 (2011). (6): p. 467-471.

[111] D. Naumenko, V. Snitka, B. Snopok, S. Arpiainen and H. Lipsanen, Graphene-enhanced Raman imaging of TiO2 nanoparticles. Nanotechnology, 23 (2012). (46): p. 465703.

[112] B. Erdem, R.A. Hunsicker, G.W. Simmons, E.D. Sudol, V.L. Dimonie and M.S. El-Aasser, XPS and FTIR surface characterization of TiO2 particles used in polymer encapsulation. Langmuir, 17 (2001). (9): p. 2664-2669.

[113] L. Gu, H. Zhang, Z. Jiao, M. Li, M. Wu and Y. Lei, Glucosamine-induced growth of highly distributed TiO 2 nanoparticles on graphene nanosheets as high-performance photocatalysts. RSC Advances, 6 (2016). (71): p. 67039-67048.

[114] D. Peng, W. Qin, X. Wu and Y. Pan, Improvement of the resistance performance of carbon/cyanate ester composites during vacuum electron radiation by

reduced graphene oxide modified TiO 2. RSC Advances, 5 (2015). (94): p. 77138-77146.

[115] J.S. Lee, K.H. You and C.B. Park, Highly photoactive, low bandgap TiO2 nanoparticles wrapped by graphene. Advanced Materials, 24 (2012). (8): p. 1084-1088.

[116] S.A. El-Safty, M.A. Shenashen, M. Ismael and M. Khairy, Encapsulation of proteins into tunable and giant mesocage alumina. Chemical Communications, 48 (2012). (53): p. 6708-6710.

[117] S. El-Safty, A. Shahat, M.R. Awual and M. Mekawy, Large three-dimensional mesocage pores tailoring silica nanotubes as membrane filters: nanofiltration and permeation flux of proteins. Journal of Materials Chemistry, 21 (2011). (15): p. 5593-5603.

[118] M. Rismanchian, J. Akbari and R. Keshavarzi, Photocatalytic removal of gaseous toluene by titanium dioxide coated on nickel foam: Influence of relative humidity and toluene concentration. International Journal of Environmental Health Engineering, 3 (2014). (1): p. 29.

[119] H. Chen, X. Tan, J. Zhang, Q. Lu, X. Ou, Y. Ruo and S. Chen, An electrogenerated chemiluminescent biosensor based on a gC 3 N 4–hemin nanocomposite and hollow gold nanoparticles for the detection of lactate. RSC Advances, 4 (2014). (106): p. 61759-61766.

[120] H. Ju, X. Zhang and J. Wang, Nanobiosensing: principles, development and application. 2011: Springer Science & Business Media.

[121] S. Suman, R. Singhal, A.L. Sharma, B. Malthotra and C. Pundir, Development of a lactate biosensor based on conducting copolymer bound lactate oxidase. Sensors and Actuators B: Chemical, 107 (2005). (2): p. 768-772.

[122] T.-M. Park, E.I. Iwuoha, M.R. Smyth, R. Freaney and A.J. McShane, Sol-gel based amperometric biosensor incorporating an osmium redox polymer as mediator for detection of L-lactate. Talanta, 44 (1997). (6): p. 973-978.

[123] J. Bai and B. Zhou, Titanium dioxide nanomaterials for sensor applications. Chemical reviews, 114 (2014). (19): p. 10131-10176.

[124] N. Chauhan, J. Narang and C. Pundir, Fabrication of multiwalled carbon

nanotubes/polyaniline modified Au electrode for ascorbic acid determination. Analyst, 136 (2011). (9): p. 1938-1945.

[125] C. Shan, H. Yang, D. Han, Q. Zhang, A. Ivaska and L. Niu, Electrochemical determination of NADH and ethanol based on ionic liquid-functionalized graphene. Biosensors and Bioelectronics, 25 (2010). (6): p. 1504-1508.

[126] J. Huang, J. Li, Y. Yang, X. Wang, B. Wu, J.-i. Anzai, T. Osa and Q. Chen, Development of an amperometric l-lactate biosensor based on l-lactate oxidase immobilized through silica sol–gel film on multi-walled carbon nanotubes/platinum nanoparticle modified glassy carbon electrode. Materials Science and Engineering: C, 28 (2008). (7): p. 1070-1075.

[127] M. Tribet, B. Covelo, A. Sicilia-Zafra, R. Navarrete-Casas, D. Choquesillo-Lazarte, J. González-Pérez, A. Castineiras and J. Niclós-Gutiérrez, Ternary copper (II) complexes with N-carboxymethyl-l-prolinato (2−) ion and imidazole or creatinine: A comparative study of the interligand interactions influencing the molecular recognition and stability. Journal of inorganic biochemistry, 99 (2005). (7): p. 1424-1432.

[128] X.-Y. Peng, X.-X. Liu, D. Diamond and K.T. Lau, Synthesis of electrochemically-reduced graphene oxide film with controllable size and thickness and its use in supercapacitor. Carbon, 49 (2011). (11): p. 3488-3496.

[129] W.R. de Araújo, M.O. Salles and T.R. Paixão, Development of an enzymeless electroanalytical method for the indirect detection of creatinine in urine samples. Sensors and Actuators B: Chemical, 173 (2012). p. 847-851.

[130] E.P. Randviir, D.K. Kampouris and C.E. Banks, An improved electrochemical creatinine detection method via a Jaffe-based procedure. Analyst, 138 (2013). (21): p. 6565-6572.

[131] T. Wen, W. Zhu, C. Xue, J. Wu, Q. Han, X. Wang, X. Zhou and H. Jiang, Novel electrochemical sensing platform based on magnetic field-induced self-assembly of Fe3O4@ Polyaniline nanoparticles for clinical detection of creatinine. Biosensors and Bioelectronics, 56 (2014). p. 180-185.

[132] A. Erlenkötter, M. Fobker and G.-C. Chemnitius, Biosensors and flow-through system for the determination of creatinine in hemodialysate. Analytical and

bioanalytical chemistry, 372 (2002). (2): p. 284-292.

[133] J.-C. Chen, A. Kumar, H.-H. Chung, S.-H. Chien, M.-C. Kuo and J.-M. Zen, An enzymeless electrochemical sensor for the selective determination of creatinine in human urine. Sensors and Actuators B: Chemical, 115 (2006). (1): p. 473-480.

จุฬาลงกรณ์มหาวิทยาลัย
CHULALONGKORN UNIVERSITY

[1]   F. Alam, S. RoyChoudhury, A.H. Jalal, Y. Umasankar, S. Forouzanfar, N. Akter, S. Bhansali and N. Pala, Lactate biosensing: The emerging point-of-care and personal health monitoring. Biosensors and Bioelectronics, 117 (2018). p. 818-829.

[2]   A. Uzunoglu and L.A. Stanciu, Novel CeO2–CuO-decorated enzymatic lactate biosensors operating in low oxygen environments. Analytica Chimica Acta, 909 (2016). p. 121-128.

[3]   D.C. Angus, W.T. Linde-Zwirble, J. Lidicker, G. Clermont, J. Carcillo and M.R. Pinsky, Epidemiology of severe sepsis in the United States: analysis of incidence, outcome, and associated costs of care. Critical care medicine, 29 (2001). (7): p. 1303-1310.

[4]   R.A. Fowler, M. Hill-Popper, J. Stasinos, C. Petrou, G.D. Sanders and A.M. Garber, Cost-effectiveness of recombinant human activated protein C and the influence of severity of illness in the treatment of patients with severe sepsis. Journal of critical care, 18 (2003). (3): p. 181-191.

[5]   U. Lad, S. Khokhar and G.M. Kale, *Electrochemical creatinine biosensors*. 2008, ACS Publications.

[6]   V. Kumar, S. Hebbar, R. Kalam, S. Panwar, S. Prasad, S. Srikanta, P. Krishnaswamy and N. Bhat, Creatinine-iron complex and its use in electrochemical measurement of urine creatinine. IEEE Sensors Journal, 18 (2017). (2): p. 830-836.

[7]   C.-H. Chen and M.S. Lin, A novel structural specific creatinine sensing scheme for the determination of the urine creatinine. Biosensors and Bioelectronics, 31 (2012). (1): p. 90-94.

[8]   J. Ping, Y. Wang, Y. Ying and J. Wu, Application of electrochemically reduced graphene oxide on screen-printed ion-selective electrode. Analytical chemistry, 84 (2012). (7): p. 3473-3479.

[9]   C.W. Foster, J. Pillay, J.P. Metters and C.E. Banks, Cobalt phthalocyanine modified electrodes utilised in electroanalysis: Nano-structured modified electrodes vs. bulk modified screen-printed electrodes. Sensors, 14 (2014). (11): p. 21905-21922.

[10]   P. Najafisayar and M. Bahrololoom, The effect of pulse electropolymerization on the electrochemical properties of polythiophene films. Electrochimica Acta, 114 (2013). p. 462-473.

[11]   D. Ariyanayagamkumarappa and I. Zhitomirsky, Electropolymerization of polypyrrole films on stainless steel substrates for electrodes of electrochemical supercapacitors. Synthetic Metals, 162 (2012). (9-10): p. 868-872.

[12]   S.Y. Chae, G. Rahman and O.-s. Joo, Elucidation of the structural and charge separation properties of titanium-doped hematite films deposited by electrospray method for photoelectrochemical water oxidation. Electrochimica Acta, 297 (2019). p. 784-793.

[13]   J.C. Arrebola, A. Caballero, L. Hernán, M. Melero, J. Morales and E.R. Castellón, Electrochemical properties of LiNi0. 5Mn1. 5O4 films prepared by spin-coating deposition. Journal of power sources, 162 (2006). (1): p. 606-613.

[14]   J. Nielsen, M. Day, C. Dudenhoefer, H. Paris, K.F. Peters, D. Thomas, K. Ward and J. Yu. *Thermal inkjet system to enable picoliter dispense of pharmaceutical compounds*. in *NIP & Digital Fabrication Conference*. 2011. Society for Imaging Science and Technology.

[15]   A. Turner, I. Karube and G.S. Wilson, Biosensors: fundamentals and applications. 1987: Oxford university press.

[16]   D.R. Thevenot, K. Toth, R.A. Durst and G.S. Wilson, Electrochemical biosensors: recommended definitions and classification. Pure and applied chemistry, 71 (1999). (12): p. 2333-2348.

[17]   J.D. Newman and S.J. Setford, Enzymatic biosensors. Molecular Biotechnology, 32 (2006). (3): p. 249-268.

[18]   L.C. Clark Jr and C. Lyons, Electrode systems for continuous monitoring in cardiovascular surgery. Annals of the New York Academy of sciences, 102 (1962). (1): p. 29-45.

[19]   S. Carrara, S. Ghoreishizadeh, J. Olivo, I. Taurino, C. Baj-Rossi, A. Cavallini, M. Op de Beeck, C. Dehollain, W. Burleson and F.G. Moussy, Fully integrated biochip platforms for advanced healthcare. Sensors, 12 (2012). (8): p. 11013-11060.

[20]   C.R. Lowe, Biosensors. Trends in biotechnology, 2 (1984). (3): p. 59-65.

[21]   D.R. Thévenot, K. Toth, R.A. Durst and G.S. Wilson, Electrochemical biosensors: recommended definitions and classification. Analytical Letters, 34 (2001). (5): p. 635-659.

[22]   B.R. Eggins, Chemical sensors and biosensors. Vol. 28. 2008: John Wiley & Sons.

[23]   X. Zhang, H. Ju and J. Wang, Electrochemical sensors, biosensors and their biomedical applications. 2011: Academic Press.

[24]   D. Grieshaber, R. MacKenzie, J. Vörös and E. Reimhult, Electrochemical biosensors-sensor principles and architectures. Sensors, 8 (2008). (3): p. 1400-1458.

[25]   A. Padwa, Comprehensive heterocyclic chemistry III. Katritzky, AR, (2008). p. 1-105.

[26]   S. Brahim, D. Narinesingh and A. Guiseppi-Elie, Amperometric determination of cholesterol in serum using a biosensor of cholesterol oxidase contained within a polypyrrole–hydrogel membrane. Analytica chimica acta, 448 (2001). (1-2): p. 27-36.

[27]   S. Mundinamani and M. Rabinal, Cyclic voltammetric studies on the role of electrode, electrode surface modification and electrolyte solution of an electrochemical cell. J. Appl. Chem, 7 (2014). p. 45-52.

[28]   P.T. Kissinger and W.R. Heineman, Cyclic voltammetry. Journal of Chemical Education, 60 (1983). (9): p. 702.

[29]   A.J. Bard and L.R. Faulkner, Fundamentals and applications. Electrochemical Methods, 2 (2001). p. 482.

[30]   P.D. Voegel and R.P. Baldwin, Electrochemical detection in capillary electrophoresis. Electrophoresis, 18 (1997). (12‑13): p. 2267-2278.

[31]   A.J. Blasco and A. Escarpa, *Electrochemical detection in capillary electrophoresis on microchips*, in *Comprehensive Analytical Chemistry*. 2005, Elsevier. p. 703-758.

[32]   G.S. Wilson and Y. Hu, Enzyme-based biosensors for in vivo measurements. Chemical Reviews, 100 (2000). (7): p. 2693-2704.

[33]   V. Bhatt, Essentials of Coordination Chemistry: A Simplified Approach with 3D Visuals. 2015: Academic Press.

[34]   N.J. Ronkainen, H.B. Halsall and W.R. Heineman, Electrochemical biosensors. Chemical Society Reviews, 39 (2010). (5): p. 1747-1763.

[35]   W. Putzbach and N.J. Ronkainen, Immobilization techniques in the fabrication of nanomaterial-based electrochemical biosensors: A review. Sensors, 13 (2013). (4): p. 4811-4840.

[36]   A.K. Sarma, P. Vatsyayan, P. Goswami and S.D. Minteer, Recent advances in material science for developing enzyme electrodes. Biosensors and Bioelectronics, 24 (2009). (8): p. 2313-2322.

[37]   C. Yuan, L. Yang, L. Hou, L. Shen, X. Zhang and X.W. Lou, Growth of ultrathin mesoporous Co_3O_4 nanosheet arrays on Ni foam for high-performance electrochemical capacitors. Energy & Environmental Science, 5 (2012). (7): p. 7883-7887.

[38]   M. Khairy and S.A. El-Safty, Hemoproteins–nickel foam hybrids as effective supercapacitors. Chemical Communications, 50 (2014). (11): p. 1356-1358.

[39]   S.A. El-Safty, M. Shenashen and M. Khairy, Bioadsorption of proteins on large mesocage-shaped mesoporous alumina monoliths. Colloids and Surfaces B: Biointerfaces, 103 (2013). p. 288-297.

[40]   W. Lu, X. Qin, A.M. Asiri, A.O. Al-Youbi and X. Sun, Ni foam: a novel three-dimensional porous sensing platform for sensitive and selective nonenzymatic glucose detection. Analyst, 138 (2013). (2): p. 417-420.

[41]   N. Akhtar, S.A. El-Safty and M. Khairy, Simple and sensitive electrochemical sensor-based three-dimensional porous Ni-hemoglobin composite electrode. Chemosensors, 2 (2014). (4): p. 235-250.

[42]   N. Akhtar, S.A. El-Safty, M. Khairy and W.A. El-Said, Fabrication of a highly selective nonenzymatic amperometric sensor for hydrogen peroxide based on nickel foam/cytochrome c modified electrode. Sensors and Actuators B: Chemical, 207 (2015). p. 158-166.

[43]   M.M. Rahman, A. Ahammad, J.-H. Jin, S.J. Ahn and J.-J. Lee, A comprehensive review of glucose biosensors based on nanostructured metal-oxides. Sensors, 10 (2010). (5): p. 4855-4886.

[44]   J. Yu and H. Ju, Amperometric biosensor for hydrogen peroxide based on hemoglobin entrapped in titania sol–gel film. Analytica Chimica Acta, 486 (2003). (2): p. 209-216.

[45]   X. Xu, J. Zhao, D. Jiang, J. Kong, B. Liu and J. Deng, TiO2 sol-gel derived amperometric biosensor for H2O2 on the electropolymerized phenazine methosulfate modified electrode. Analytical and bioanalytical chemistry, 374 (2002). (7-8): p. 1261-1266.

[46]   J. Kochana and J. Adamski, Detection of NADH and ethanol at a graphite electrode modified with titania sol-gel/Meldola's Blue/MWCNT/Nafion nanocomposite film. Open Chemistry, 10 (2012). (1): p. 224-231.

[47]   M. Tasviri, H.-A. Rafiee-Pour, H. Ghourchian and M.R. Gholami, Amine functionalized TiO 2–carbon nanotube composite: synthesis, characterization and application to glucose biosensing. Applied Nanoscience, 1 (2011). (4): p. 189-195.

[48]   Y. Shao, J. Wang, H. Wu, J. Liu, I.A. Aksay and Y. Lin, Graphene based electrochemical sensors and biosensors: a review. Electroanalysis, 22 (2010). (10): p. 1027-1036.

[49]   H.D. Jang, S.K. Kim, H. Chang, K.-M. Roh, J.-W. Choi and J. Huang, A glucose biosensor based on TiO2–Graphene composite. Biosensors and Bioelectronics, 38 (2012). (1): p. 184-188.

[50]   E. Casero, C. Alonso, M.D. Petit-Domínguez, L. Vázquez, A.M. Parra-Alfambra, P. Merino, S. Álvarez-García, A. de Andrés, E. Suárez and F. Pariente, Lactate biosensor based on a bionanocomposite composed of titanium oxide nanoparticles, photocatalytically reduced graphene, and lactate oxidase. Microchimica Acta, 181 (2014). (1-2): p. 79-87.

[51]   J. Uribarri, M.S. Oh and H.J. Carroll, D-lactic acidosis: a review of clinical presentation, biochemical features, and pathophysiologic mechanisms. MEDICINE-BALTIMORE-, 77 (1998). p. 73-82.

[52]   G.J. Kost and M. McQueen, New whole blood analyzers and their impact on cardiac and critical care. Critical reviews in clinical laboratory sciences, 30 (1993). (2): p. 153-202.

[53]   M.L. Goodwin, J.E. Harris, A. Hernández and L.B. Gladden, Blood lactate measurements and analysis during exercise: a guide for clinicians. Journal of diabetes science and technology, 1 (2007). (4): p. 558-569.

[54]   S.B. Barker and W.H. Summerson, The colorimetric determination of lactic acid in biological material. Journal of Biological Chemistry, 138 (1941). p. 535-554.

[55]   B. Heinemann, A rapid colorimetric method for the determination of lactic acid in milk. Journal of Dairy Science, 23 (1940). (10): p. 969-972.

[56]   F. Wu, Y. Huang and C. Huang, Chemiluminescence biosensor system for lactic acid using natural animal tissue as recognition element. Biosensors and Bioelectronics, 21 (2005). (3): p. 518-522.

[57]   J. Ren, A. Dean Sherry and C.R. Malloy, Noninvasive monitoring of lactate dynamics in human forearm muscle after exhaustive exercise by 1H‑magnetic resonance spectroscopy at 7 tesla. Magnetic resonance in medicine, 70 (2013). (3): p. 610-619.

[58]   N. Nikolaus and B. Strehlitz, Amperometric lactate biosensors and their application in (sports) medicine, for life quality and wellbeing. Microchimica Acta, 160 (2008). (1-2): p. 15-55.

[59]   L. Han, R. Liu, C. Li, H. Li, C. Li, G. Zhang and J. Yao, Controlled synthesis of double-shelled CeO 2 hollow spheres and enzyme-free electrochemical bio-sensing properties for uric acid. Journal of Materials Chemistry, 22 (2012). (33): p. 17079-17085.

[60]   Y. Haldorai, J.Y. Kim, A.E. Vilian, N.S. Heo, Y.S. Huh and Y.-K. Han, An enzyme-free electrochemical sensor based on reduced graphene oxide/Co3O4 nanospindle composite for sensitive detection of nitrite. Sensors and Actuators B: Chemical, 227 (2016). p. 92-99.

[61]   J. Zhou, Y. Zhao, J. Bao, D. Huo, H. Fa, X. Shen and C. Hou, One-step electrodeposition of Au-Pt bimetallic nanoparticles on MoS2 nanoflowers for hydrogen peroxide enzyme-free electrochemical sensor. Electrochimica Acta, 250 (2017). p. 152-158.

[62]   S. Kim, K. Kim, H.-J. Kim, H.-N. Lee, T.J. Park and Y.M. Park, Non-enzymatic electrochemical lactate sensing by NiO and Ni (OH) 2 electrodes: A mechanistic investigation. Electrochimica Acta, 276 (2018). p. 240-246.

[63]   N. Shen, H. Xu, W. Zhao, Y. Zhao and X. Zhang, Highly Responsive and Ultrasensitive Non-Enzymatic Electrochemical Glucose Sensor Based on Au Foam. Sensors, 19 (2019). (5): p. 1203.

[64]   T. Tsuchida and K. Yoda, Multi-enzyme membrane electrodes for determination of creatinine and creatine in serum. Clinical Chemistry, 29 (1983). (1): p. 51-55.

[65]   S. Yadav, A. Kumar and C. Pundir, Amperometric creatinine biosensor based on covalently coimmobilized enzymes onto carboxylated multiwalled carbon nanotubes/polyaniline composite film. Analytical biochemistry, 419 (2011). (2): p. 277-283.

[66]   H.H. Taussky, A procedure increasing the specificity of the Jaefe reaction for the determination of creatine and creatinine in urine and peasma. Clinica Chimica Acta, 1 (1956). (3): p. 210-224.

[67]   R. Vaishya, S. Arora, B. Singh and V. Mallika, Modification of Jaffe's kinetic method decreases bilirubin interference: A preliminary report. Indian Journal of clinical biochemistry, 25 (2010). (1): p. 64-66.

[68]   S. Yadav, R. Devi, A. Kumar and C. Pundir, Tri-enzyme functionalized ZnO-NPs/CHIT/c-MWCNT/PANI composite film for amperometric determination of creatinine. Biosensors and Bioelectronics, 28 (2011). (1): p. 64-70.

[69]   T. Osaka, S. Komaba and A. Amano, Highly sensitive microbiosensor for creatinine based on the combination of inactive polypyrrole with polyion complexes. Journal of the Electrochemical Society, 145 (1998). (2): p. 406-408.

[70]   M. Zhybak, V. Beni, M. Vagin, E. Dempsey, A. Turner and Y. Korpan, Creatinine and urea biosensors based on a novel ammonium ion-selective copper-polyaniline nano-composite. Biosensors and Bioelectronics, 77 (2016). p. 505-511.

[71]   S. Yadav, R. Devi, P. Bhar, S. Singhla and C. Pundir, Immobilization of creatininase, creatinase and sarcosine oxidase on iron oxide nanoparticles/chitosan-g-polyaniline modified Pt electrode for detection of creatinine. Enzyme and microbial technology, 50 (2012). (4-5): p. 247-254.

[72]   V. Serafín, P. Hernández, L. Agüí, P. Yáñez-Sedeño and J. Pingarrón, Electrochemical biosensor for creatinine based on the immobilization of creatininase,

creatinase and sarcosine oxidase onto a ferrocene/horseradish peroxidase/gold nanoparticles/multi-walled carbon nanotubes/Teflon composite electrode. Electrochimica Acta, 97 (2013). p. 175-183.

[73]   T. Yasukawa, Y. Kiba and F. Mizutani, A Dual Electrochemical Sensor Based on a Test-strip Assay for the Quantitative Determination of Albumin and Creatinine. Analytical Sciences, 31 (2015). (7): p. 583-589.

[74]   A. Apilux, W. Dungchai, W. Siangproh, N. Praphairaksit, C.S. Henry and O. Chailapakul, Lab-on-paper with dual electrochemical/colorimetric detection for simultaneous determination of gold and iron. Analytical chemistry, 82 (2010). (5): p. 1727-1732.

[75]   A.W. Martinez, S.T. Phillips, M.J. Butte and G.M. Whitesides, Patterned paper as a platform for inexpensive, low‐volume, portable bioassays. Angewandte Chemie International Edition, 46 (2007). (8): p. 1318-1320.

[76]   W. Dungchai, O. Chailapakul and C.S. Henry, Electrochemical detection for paper-based microfluidics. Analytical chemistry, 81 (2009). (14): p. 5821-5826.

[77]   N. Ruecha, R. Rangkupan, N. Rodthongkum and O. Chailapakul, Novel paper-based cholesterol biosensor using graphene/polyvinylpyrrolidone/polyaniline nanocomposite. Biosensors and Bioelectronics, 52 (2014). p. 13-19.

[78]   X. Li, C. Zhao and X. Liu, A paper-based microfluidic biosensor integrating zinc oxide nanowires for electrochemical glucose detection. Microsystems & Nanoengineering, 1 (2015). p. 15014.

[79]   Y. Wang, S. Wang, L. Tao, Q. Min, J. Xiang, Q. Wang, J. Xie, Y. Yue, S. Wu and X. Li, A disposable electrochemical sensor for simultaneous determination of norepinephrine and serotonin in rat cerebrospinal fluid based on MWNTs-ZnO/chitosan composites modified screen-printed electrode. Biosensors and Bioelectronics, 65 (2015). p. 31-38.

[80]   H. Beitollai, F. Garkani Nejad, S. Tajik, S. Jahani and P. Biparva, Voltammetric determination of amitriptyline based on graphite screen printed electrode modified with a Copper Oxide nanoparticles. International Journal of Nano Dimension, 8 (2017). (3): p. 197-205.

[81]   M. Mitewa, Coordination properties of the bioligands creatinine and creatine in various reaction media. Coordination chemistry reviews, 140 (1995). p. 1-25.

[82]   J. Raveendran, P. Resmi, T. Ramachandran, B.G. Nair and T.S. Babu, Fabrication of a disposable non-enzymatic electrochemical creatinine sensor. Sensors and Actuators B: Chemical, 243 (2017). p. 589-595.

[83]   S. Reddy, B.K. Swamy and H. Jayadevappa, CuO nanoparticle sensor for the electrochemical determination of dopamine. Electrochimica Acta, 61 (2012). p. 78-86.

[84]   J. Ping, S. Ru, K. Fan, J. Wu and Y. Ying, Copper oxide nanoparticles and ionic liquid modified carbon electrode for the non-enzymatic electrochemical sensing of hydrogen peroxide. Microchimica Acta, 171 (2010). (1-2): p. 117-123.

[85]   P.M. Nia, W.P. Meng, F. Lorestani, M. Mahmoudian and Y. Alias, Electrodeposition of copper oxide/polypyrrole/reduced graphene oxide as a nonenzymatic glucose biosensor. Sensors and Actuators B: Chemical, 209 (2015). p. 100-108.

[86]   S. Chaiyo, E. Mehmeti, K. Žagar, W. Siangproh, O. Chailapakul and K. Kalcher, Electrochemical sensors for the simultaneous determination of zinc, cadmium and lead using a Nafion/ionic liquid/graphene composite modified screen-printed carbon electrode. Analytica chimica acta, 918 (2016). p. 26-34.

[87]   H. Xu, H.-Y. Xiong, Q.-X. Zeng, L. Jia, Y. Wang and S.-F. Wang, Direct electrochemistry and electrocatalysis of heme proteins immobilized in single-wall carbon nanotubes-surfactant films in room temperature ionic liquids. Electrochemistry Communications, 11 (2009). (2): p. 286-289.

[88]   H. Naeim, F. Kheiri, M. Sirousazar and A. Afghan, Ionic liquid/reduced graphene oxide/nickel-palladium nanoparticle hybrid synthesized for non-enzymatic electrochemical glucose sensing. Electrochimica Acta, 282 (2018). p. 137-146.

[89]   Y. Li, X. Zhai, H. Wang, X. Liu, L. Guo, X. Ji, L. Wang, H. Qiu and X. Liu, Non-enzymatic sensing of uric acid using a carbon nanotube ionic-liquid paste electrode modified with poly (β-cyclodextrin). Microchimica Acta, 182 (2015). (11-12): p. 1877-1884.

[90]   J.S. Bunch, A.M. Van Der Zande, S.S. Verbridge, I.W. Frank, D.M. Tanenbaum, J.M. Parpia, H.G. Craighead and P.L. McEuen, Electromechanical resonators from graphene sheets. Science, 315 (2007). (5811): p. 490-493.

[91]   K.R. Ratinac, W. Yang, J.J. Gooding, P. Thordarson and F. Braet, Graphene and related materials in electrochemical sensing. Electroanalysis, 23 (2011). (4): p. 803-826.

[92]   H.C. Schniepp, J.-L. Li, M.J. McAllister, H. Sai, M. Herrera-Alonso, D.H. Adamson, R.K. Prud'homme, R. Car, D.A. Saville and I.A. Aksay, Functionalized single graphene sheets derived from splitting graphite oxide. The Journal of Physical Chemistry B, 110 (2006). (17): p. 8535-8539.

[93]   Z. Wang, X. Zhou, J. Zhang, F. Boey and H. Zhang, Direct electrochemical reduction of single-layer graphene oxide and subsequent functionalization with glucose oxidase. The Journal of Physical Chemistry C, 113 (2009). (32): p. 14071-14075.

[94]   Z. Wang, H. Wang, Z. Zhang, X. Yang and G. Liu, Sensitive electrochemical determination of trace cadmium on a stannum film/poly (p-aminobenzene sulfonic acid)/electrochemically reduced graphene composite modified electrode. Electrochimica Acta, 120 (2014). p. 140-146.

[95]   D. Li, M.B. Müller, S. Gilje, R.B. Kaner and G.G. Wallace, Processable aqueous dispersions of graphene nanosheets. Nature nanotechnology, 3 (2008). (2): p. 101.

[96]   S. Mutyala and J. Mathiyarasu, A reagentless non-enzymatic hydrogen peroxide sensor presented using electrochemically reduced graphene oxide modified glassy carbon electrode. Materials Science and Engineering: C, 69 (2016). p. 398-406.

[97]   J.-M. Jian, L. Fu, J. Ji, L. Lin, X. Guo and T.-L. Ren, Electrochemically reduced graphene oxide/gold nanoparticles composite modified screen-printed carbon electrode for effective electrocatalytic analysis of nitrite in foods. Sensors and Actuators B: Chemical, 262 (2018). p. 125-136.

[98]   G.C. Bandara, C.A. Heist and V.T. Remcho, Patterned polycaprolactone-filled glass microfiber microfluidic devices for total protein content analysis. Talanta, 176 (2018). p. 589-594.

[99]   G.C. Bandara, C.A. Heist and V.T. Remcho, Chromatographic Separation and Visual Detection on Wicking Microfluidic Devices: Quantitation of Cu2+ in Surface, Ground, and Drinking Water. Analytical chemistry, 90 (2018). (4): p. 2594-2600.

[100]   R.E. Jones, W. Zheng, J.C. McKew and C.Z. Chen, An alternative direct compound dispensing method using the HP D300 digital dispenser. Journal of laboratory automation, 18 (2013). (5): p. 367-374.

[101]   N. Promphet, P. Rattanawaleedirojn and N. Rodthongkum, Electroless NiP-TiO2 sol-RGO: A smart coating for enhanced corrosion resistance and conductivity of steel. Surface and Coatings Technology, 325 (2017). p. 604-610.

[102]   P. Rattanawaleedirojn, K. Saengkiettiyut, Y. Boonyongmaneerat, S. Sangsuk, N. Promphet and NTable 1. Rodthongkum, TiO 2 sol-embedded in electroless Ni–P coating: a novel approach for an ultra-sensitive sorbitol sensor. RSC Advances, 6 (2016). (73): p. 69261-69269.

[103]   S. Jampasa, W. Wonsawat, N. Rodthongkum, W. Siangproh, P. Yanatatsaneejit, T. Vilaivan and O. Chailapakul, Electrochemical detection of human papillomavirus DNA type 16 using a pyrrolidinyl peptide nucleic acid probe immobilized on screen-printed carbon electrodes. Biosensors and Bioelectronics, 54 (2014). p. 428-434.

[104]   S. Chaiyo, E. Mehmeti, W. Siangproh, T.L. Hoang, H.P. Nguyen, O. Chailapakul and K. Kalcher, Non-enzymatic electrochemical detection of glucose with a disposable paper-based sensor using a cobalt phthalocyanine–ionic liquid–graphene composite. Biosensors and Bioelectronics, 102 (2018). p. 113-120.

[105]   S. Jampasa, W. Siangproh, K. Duangmal and O. Chailapakul, Electrochemically reduced graphene oxide-modified screen-printed carbon electrodes for a simple and highly sensitive electrochemical detection of synthetic colorants in beverages. Talanta, 160 (2016). p. 113-124.

[106]   F. Bugamelli, C. Marcheselli, E. Barba and M. Raggi, Determination of l-dopa, carbidopa, 3-O-methyldopa and entacapone in human plasma by HPLC–ED. Journal of pharmaceutical and biomedical analysis, 54 (2011). (3): p. 562-567.

[107]   G.D. Tarigh, F. Shemirani and N.S. Maz'hari, Fabrication of a reusable magnetic multi-walled carbon nanotube–TiO 2 nanocomposite by electrostatic adsorption:

enhanced photodegradation of malachite green. RSC Advances, 5 (2015). (44): p. 35070-35079.

[108] R. Rahimi, S. Zargari and Z. Sadat Shojaei. *Photoelectrochemical investigation of TiO2-graphene nanocomposites*. in *Proceedings of the 18th International Electronic Conference on Synthetic Organic Chemistry, Basel, Switzerland*. 2014.

[109] M.-y. Duan, J. Li, G. Mele, C. Wang, X.-f. Lu, G. Vasapollo and F.-x. Zhang, Photocatalytic activity of novel tin porphyrin/TiO2 based composites. The Journal of Physical Chemistry C, 114 (2010). (17): p. 7857-7862.

[110] J.-J. Shim, Ionic liquid mediated synthesis of graphene–TiO2 hybrid and its photocatalytic activity. Materials Science and Engineering: B, 180 (2014). p. 38-45.

[111] Y.-p. Zhang, J.-j. Xu, Z.-h. Sun, C.-z. Li and C.-x. Pan, Preparation of graphene and TiO 2 layer by layer composite with highly photocatalytic efficiency. Progress in Natural Science: Materials International, 21 (2011). (6): p. 467-471.

[112] D. Naumenko, V. Snitka, B. Snopok, S. Arpiainen and H. Lipsanen, Graphene-enhanced Raman imaging of TiO2 nanoparticles. Nanotechnology, 23 (2012). (46): p. 465703.

[113] B. Erdem, R.A. Hunsicker, G.W. Simmons, E.D. Sudol, V.L. Dimonie and M.S. El-Aasser, XPS and FTIR surface characterization of TiO2 particles used in polymer encapsulation. Langmuir, 17 (2001). (9): p. 2664-2669.

[114] L. Gu, H. Zhang, Z. Jiao, M. Li, M. Wu and Y. Lei, Glucosamine-induced growth of highly distributed TiO 2 nanoparticles on graphene nanosheets as high-performance photocatalysts. RSC Advances, 6 (2016). (71): p. 67039-67048.

[115] D. Peng, W. Qin, X. Wu and Y. Pan, Improvement of the resistance performance of carbon/cyanate ester composites during vacuum electron radiation by reduced graphene oxide modified TiO 2. RSC Advances, 5 (2015). (94): p. 77138-77146.

[116] J.S. Lee, K.H. You and C.B. Park, Highly photoactive, low bandgap TiO2 nanoparticles wrapped by graphene. Advanced Materials, 24 (2012). (8): p. 1084-1088.

[117] S.A. El-Safty, M.A. Shenashen, M. Ismael and M. Khairy, Encapsulation of proteins into tunable and giant mesocage alumina. Chemical Communications, 48 (2012). (53): p. 6708-6710.

[118]   S. El-Safty, A. Shahat, M.R. Awual and M. Mekawy, Large three-dimensional mesocage pores tailoring silica nanotubes as membrane filters: nanofiltration and permeation flux of proteins. Journal of Materials Chemistry, 21 (2011). (15): p. 5593-5603.

[119]   M. Rismanchian, J. Akbari and R. Keshavarzi, Photocatalytic removal of gaseous toluene by titanium dioxide coated on nickel foam: Influence of relative humidity and toluene concentration. International Journal of Environmental Health Engineering, 3 (2014). (1): p. 29.

[120]   H. Chen, X. Tan, J. Zhang, Q. Lu, X. Ou, Y. Ruo and S. Chen, An electrogenerated chemiluminescent biosensor based on a gC 3 N 4–hemin nanocomposite and hollow gold nanoparticles for the detection of lactate. RSC Advances, 4 (2014). (106): p. 61759-61766.

[121]   H. Ju, X. Zhang and J. Wang, Nanobiosensing: principles, development and application. 2011: Springer Science & Business Media.

[122]   S. Suman, R. Singhal, A.L. Sharma, B. Malthotra and C. Pundir, Development of a lactate biosensor based on conducting copolymer bound lactate oxidase. Sensors and Actuators B: Chemical, 107 (2005). (2): p. 768-772.

[123]   T.-M. Park, E.I. Iwuoha, M.R. Smyth, R. Freaney and A.J. McShane, Sol-gel based amperometric biosensor incorporating an osmium redox polymer as mediator for detection of L-lactate. Talanta, 44 (1997). (6): p. 973-978.

[124]   J. Bai and B. Zhou, Titanium dioxide nanomaterials for sensor applications. Chemical reviews, 114 (2014). (19): p. 10131-10176.

[125]   N. Chauhan, J. Narang and C. Pundir, Fabrication of multiwalled carbon nanotubes/polyaniline modified Au electrode for ascorbic acid determination. Analyst, 136 (2011). (9): p. 1938-1945.

[126]   C. Shan, H. Yang, D. Han, Q. Zhang, A. Ivaska and L. Niu, Electrochemical determination of NADH and ethanol based on ionic liquid-functionalized graphene. Biosensors and Bioelectronics, 25 (2010). (6): p. 1504-1508.

[127]   J. Huang, J. Li, Y. Yang, X. Wang, B. Wu, J.-i. Anzai, T. Osa and Q. Chen, Development of an amperometric l-lactate biosensor based on l-lactate oxidase immobilized through silica sol–gel film on multi-walled carbon nanotubes/platinum

nanoparticle modified glassy carbon electrode. Materials Science and Engineering: C, 28 (2008). (7): p. 1070-1075.

[128]   M. Tribet, B. Covelo, A. Sicilia-Zafra, R. Navarrete-Casas, D. Choquesillo-Lazarte, J. González-Pérez, A. Castineiras and J. Niclós-Gutiérrez, Ternary copper (II) complexes with N-carboxymethyl-l-prolinato (2−) ion and imidazole or creatinine: A comparative study of the interligand interactions influencing the molecular recognition and stability. Journal of inorganic biochemistry, 99 (2005). (7): p. 1424-1432.

[129]   X.-Y. Peng, X.-X. Liu, D. Diamond and K.T. Lau, Synthesis of electrochemically-reduced graphene oxide film with controllable size and thickness and its use in supercapacitor. Carbon, 49 (2011). (11): p. 3488-3496.

[130]   W.R. de Araújo, M.O. Salles and T.R. Paixão, Development of an enzymeless electroanalytical method for the indirect detection of creatinine in urine samples. Sensors and Actuators B: Chemical, 173 (2012). p. 847-851.

[131]   E.P. Randviir, D.K. Kampouris and C.E. Banks, An improved electrochemical creatinine detection method via a Jaffe-based procedure. Analyst, 138 (2013). (21): p. 6565-6572.

[132]   T. Wen, W. Zhu, C. Xue, J. Wu, Q. Han, X. Wang, X. Zhou and H. Jiang, Novel electrochemical sensing platform based on magnetic field-induced self-assembly of Fe3O4@ Polyaniline nanoparticles for clinical detection of creatinine. Biosensors and Bioelectronics, 56 (2014). p. 180-185.

[133]   A. Erlenkötter, M. Fobker and G.-C. Chemnitius, Biosensors and flow-through system for the determination of creatinine in hemodialysate. Analytical and bioanalytical chemistry, 372 (2002). (2): p. 284-292.

[134]   J.-C. Chen, A. Kumar, H.-H. Chung, S.-H. Chien, M.-C. Kuo and J.-M. Zen, An enzymeless electrochemical sensor for the selective determination of creatinine in human urine. Sensors and Actuators B: Chemical, 115 (2006). (1): p. 473-480.

VITA

NAME	Siraprapa Boobphahom
DATE OF BIRTH	3 March 1989
PLACE OF BIRTH	Srisaket
INSTITUTIONS ATTENDED	M.Sc (Biochemistry), Chulalongkorn University, Bangkok, Thailand
	B.Sc. (Chemistry), University of Srinakharinwirot, Bangkok, Thailand
HOME ADDRESS	1/1 Palochai Rd. Soi 7, Tambol Nai Meaung, Ampoe Meaung, Ubon Rachatanee Province
PUBLICATION	Boobphahom, S., Rattanawaleedirojn, P., Boonyongmaneerat, Y., Rengpipat, S., Chailapakul, O., & Rodthongkum, N. (2019). TiO2 sol/graphene modified 3D porous Ni foam: A novel platform for enzymatic electrochemical biosensor. Journal of Electroanalytical Chemistry, 833, 133-142.
	Boobphahom, S., Ruecha, N., Rodthongkum, N., Chailapakul, O., & Remcho, V. T. (2019). A copper oxide-ionic liquid/reduced graphene oxide composite sensor enabled by digital dispensing: Non-enzymatic paper-based microfluidic determination of creatinine in human blood serum. Analytica chimica acta, 1083, 110-118.